

ANALYSIS OF FLOW THROUGH EIGHTEEN-FOOT  
BROKEN BACK CULVERTS

By

NICHOLAS MICHAEL JOHNSON

Bachelor of Science in Civil Engineering

Oklahoma State University

Stillwater, OK

2011

Submitted to the Faculty of the  
Graduate College of the  
Oklahoma State University  
in partial fulfillment of  
the requirements for  
the Degree of  
MASTER OF SCIENCE  
May, 2013

ANALYSIS OF FLOW THROUGH EIGHTEEN-  
FOOT BROKEN BACK CULVERTS

Thesis Approved:

Avdhesh K. Tyagi

---

Thesis Adviser

Dee A. Sanders

---

John N. Veenstra

---

## ACKNOWLEDGEMENTS

First, I wish to thank God that He has provided me these opportunities and the natural stubbornness to see this degree through. Without the time I spent meditating with Him I know I would not have been able to finish.

I would like to thank my parents, Michael and Gina Johnson, for not taking the easy road and teaching me and my siblings themselves day in and day out throughout our primary schooling. It was because of their love and effort that I learned to persevere to completion when I considered something important. It was in that little schoolroom where we spent so much time together that I developed my love of learning and appreciation for education.

I would like to thank my advisor, Avdhesh Tyagi, for working with me through difficult schedules and limited meetings to make the most of my time with him. I would not complete this degree without his constant support and instruction.

I would also like to acknowledge that Oklahoma Department of Transportation, Oklahoma Transportation Commission, and Federal Highway Administration provided the funding that made this research possible.

Name: NICHOLAS MICHAEL JOHNSON

Date of Degree: MAY, 2013

Title of Study: ANALYSIS OF FLOW THROUGH EIGHTEEN-FOOT BROKEN  
BACK CULVERTS

Major Field: CIVIL ENGINEERING

Abstract: Many culverts in Oklahoma are subject to detrimental scour. This study examines the flow through broken-back culverts with drops ranging from six to twenty-four feet. After this initial look at the flow through these culverts under the current practice of allowing the flow to pass through with its high energy, the eighteen-foot culverts are singled out and examined.

Next, culverts with abnormally high ceilings are examined to see what culvert dimensions would be needed to fully develop a hydraulic jump with the use of sills and friction blocks. This will allow new culverts to be constructed in a way to most efficiently induce the hydraulic jump and minimize the outlet energy, and so minimize the degradation of the area directly downstream of the culvert.

Thirdly, culverts with standard height ceilings are examined to see what arrangement of sills and frictions blocks will produce the most efficient jump in standard field conditions. This will allow existing culverts that are otherwise sound to be retrofitted to minimize further downstream degradation.

Finally, there will be a summary of conclusions to the three parts of the study-the flow regimes present in the culverts, open channel flow analysis of eighteen foot drop broken-back culverts and pressure flow analysis of eighteen foot drop broken-back culverts. This will look at the relevance of the eighteen-foot drop broken-back culvert, and give a brief overview of the differences between the new version of the culvert and the retrofitted culvert.

## TABLE OF CONTENTS

| Chapter  | Page |
|--|------|
| I. INTRODUCTION.....   | 1    |
| II. REVIEW OF LITERATURE.....  | 3    |
| III. FLOW REGIMES IN BROKEN-BACK CULVERTS.....   | 12   |
| 3.1 Abstract.....  | 12   |
| 3.2 Introduction.....  | 13   |
| 3.3 Literature Review.....   | 13   |
| 3.4 Laboratory Models.....   | 15   |
| 3.5 Flow in the Barrel.....  | 17   |
| 3.6 Hydraulic Jump.....  | 18   |
| 3.7 Mathematical Considerations.....   | 23   |
| 3.7.1 Froude Number.....   | 23   |
| 3.7.2 Bernoulli Equation.....  | 24   |
| 3.8 Discussion of Results.....   | 25   |
| 3.9 Conclusion.....  | 25   |
| 3.10 Acknowledgements.....   | 26   |
| 3.11 References.....   | 26   |
| IV. ENERGY DISSIPATION IN EIGHTEEN-FOOT DROP BROKEN-BACK<br>CULVERTS UNDER OPEN CHANNEL FLOW CONDITIONS..... | 29   |
| 4.1 Abstract.....  | 29   |
| 4.2 Introduction.....  | 29   |
| 4.3 Laboratory Model.....  | 33   |
| 4.4 Data Collection and Analysis.....  | 40   |
| 4.5 Results.....   | 42   |
| 4.6 Conclusion.....  | 48   |
| 4.7 Acknowledgements.....  | 50   |
| 4.8 Notation.....  | 50   |
| 4.9 References.....  | 51   |

| Chapter  | Page |
|--|------|
| V. ENERGY DISSIPATION IN EIGHTEEN-FOOT DROP BROKEN-BACK<br>CULVERTS UNDER PRESSURE FLOW CONDITIONS ..... | 53   |
| 5.1 Abstract .....   | 53   |
| 5.2 Introduction.....  | 54   |
| 5.3 Theory .....   | 58   |
| 5.4 Experimental Setup and Instrumentation.....  | 61   |
| 5.4.1 Laboratory Model .....   | 61   |
| 5.4.2 Experimental Procedure and Data Collection.....  | 69   |
| 5.5 Data Analysis .....  | 70   |
| 5.6 Results.....   | 76   |
| 5.7 Conclusion .....   | 77   |
| 5.8 Acknowledgements.....  | 78   |
| 5.9 Notation.....  | 79   |
| 5.10 References.....   | 80   |
| VI. CONCLUSION.....  | 82   |
| REFERENCES .....   | 84   |
| APPENDIX.....  | 89   |

## LIST OF TABLES

| Table   | Page |
|---|------|
| 3.1: Parameters for the Four Flow Conditions.....   | 19   |
| 4.1: Hydraulic Parameters for Experiment 1 .....  | 44   |
| 4.2: Hydraulic Parameters for Experiment 5 .....  | 46   |
| 4.3: Hydraulic Parameters for Experiment 6 .....  | 48   |
| 5.1: Hydraulic Parameters for Experiment 19 .....   | 72   |
| 5.2: Hydraulic Parameters for Experiment 24 .....   | 74   |
| 5.3: Hydraulic Parameters for Experiment 25 .....   | 76   |
| A.1: Experiment 1 for 1% slope using Open Channel Flow Condition with No Sill<br>in the Culvert.....  | 90   |
| A.2: Experiment 2 for 1% Slope Using Open Channel Flow Condition with a 2”<br>End Sill.....   | 91   |
| A.3: Experiment 3 for 1% Slope Using Open Channel Flow Condition with a 3”<br>End Sill.....   | 92   |
| A.4: Experiment 4 for 1% Slope Using Open Channel Flow Condition with a 3”<br>Sill 33” from the End .....   | 93   |
| A.5: Experiment 5 for 1% Slope Using Open Channel Flow Condition with a 3”<br>Sill 26” from the End .....   | 94   |
| A.6: Experiment 6 for 1% Slope Using Open Channel Flow Condition with a 3”<br>Sill 26” from the End and 15 Flat Faced Friction Blocks at 12” from the Toe ..              | 95   |
| A.7: Experiment 7 for 1% Slope Using Open Channel Flow Condition with a 3”<br>Sill 26” from the End and 30 Flat Faced Friction Blocks at 12” from the Toe ..              | 96   |
| A.8: Experiment 8 for 1% Slope Using Open Channel Flow Condition with a 3”<br>Sill 26” from the End and 45 Flat Faced Friction Blocks at 12” from the Toe ..              | 97   |
| A.9: Experiment 9 for 0.6% Slope Using Open Channel Flow Condition with No<br>Sill in the Culvert .....   | 98   |
| A.10: Experiment 10 for 0.6% Slope Using Open Channel Flow Condition with a<br>3” Sill at 26” from the End .....  | 99   |
| A.11: Experiment 11 for 0.6% Slope Using Open Channel Flow Condition with a<br>3” Sill at 26” from the End and 15 Flat Faced Friction Blocks at 12” from the<br>Toe ..... | 100  |

| Table   | Page |
|---|------|
| A.12: Experiment 12 for 0.6% Slope Using Open Channel Flow Condition with a 3" Sill at 26" from the End with 30 Flat Faced Friction Blocks at 12" from the Toe .....            | 101  |
| A.13: Experiment 13 for 0.6% Slope Using Open Channel Flow Condition with a 3" Sill at 26" from the End with 45 Flat Faced Friction Blocks at 12" from the Toe .....            | 102  |
| A.14: Experiment 14 for 0.3% Slope Using Open Channel Flow Condition with No Sill in the Culvert .....  | 103  |
| A.15: Experiment 15 for 0.3% Slope Using Open Channel Flow Condition with a 3" Sill at 26" from the End .....   | 104  |
| A.16: Experiment 16 for 0.3% Slope Using Open Channel Flow Condition with a 3" Sill at 26" from the End with 15 Flat Faced Friction Blocks at 12" from the Toe .....            | 105  |
| A.17: Experiment 17 for 0.3% Slope Using Open Channel Flow Condition with a 3" Sill at 26" from the End with 30 Flat Faced Friction Blocks at 12" from the Toe .....            | 106  |
| A.18: Experiment 18 for 0.3% Slope Using Open Channel Flow Condition with a 3" Sill at 26" from the End with 45 Flat Faced Friction Blocks at 12" from the Toe .....            | 107  |
| A.19: Experiment 19 for 1.0% Slope Horizontal Channel Using Pressure Flow Condition without any Friction Blocks.....  | 108  |
| A.20: Experiment 20 for 1.0% Slope Using Pressure Flow Condition with a 2" End Sill.....  | 109  |
| A.21: Experiment 21 for 1.0% Slope Using Pressure Flow Condition with a 2" Sill at 34" from the End.....  | 110  |
| A.22: Experiment 22 for 1.0% Slope Using Pressure Flow Condition with a 2.5" Sill at 26" from the End .....   | 111  |
| A.23: Experiment 23 for 1.0% Slope Using Pressure Flow Condition with a 2" Sill at 30" from the End.....  | 112  |
| A.24: Experiment 24 for 1.0% Slope Using Pressure Flow Condition and a 1.5" Sill at 37" from the End and 2" Sill at 27" from the End .....                                      | 113  |
| A.25: Experiment 25 for 1% Slope Using Pressure Flow Condition with 15 Flat Faced Friction Blocks and a 1.5" Sill at 37" from the End and a 2" Sill at 27" from the End .....   | 114  |
| A.26: Experiment 26 for 1.0% Slope Using Pressure Flow Condition with 30 Flat Faced Friction Blocks and a 1.5" Sill at 37" from the End and a 2" sill at 27" from the End ..... | 115  |
| A.27: Experiment 27 for 1.0% Slope Using Pressure Flow Condition with 45 Flat Faced Friction Blocks and a 1.5" Sill at 37" from the End and a 2" Sill at 27" from the End ..... | 116  |
| A.28: Experiment 28 for 0.6% Slope Horizontal Channel Using Pressure Flow Condition without any Friction Blocks.....  | 117  |
| A.29: Experiment 29 for 0.6% Slope Using Pressure Flow Condition and a 1.5" Sill at 37" from the End and a 2" Sill at 27" from the End.....                                     | 118  |



|   |     |
|---|-----|
| A.30: Experiment 30 for 0.6% Slope Using Pressure Flow Condition with 15 Flat Faced Friction Blocks and a 1.5” Sill at 37” from the End and a 2” Sill at 27” from the End ..... | 119 |
| A.31: Experiment 31 for 0.6% Slope Using Pressure Flow Condition with 30 Flat Faced Friction Blocks and a 1.5” Sill at 37” from the End and a 2” Sill at 27” from the End ..... | 120 |
| A.32: Experiment 32 for 0.6% Slope Using Pressure Flow Condition with 45 Flat Faced Friction Blocks and a 1.5” Sill at 37” from the End and a 2” Sill at 27” from the End ..... | 121 |
| A.33: Experiment 33 for 0.3% Slope Horizontal Channel Using Pressure Flow Condition without any Friction Blocks.....  | 122 |
| A.34: Experiment 34 for 0.3% Slope Using Pressure Flow Condition and a 1.5” Sill at 37” from the End and a 2” Sill at 27” from the End.....                                     | 123 |
| A.35: Experiment 35 for 0.3% Slope Using Pressure Flow Condition with 15 Flat Faced Friction Blocks and a 1.5” Sill at 37” from the End and a 2” Sill at 27” from the End ..... | 124 |
| A.36: Experiment 36 for 0.3% Slope Using Pressure Flow Condition with 30 Flat Faced Friction Blocks and a 1.5” Sill at 37” from the End and a 2” Sill at 27” From the End.....  | 125 |
| A.37: Experiment 37 for 0.3% Slope Using Pressure Flow Condition with 45 Flat Faced Friction Blocks and a 1.5” Sill at 37” from the End and a 2” Sill at 27” from the End ..... | 126 |

## LIST OF FIGURES

| Figure   | Page |
|--|------|
| 3.1: Broken-Back Culvert Model Schematic .....   | 15   |
| 3.2: 6 Ft Drop A Case .....  | 20   |
| 3.3: 6 Ft Drop B Case .....  | 20   |
| 3.4: 6 Ft Drop C Case .....  | 20   |
| 3.5: 12 Ft Drop A Case .....   | 21   |
| 3.6: 12 Ft Drop B Case .....   | 21   |
| 3.7: 12 Ft Drop C Case .....   | 21   |
| 3.8: 18 Ft Drop A Case .....   | 22   |
| 3.9: 18 Ft Drop B Case .....   | 22   |
| 3.10: 18 Ft Drop C Case .....  | 22   |
| 3.11: 24 Ft Drop A Case .....  | 23   |
| 3.12: 24 Ft Drop B Case .....  | 23   |
| 3.13: 24 Ft Drop C Case .....  | 23   |
| 4.1: Open Channel Flow Conditions Model Isometric .....  | 34   |
| 4.2: Plan View of Model .....  | 35   |
| 4.3: Profile View of Laboratory Model .....  | 35   |
| 4.4: Profile and Plan View of Reservoir Inlet (Upstream).....  | 36   |
| 4.5: Plan View of Culvert Outlet (Downstream) .....  | 36   |
| 4.6: Side View of Laboratory Model .....   | 37   |
| 4.7: Front View of Laboratory Model.....   | 38   |
| 4.8: Example of Sill and Friction Block Configuration.....   | 39   |
| 4.9: Example of Friction Block .....   | 40   |
| 4.10: Typical Sill Dimensions.....   | 40   |
| 4.11: Experiment 1A with No Sill or Friction Blocks .....  | 43   |
| 4.12: Experiment 1B with No Sill or Friction Blocks .....  | 43   |
| 4.13: Experiment 1C with No Sill or Friction Blocks .....  | 44   |
| 4.14: Experiment 5A with a 3" Sill at 26" from the End of the Culvert.....                                       | 45   |
| 4.15: Experiment 5B with a 3" Sill at 26" from the End of the Culvert.....                                       | 45   |
| 4.16: Experiment 5C with a 3" Sill at 26" from the End of the Culvert.....                                       | 45   |
| 4.17: Experiment 6A with a 3" Sill at 26" from the End of the Culvert and 15 Flat<br>Faced Friction Blocks ..... | 47   |
| 4.18: Experiment 6B with a 3" Sill at 26" from the End of the Culvert and 15 Flat<br>Faced Friction Blocks ..... | 47   |

| Figure   | Page |
|--|------|
| 4.19: Experiment 6C with a 3” Sill at 26” from the End of the Culvert and 15 Flat Faced Friction Blocks .....  | 47   |
| 4.20: Hydraulic Jump Characteristics for Experiment 5B 1.0d .....  | 49   |
| 4.21: Hydraulic Jump Characteristics for Experiment 5C 1.2d .....  | 49   |
| 5.1: Pressure Flow Laboratory Model .....  | 62   |
| 5.2: Profile and Plan View of Reservoir Inlet (Upstream).....  | 62   |
| 5.3: Plan View of Culvert Outlet (Downstream) .....  | 63   |
| 5.4: Profile View of Laboratory Model .....  | 63   |
| 5.5: Plan View of Laboratory Model .....   | 63   |
| 5.6: Dimensions of Broken-Back Culvert to Apply Pressure Flow Condition.....   | 64   |
| 5.7: Front View of Laboratory Model.....   | 65   |
| 5.8: Side View of Laboratory Model .....   | 66   |
| 5.9: Downstream Plywood Channel after Wingwall .....   | 66   |
| 5.10: Reservoir and Channel Inlet for Culvert Model .....  | 67   |
| 5.11: Typical Sill Dimensions.....   | 68   |
| 5.12: Example of Flat Faced Friction Block.....  | 68   |
| 5.13: Example of Flat Faced Friction Blocks Arranged on Model Bottom.....  | 69   |
| 5.14: Hydraulic Jump Variables in a Broken-Back Culvert .....  | 70   |
| 5.15: Experiment 19A with No Sill or Friction Blocks .....   | 71   |
| 5.16: Experiment 19B with No Sill or Friction Blocks .....   | 71   |
| 5.17: Experiment 19C with No Sill or Friction Blocks .....   | 71   |
| 5.18: Experiment 24A with a 1.5” Sill at 37” from the End and a 2” Sill located at 27” from the End of the Culvert .....                                   | 73   |
| 5.19: Experiment 24B with a 1.5” Sill at 37” from the End and a 2” Sill located at 27” from the End of the Culvert .....                                   | 73   |
| 5.20: Experiment 24C with a 1.5” Sill at 37” from the End and a 2” Sill located at 27” from the End of the Culvert .....                                   | 73   |
| 5.21: Experiment 25A with a 1.5” Sill at 37” from the End and a 2” Sill located at 27” from the End of the Culvert and 15 Flat Faced Friction Blocks ..... | 75   |
| 5.22: Experiment 25B with a 1.5” Sill at 37” from the End and a 2” Sill located at 27” from the End of the Culvert and 15 Flat Faced Friction Blocks ..... | 75   |
| 5.23: Experiment 25C with a 1.5” Sill at 37” from the End and a 2” Sill located at 27” from the End of the Culvert and 15 Flat Faced Friction Blocks ..... | 75   |
| A.1: Experiment 1A for 1% Slope.....   | 90   |
| A.2: Experiment 1B for 1% Slope .....  | 90   |
| A.3: Experiment 1C for 1% Slope .....  | 90   |
| A.4: Experiment 2A for 1% Slope.....   | 91   |
| A.5: Experiment 2B for 1% Slope .....  | 91   |
| A.6: Experiment 2C for 1% Slope .....  | 91   |
| A.7: Experiment 3A for 1% Slope.....   | 92   |
| A.8: Experiment 3B for 1% Slope .....  | 92   |
| A.9: Experiment 3C for 1% Slope .....  | 92   |
| A.10: Experiment 4A for 1% Slope.....  | 93   |
| A.11: Experiment 4B for 1% Slope .....   | 93   |

| Figure                                    | Page |
|---|------|
| A.12: Experiment 4C for 1% Slope .....    | 93   |
| A.13: Experiment 5A for 1% Slope .....    | 94   |
| A.14: Experiment 5B for 1% Slope .....    | 94   |
| A.15: Experiment 5C for 1% Slope .....    | 94   |
| A.16: Experiment 6A for 1% Slope .....    | 95   |
| A.17: Experiment 6B for 1% Slope .....    | 95   |
| A.18: Experiment 6C for 1% Slope .....    | 95   |
| A.19: Experiment 7A for 1% Slope .....    | 96   |
| A.20: Experiment 7B for 1% Slope .....    | 96   |
| A.21: Experiment 7C for 1% Slope .....    | 96   |
| A.22: Experiment 8A for 1% Slope .....    | 97   |
| A.23: Experiment 8B for 1% Slope .....    | 97   |
| A.24: Experiment 8C for 1% Slope .....    | 97   |
| A.25: Experiment 9A for 0.6% Slope .....  | 98   |
| A.26: Experiment 9B for 0.6% Slope .....  | 98   |
| A.27: Experiment 9C for 0.6% Slope .....  | 98   |
| A.28: Experiment 10A for 0.6% Slope ..... | 99   |
| A.29: Experiment 10B for 0.6% Slope ..... | 99   |
| A.30: Experiment 10C for 0.6% Slope ..... | 99   |
| A.31: Experiment 11A for 0.6% Slope ..... | 100  |
| A.32: Experiment 11B for 0.6% Slope ..... | 100  |
| A.33: Experiment 11C for 0.6% Slope ..... | 100  |
| A.34: Experiment 12A for 0.6% Slope ..... | 101  |
| A.35: Experiment 12B for 0.6% Slope ..... | 101  |
| A.36: Experiment 12C for 0.6% Slope ..... | 101  |
| A.37: Experiment 13A for 0.6% Slope ..... | 102  |
| A.38: Experiment 13B for 0.6% Slope ..... | 102  |
| A.39: Experiment 13C for 0.6% Slope ..... | 102  |
| A.40: Experiment 14A for 0.3% Slope ..... | 103  |
| A.41: Experiment 14B for 0.3% Slope ..... | 103  |
| A.42: Experiment 14C for 0.3% Slope ..... | 103  |
| A.43: Experiment 15A for 0.3% Slope ..... | 104  |
| A.44: Experiment 15B for 0.3% Slope ..... | 104  |
| A.45: Experiment 15C for 0.3% Slope ..... | 104  |
| A.46: Experiment 16A for 0.3% Slope ..... | 105  |
| A.47: Experiment 16B for 0.3% Slope ..... | 105  |
| A.48: Experiment 16C for 0.3% Slope ..... | 105  |
| A.49: Experiment 17A for 0.3% Slope ..... | 106  |
| A.50: Experiment 17B for 0.3% Slope ..... | 106  |
| A.51: Experiment 17C for 0.3% Slope ..... | 106  |
| A.52: Experiment 18A for 0.3% Slope ..... | 107  |
| A.53: Experiment 18B for 0.3% Slope ..... | 107  |
| A.54: Experiment 18C for 0.3% Slope ..... | 107  |
| A.55: Experiment 19A for 1% Slope .....   | 108  |

| Figure                                    | Page |
|---|------|
| A.56: Experiment 19B for 1% Slope .....   | 108  |
| A.57: Experiment 19C for 1% Slope .....   | 108  |
| A.58: Experiment 20A for 1% Slope .....   | 109  |
| A.59: Experiment 20B for 1% Slope .....   | 109  |
| A.60: Experiment 20C for 1% Slope .....   | 109  |
| A.61: Experiment 21A for 1% Slope .....   | 110  |
| A.62: Experiment 21B for 1% Slope .....   | 110  |
| A.63: Experiment 21C for 1% Slope .....   | 110  |
| A.64: Experiment 22A for 1% Slope .....   | 111  |
| A.65: Experiment 22B for 1% Slope .....   | 111  |
| A.66: Experiment 22C for 1% Slope .....   | 111  |
| A.67: Experiment 23A for 1% Slope .....   | 112  |
| A.68: Experiment 23B for 1% Slope .....   | 112  |
| A.69: Experiment 23C for 1% Slope .....   | 112  |
| A.70: Experiment 24A for 1% Slope .....   | 113  |
| A.71: Experiment 24B for 1% Slope .....   | 113  |
| A.72: Experiment 24C for 1% Slope .....   | 113  |
| A.73: Experiment 25A for 1% Slope .....   | 114  |
| A.74: Experiment 25B for 1% Slope .....   | 114  |
| A.75: Experiment 25C for 1% Slope .....   | 114  |
| A.76: Experiment 26A for 1% Slope .....   | 115  |
| A.77: Experiment 26B for 1% Slope .....   | 115  |
| A.78: Experiment 26C for 1% Slope .....   | 115  |
| A.79: Experiment 27A for 1% Slope .....   | 116  |
| A.80: Experiment 27B for 1% Slope .....   | 116  |
| A.81: Experiment 27C for 1% Slope .....   | 116  |
| A.82: Experiment 28A for 0.6% Slope ..... | 117  |
| A.83: Experiment 28B for 0.6% Slope ..... | 117  |
| A.84: Experiment 28C for 0.6% Slope ..... | 117  |
| A.85: Experiment 29A for 0.6% Slope ..... | 118  |
| A.86: Experiment 29B for 0.6% Slope ..... | 118  |
| A.87: Experiment 29C for 0.6% Slope ..... | 118  |
| A.88: Experiment 30A for 0.6% Slope ..... | 119  |
| A.89: Experiment 30B for 0.6% Slope ..... | 119  |
| A.90: Experiment 30C for 0.6% Slope ..... | 119  |
| A.91: Experiment 31A for 0.6% Slope ..... | 120  |
| A.92: Experiment 31B for 0.6% Slope ..... | 120  |
| A.93: Experiment 31C for 0.6% Slope ..... | 120  |
| A.94: Experiment 32A for 0.6% Slope ..... | 121  |
| A.95: Experiment 32B for 0.6% Slope ..... | 121  |
| A.96: Experiment 32C for 0.6% Slope ..... | 121  |
| A.97: Experiment 33A for 0.3% Slope ..... | 122  |
| A.98: Experiment 33B for 0.3% Slope ..... | 122  |
| A.99: Experiment 33C for 0.3% Slope ..... | 122  |

| Figure  | Page |
|---|------|
| A.100: Experiment 34A for 0.3% Slope .....                            | 123  |
| A.101: Experiment 34B for 0.3% Slope .....                            | 123  |
| A.102: Experiment 34C for 0.3% Slope .....                            | 123  |
| A.103: Experiment 35A for 0.3% Slope .....                            | 124  |
| A.104: Experiment 35B for 0.3% Slope .....                            | 124  |
| A.105: Experiment 35C for 0.3% Slope .....                            | 124  |
| A.106: Experiment 36A for 0.3% Slope .....                            | 125  |
| A.107: Experiment 36B for 0.3% Slope .....                            | 125  |
| A.108: Experiment 36C for 0.3% Slope .....                            | 125  |
| A.109: Experiment 37A for 0.3% Slope .....                            | 126  |
| A.110: Experiment 37B for 0.3% Slope .....                            | 126  |
| A.111: Experiment 37C for 0.3% Slope .....                            | 126  |
| A.112: ADV Plugged to Measure the Downstream Velocity $V_{d/s}$ ..... | 127  |
| A.113: ADV Instrument .....   | 127  |
| A.114: ADV Mount Over Flume .....                                     | 128  |
| A.115: Pitot Tube Plugged in Culverts Downstream to $V_{d/s}$ .....   | 129  |
| A.116: Pitot Tube Plugged in Culverts Upstream to $V_{u/p}$ .....     | 130  |
| A.117: Pitot Tube .....   | 131  |

## CHAPTER I

### INTRODUCTION

A recent research study conducted by the Oklahoma Transportation Center at Oklahoma State University indicated that there are 121 scour-critical culverts on the Interstate System (ISTAT), the National Highway System (NHS), and the State Transportation Program (STP) in Oklahoma (Tyagi, 2002). The average replacement cost of these culverts is about \$121M. A survey of culverts in Oklahoma indicates that the drop in flowline between upstream and downstream ends ranges between 6 and 24 feet.

This thesis presents broken-back culverts with a drop of 18 feet. A drop of 18 feet was used in the laboratory model because it is close to the middle limit. Results of this research could maximize the energy loss within the culvert, thus minimizing the scour around the culvert and decreasing the degradation in the downstream channel. This reduces the construction and rehabilitation costs of culverts in Oklahoma. The project is supported by the Bridge Division, Oklahoma Department of Transportation (ODOT).

The purpose of this project is to develop a methodology to analyze broken-back culverts in Oklahoma such that the energy is mostly dissipated within the culverts to minimize the degradation downstream. The purpose of a culvert is to safely pass water underneath the

roadways constructed in hilly topography or on the side of a relatively steep hill. A broken-back culvert is used in areas of high relief and steep topography since it has one or more breaks in profile slope. This project investigates culverts with a drop that may result in effective energy dissipation inside the culvert and consequently minimize the scour downstream of broken-back culverts.

The research investigation includes the following tasks: 1) obtain and review existing research currently available for characterizing the hydraulic jump in culverts; 2) examine the various flow regimes of current broken-back culverts; 3) build a scale model to represent a prototype of a broken-back culvert 150 feet long, with two barrels of 10 X 10 feet, and a vertical drop of 18 feet; 4) simulate different flow conditions for 0.8, 1.0 and 1.2 times the culvert depth ( $d$ ) in the scale model constructed in Task 2; 5) evaluate the energy dissipation between upstream and downstream ends of the broken-back culvert with and without friction blocks of different shapes; 6) observe in physical experiments the efficiency of the hydraulic jump with and without friction blocks between upstream and downstream ends of the culvert and the location of the hydraulic jump from the toe of the drop in the culvert.



## CHAPTER II

### REVIEW OF LITERATURE

There are four basic regimes of flow: subcritical-laminar, supercritical-laminar, subcritical-turbulent, and supercritical-turbulent (Chow, 1959).

Smith and Oak (1994) conducted experiments to determine the inlet efficiency of a culvert. They found that projecting a slightly larger frame of the culvert upstream increased inlet efficiency. This study was done on circular culverts and showed the relationship between inlet styles and inlet efficiency.

Pegram and others (1999) conducted various experiments looking at skimming flow over stepped spillways. The turbulence associated with this study and the examination of model versus prototype scale impacts make it especially interesting in view of anticipated hydraulic jump. They found that a scale of down to 1:20 can faithfully give results in a model highly indicative of prototype reactions.

Campbell and others (1985) found that for supercritical flows the mass flow rate is controlled by the inlet conditions; but for subcritical flows the mass flow rate becomes controlled by the material properties of the flow and the channel declination. This indicates that sedimentation will

be more likely in the subcritical flow after the induced hydraulic jump in the culverts of this study.

Chanson (1996) discussed the occurrence of undular jump characteristics in culverts. He concluded that in standard culverts the flow can reasonably be predicted by using critical flow assumptions. He warned that this could not accurately predict all parameters in the culvert, but can be used for reasonable approximations in undular flow conditions. His study indicated the lack of experimental data in culvert studies at that time.

Stahl and Hager (1998) conducted various experiments analyzing hydraulic jump in circular conduits. They note that in jump conditions where the surface is not allowed to be free but becomes pressurized the characteristics begin to deviate from those in classical hydraulic jump. This deviation from classical hydraulic jump has prompted the study of extended height culverts as well as the observation of incomplete jump formation in typical box culverts with induced jump.

Moawad and others (1994) found that culverts are more susceptible to damage when fully submerged due to uplift around the inlet. They concluded that scour mitigation measures such as aprons should be placed at the inlet of the culvert due to the increase in deterioration of the culvert possible from this uplift aggravated by scour.

Nettleton and McCorquodale (1989) studied the hydraulic jump induced in stilling basins by way of baffle blocks. They concluded that there is an optimal placement for the jump inducers: too close and a large hump will form, too far back and the jump length increases. They determined that a continuous end sill would produce better results, but their scope only covered the baffle blocks.

There are 121 scour-critical culverts on the Interstate System (ISTAT), the National Highway System (NHS), and the State Transportation Program (STP) in Oklahoma according to a research

study conducted by the Oklahoma Transportation Center at Oklahoma State University (Tyagi, 2002). The average replacement cost of these culverts is about \$121M. A survey of culverts in Oklahoma indicates that the drop in flowline between upstream and downstream ends ranges between 6 and 24 feet (Rusch, 2008). In this research, a drop of 18 feet was used in the laboratory model. Advantages of this research are to maximize the energy loss within the culvert, thus minimizing the scour around the culvert and decreasing the degradation downstream in the channel. This reduces the construction and rehabilitation costs of culverts.

The hydraulic jump is a natural phenomenon produced by a sudden rise in water level due to change from supercritical flow to subcritical flow, that is, when there is a sudden decrease in velocity of the flow. This sudden change in the velocity causes the considerable turbulence and loss of energy. Consequently, hydraulic jump on broken-back culvert is generally used as an energy dissipater, and it has been recognized as an effective method for many years. Several investigators have studied hydraulic jump on culvert sloping aprons, Hotchkiss et al. (2005), Tyagi et al. (2010), and others have created expressions for jumps on sloping open rectangular channel [ (Li (1995), Husain et al. (1994), Sholichin and Akib (2010), Demetriou, and Dimitriou, (2008)].

Li (1995) studied how to find the location and length of the hydraulic jump in  $1^\circ$  through  $5^\circ$  slopes of rectangular channels. He examined many experimental laboratory models to get the relationship between upstream flow Froude number and ratio of jump length and sequent depth after jump  $L/y_2$ . Li used the HEC-2 software to locate the heel of a hydraulic jump to get the length of the jump and toe of the jump. The scale between the models and the prototypes was 1:65. Researchers concluded that estimation of sequent depth for a hydraulic jump had to take the channel bed slope into account if the bed slope was greater than  $3^\circ$ , and  $y_2/y_1$ , and  $F_{r1}$ , had a linear relation and could be used to estimate the sequent depth. Li recommended some rules such as using a solid triangular sill which could be arranged at the end of the basin apron to lift the

water and reduce the scour from the leaving flow, and if the  $F_{r1}$  ranged between 4.5 and 9, the tailwater depth was lowered by 5% of the sequent water depth.

Demetriou and Dimitriou (2008) carried out many laboratory experiments to measure the energy loss efficiency in hydraulic jump within sloped rectangular open channels. The authors used channel inclination angles  $\phi$  between  $2^\circ$  and  $16^\circ$ , and the Froude numbers,  $F_{r1}$ , ranged between 2 and 16. The authors concluded that the dimensionless energy loss was increasing with  $F_{r1}$  for  $\phi$ =constant, while for  $F_{r1}$  =constant this relative energy loss was also increasing with angle  $\phi$ .

Husain et al. (1994) performed many experiments on the sloping floor of open rectangular channels with negative and positive step to predict the length and depth of hydraulic jump and to analyze the sequent depth ratio. They found that the negative step has advantages over the positive with respect to stability and compactness of hydraulic jump. They developed a set of non-dimensional equations in terms of profile coefficient, and they used multiple linear regression analysis on jumps with or without a step. In Froude numbers between 4 to 12 and slope,  $S$ , between 1 and 10, the length and sequent depth ratio can accurately be predicted.

Numerous studies have examined the characteristics of the hydraulic jump. Bhutto et al. (1989) provided analytical solutions for computing sequent depth and relative energy loss for free hydraulic jump in horizontal and sloping rectangular channels from their experimental studies. They used the ratio of jump length to jump depth and the Froude number to compute the length of free jump on a horizontal bed. Jump factor and shape factor were evaluated experimentally for free jump on a sloping bed. To check the efficiency of the equations, they made comparisons with previous solutions by other researchers and found that the equations they derived could be used instead of previous solutions.

Defina and Susin (2003) investigated the stability of a stationary hydraulic jump situated over a lane sloping topography in a rectangular channel of uniform width with assuming inviscid flow

conditions. On upslope flow, it was found that hydraulic jump is unstable and if the jump is slightly displaced from its stationary point, it will move further away in the same direction. In the channel with adverse slope, they indicated that a stationary jump can be produced. They calculated the ratio of bed to friction slope such as energy dissipation per unit weight and unit length, and the result was quite large. They found that the equilibrium state is weakly perturbed when the theoretical stability condition was inferred in terms of the speed adopted by the jump.

Beirami and Chamani (2006) studied a large variety of hydraulic jumps on horizontal and end sloping ogee standard weirs, which were used to create supercritical flow and slopes of 0.0, -0.025, -0.05, -0.075, and -0.1 to build downstream of the weir. They presented a method to predict the sequent depth ratio that agreed with the results of investigations. Researchers observed that when the gravity force component in the jump was opposite to the flow direction, the water surface of the surface roller became undular and unstable. It was found that the negative slope of the basin reduced the sequent depth ratio, whereas a positive slope increased the sequent ratio. Beirami and Chamani (2010) reported that the energy loss in the classical jump is greater than that in any jump forming on negative or positive slopes.

Hartner et al. (2003) stated that the characteristics of the hydraulic jump depend on the Froude number ( $F_{r1}$ ). They added that in order for the hydraulic jump to occur, the flow must be supercritical, i.e. a jump can occur only when the Froude number is greater than 1.0. The hydraulic jump is classified according to its Froude number. When  $F_{r1}$  is between 1.7 and 2.5, the flow is classified as a weak jump: the rise in the water surface will be smooth with less energy dissipation. A  $F_{r1}$  between 2.5 and 4.5 results in an oscillating jump with 15-45% energy dissipation. A steady jump will occur when  $F_{r1}$  ranges from 4.5 to 9.0 and results in energy dissipation from 45% to 70%. When  $F_{r1}$  is above 9.0, a strong jump will occur with energy losses ranging from 70% to 85%.

Hotchkiss et al. (2005) proposed that by controlling the water at the outlet of a culvert, water scour around the culvert can be reduced. The effectiveness of a simple weir near the culvert outlet is compared to that of a culvert having a weir with a drop upstream in the culvert barrel. These two designs are intended to reduce the specific energy of the water at the outlet by inducing a hydraulic jump within the culvert barrel, without the aid of tailwater. The design procedure was proposed after studying the geometry and effectiveness of each jump type in energy reduction. In their research, they found the Froude number ranged from 2.6 to 6.0. It was determined that both outlet forms are effective in reducing the velocity of water and hence the energy and momentum.

Hydraulic Design of Energy Dissipators for Culverts and Channels (2006), from the Federal Highway Administration, provided design information for analyzing and mitigating problems associated with the energy dissipation at culvert outlets and in open channels. It recommends the use of the broken-back culvert design considering it as an internal energy dissipator. The proposed design for a broken-back culvert is limited to the following conditions:

- 1) The slope of the steep section must be less than or equal to 1.4:1 (V: H).
- 2) The hydraulic jump must be completed within the culvert barrel.

Many studies were carried out to examine the characteristics of the hydraulic jump. Ohtsu et al. (1996) evaluated incipient hydraulic jump conditions on flows over vertical sills. They identified two methods of obtaining an incipient jump: (1) increasing the sill height, or (2) increasing the tailwater depth until a surface roller forms upstream of the sill. For wide channels, predicted and experimental data were in agreement, but in the case of narrow channels, incipient jump was affected by channel width.

Hotchkiss et al. (2003) describe the available predictive tools for hydraulic jumps, the performance of the Broken-back Culvert Analysis Program (BCAP) in analyzing the hydraulics of a broken-back culvert, and the current applications and distribution of BCAP. They conducted

tests on the broken-back culvert made of Plexiglas to assess the performance of BCAP in predicting headwater rating curves, the locations of hydraulic jumps, and the lengths of hydraulic jumps. They conclude that accounting for the losses within the jump because of the friction in corrugated metal pipes and more accurate predicting of the locations of hydraulic jumps may be improved by predictions of flow hydraulics within the culvert barrel.

Larson (2004), in her Master's thesis entitled *Energy Dissipation in Culverts by Forcing a Hydraulic Jump at the Outlet*, suggests forcing hydraulic jumps to reduce the outlet energy. She considered two design examples to create a hydraulic jump within a culvert barrel: (1) a rectangular weir placed on a flat apron and (2) a vertical drop along with a rectangular weir. These two designs were used to study the reduction in the energy of the flow at the outlet. From these experiments she found that both designs were effective in reduction of outlet velocity, momentum, and energy. These reductions would decrease the need for downstream scour mitigation.

Lowe et al. (2011) indicated that the subcritical sequent depth is a function of the conduit shape, upstream depth, and Froude number. He studied the theoretical determination of subcritical sequent depths for pressure and free-surface jump. Lowe studied the momentum equation which consists of terms for the top width, area, and centroid of flow. Also, it was presented that the general solutions to the sequent depth problem for four prismatic conduits: rectangular, circular, elliptical, and pipe arch. Lowe provided a numerical solution for these shapes, and he neglected the effects of friction and air entrainment. The authors were concentrated on the cost of downstream energy dissipation by forcing a jump to occur within the culvert barrel.

Tyagi et al. (2009) investigated hydraulic jump under pressure and open channel flow conditions in a broken-back culvert with a 24 foot drop. It was found that for pressure flow a two sill solution induced the most desirable jump, and for open channel a single sill close to the middle of

the culvert was most desirable. The investigation was funded by the Oklahoma Transportation Center, Research and Innovative Technology Administration, Federal Highway Administration, and Oklahoma Department of Transportation.

Tyagi et al. (2010a) performed many experiments for open channel culvert conditions. Optimum energy dissipation was achieved by placing one sill at 40 feet from the outlet. Friction blocks and other modifications to the sill arrangement were not as effective.

Chamani et al. (2008) studied experimentally the energy loss of the vertical drop in the upstream with model of 0.20 m drop; they carried out laboratory experiments to collect data. They developed a model by using the theories of the shear layer and fully developed surface to estimate the energy loss. They found similarity between a turbulent surface jet and flow over the drop. The results compared with previous and their experimental data and it was found that the predictions of their model agreed well with the experimental data. Moreover, the authors used the predicted values of the energy loss to calculate the downstream depth of flow.

Mignot and Cienfuegos (2010) focused on an experimental investigation of energy dissipation and turbulence production in weak hydraulic jumps. Froude numbers ranged from 1.34 to 1.99. They observed two peak turbulence production regions for the partially developed inflow jump, one in the upper shear layer and the other in the near-wall region. The energy dissipation distribution in the jumps was measured and revealed a similar longitudinal decay of energy dissipation, which was integrated over the flow sections and maximum turbulence production values from the intermediate jump region towards its downstream section. It was found that the energy dissipation and the turbulence production were strongly affected by the inflow development. Turbulent production showed a common behavior for all measured jumps. It appeared that the elevation of maximum Turbulent Kinetic Energy (TKE) and turbulence production in the shear layer were similar.



Alikhani et al. (2010) conducted many experiments to evaluate effects of a continuous vertical end sill in a stilling basin. They measured the effects of sill position on the depth and length of a hydraulic jump without considering the tailwater depth. In the experiments, they used five different sill heights placed at three separate longitudinal distances in their 1:30 scale model. The characteristics of the hydraulic jump were measured and compared with the classical hydraulic jump under varied discharges. They proposed a new relationship between sill height and position, and sequent depth to basin length ratio. The study concluded that a 30% reduction in basin length could be accomplished by efficiently controlling the hydraulic jump length through sill height.

## CHAPTER III

### FLOW REGIMES IN BROKEN-BACK CULVERTS

#### 3.1 ABSTRACT

Broken-back culverts are used throughout the United States to pass water under roads through areas with high topography. Broken-back culverts have one or more breaks in flow path slope with steep sections having a slope of one vertical to two horizontal and mild sections having a slope of one percent or less. The culverts examined in this study were two barrel, ten foot by ten foot reinforced concrete. For every culvert modeled in this study, three simulated flow conditions were examined: a flow depth of eighty percent of the culvert height, one hundred percent of the culvert height, and finally one hundred twenty percent of the culvert height.

The study here specially looks at the Froude Number of the flow and the energy associated with the flow. These two parameters, examined in various ways, show the hydraulic jump anticipated if the jump were to be induced in the culvert.

Hydraulic jump is the natural phenomenon developed when flow depth suddenly changes due to a flow shift from supercritical to subcritical flow, which occurs when there is a sudden decrease in flow velocity. This jump can cause considerable turbulence and energy loss, making it a known effective energy dissipater. In the models for this study, the flow was supercritical-turbulent.

### 3.2 INTRODUCTION

Recent research conducted by the Oklahoma Transportation Center at Oklahoma State University indicated that 121 scour critical culverts are on the Interstate System (ISTAT), the National Highway System (NHS), and the State Transportation Program (STP) in Oklahoma (Tyagi, 2002). The change in flowline from the upstream to the downstream of these culverts varied from 6 to 24 feet.

Drops of 6, 12, 18, and 24 feet are examined in this study. The results of this study will help in determining the energy from outflow of a culvert and the possible hydraulic jump properties formed within the culvert should the hydraulic jump be artificially induced.

Culvert dimensions and hydraulic parameters for the models used in this study were provided by the Bridge Division, Oklahoma Department of Transportation (ODOT) (Rusch, 2008). This kept the model realistic to the prototypes and able to give useable data.

### 3.3 LITERATURE REVIEW

There are four basic regimes of flow: subcritical-laminar, supercritical-laminar, subcritical-turbulent, and supercritical-turbulent (Chow, 1959).

Smith and Oak (1994) conducted experiments to determine the inlet efficiency of a culvert. They found that projecting a slightly larger frame of the culvert upstream increased inlet efficiency. This study was done on circular culverts and showed the relationship between inlet styles and inlet efficiency.

Pegram and others (1999) conducted various experiments looking at skimming flow over stepped spillways. The turbulence associated with this study and the examination of model versus prototype scale impacts make it especially interesting in view of anticipated hydraulic jump. They found that a scale of down to 1:20 can faithfully give results in a model highly indicative of prototype reactions.

Campbell and others (1985) found that for supercritical flows the mass flow rate is controlled by the inlet conditions; but for subcritical flows the mass flow rate becomes controlled by the material properties of the flow and the channel declination. This indicates that sedimentation will be more likely in the subcritical flow after the induced hydraulic jump in the culverts of this study.

Chanson (1996) discussed the occurrence of undular jump characteristics in culverts. He concluded that in standard culverts the flow can reasonably be predicted by using critical flow assumptions. He warned that this could not accurately predict all parameters in the culvert, but can be used for reasonable approximations in undular flow conditions. His study indicated the lack of experimental data in culvert studies at that time.

Stahl and Hager (1998) conducted various experiments analyzing hydraulic jump in circular conduits. They note that in jump conditions where the surface is not allowed to be free but becomes pressurized the characteristics begin to deviate from those in classical hydraulic jump. This deviation from classical hydraulic jump has prompted the study of extended height culverts as well as the observation of incomplete jump formation in typical box culverts with induced jump.

Moawad and others (1994) found that culverts are more susceptible to damage when fully submerged due to uplift around the inlet. They concluded that scour mitigation measures such as aprons should be placed at the inlet of the culvert due to the increase in deterioration of the culvert possible from this uplift aggravated by scour.

Nettleton and McCorquodale (1989) studied the hydraulic jump induced in stilling basins by way of baffle blocks. They concluded that there is an optimal placement for the jump inducers: too close and a large hump will form, too far back and the jump length increases. They determined

that a continuous end sill would produce better results, but their scope only covered the baffle blocks.

Acoustic Doppler Velocimeter (ADV) is a sonar device which tracks suspended solids (particles) in a fluid medium to determine an instantaneous velocity of the particles in a sampling volume. In general, ADV devices have one transmitter head and two to four receiver heads. Since their introduction in 1993, ADVs have quickly become valuable tools for laboratory and field investigations of flow in rivers, canals, reservoirs, the oceans, around hydraulic structures and in laboratory scale models (Sontek, 2001).

### 3.4 LABORATORY MODELS

All laboratory models for this research represented two 10 foot by 10 foot barrels 150 feet long with a single break at the upstream end varying from 6 to 24 feet. The slope of the steep section was 1 (vertical) to 2 (horizontal), and the mild section slope was 1 percent. The model was constructed to 1:20 scale since this allowed for geometric similarity in a model that could easily fit the space limitations of the laboratory. This scale also enabled proper modeling of the flow rates required given the reservoir holding methods for constant head at the laboratory. An example schematic of the eighteen foot model is shown in Figure 3.1.

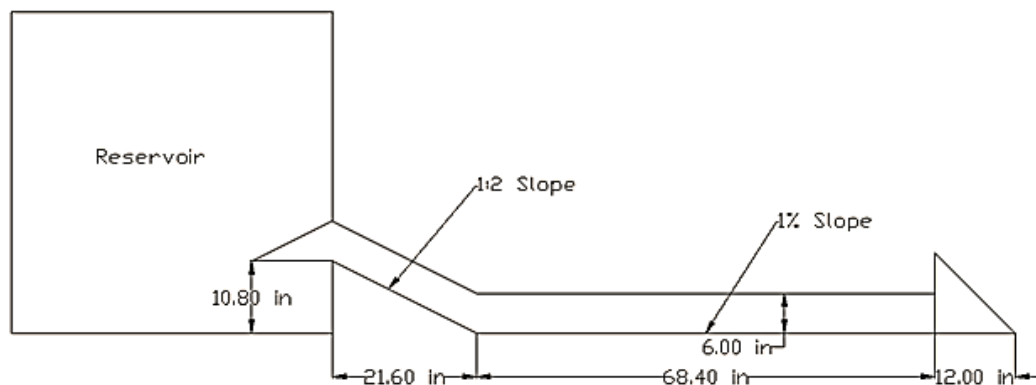


Figure 3.1: Broken Back Culvert Model Schematic

The model had two basic sections: the flume and the reservoir. The flume needed to be able to closely simulate flow in finished concrete and allow the flow to be easily observed. Plexiglas® was chosen because it offered excellent visibility of the flow in the model and had a Manning's roughness of 0.010, which is close to the Manning's roughness of 0.012 for finished concrete. It was decided that the Plexiglas® used should be 0.5 inches thick. This dimension would fit well into the model as it allowed connection hardware to be installed while not altering the interior conditions of the flume and it equated to a one foot thick wall in the prototype.

The flow in the reservoir did not need to be as closely observed as the flume and was mostly necessary to provide an observable constant head condition to the flume. Plywood was chosen for its durability and cost. It could also be altered for the various flume heights without needing to be completely rebuilt for every individual model.

A total of four flume models were constructed. These all had the same steep (1:2) and mild (1 percent) slopes, but the lengths were varied to allow for the height changes. The total length of the flume was maintained at 150 feet. The heights for the four flumes were 6 feet, 12 feet, 18 feet, and 24 feet, respectively.

Access holes were drilled into the flume ceiling to allow access of the measurement devices. When not used the holes were plugged with rubber stoppers to preserve the steady-state flow conditions of the flume. When the measurement devices were used, depending on the state of the flow the access hole would be sealed around the device by way of a rubber stopper.

Three flow measuring devices were used. A two-plate manometer was used to measure the flowrate into the reservoir. The reservoir was marked by a point gage so the flow could be made to match the depth condition desired (.8, 1.0, or 1.2 times the culvert depth). This gave the constant head for the experiment.

An Acoustic Doppler Velocimeter (ADV) was used to measure the velocity of the flow in the flume. This was the preferred device for velocity measurement since it took many samples over a relatively short period of time (about 5,000 measurements in 5 minutes for the settings used in this study). This device could not be used in some instances due to wake formation around the head of the device which gave questionable results.

When these conditions that caused questionable ADV results were encountered, a Pitot Tube was used to verify velocity readings. The Pitot Tube has long been recognized as a simple but reliable tool for measuring the head (total, static, or dynamic) of a flow. It introduces more human factors than the ADV though, and was therefore used more for verification than primary measurement.

The various depth and length characteristics of the flow were measured by a meter stick marked with both feet and inches and centimeters.

### 3.5 FLOW IN THE BARREL

There are four basic regimes of flow: subcritical-laminar, supercritical-laminar, subcritical-turbulent, and supercritical-turbulent (Chow, 1959). During a hydraulic jump, all four may be encountered at some point along the profile of the flume. A hydraulic jump can only occur in supercritical flow, since a hydraulic jump is defined as a sudden change from supercritical to subcritical flow. Whether a flow is supercritical or subcritical depends on the Froude Number. If the Froude Number is greater than 1, the flow is supercritical. If the Froude Number is less than 1, the flow is subcritical.

In the models for this study, the flow was supercritical-turbulent. The point of interest for the study was what type of jump would develop in the various models if a hydraulic jump were induced.

### 3.6 HYDRAULIC JUMP

There are five categories of hydraulic jump. These are undular jump ( $Fr=1-1.7$ ), weak jump ( $Fr=1.7-2.5$ ), oscillating jump ( $Fr=2.5-4.5$ ), steady jump ( $Fr=4.5-9.0$ ), and strong jump ( $Fr>9.0$ ) (Chow, 1959). The derivation of the Froude Number is shown in the Mathematical Considerations section. For this study, the Froude Number ranged from 1.7-4.5, meaning the anticipated hydraulic jumps were either weak or oscillating.

In weak jump scenarios, the hydraulic jump could easily be induced by a single, simple obstruction such as a sill the width of the channel (Tyagi, 2011). This sill would induce the jump and the downstream flow would be maintained at the subcritical range ( $Fr<1$ ).

In oscillating jump scenarios, the hydraulic jump could be induced by a single sill; but whenever the induced jump caused the flow to be as deep as the channel a more complex system was many times necessary. Usually, this requires a two sill system to maintain the subcritical flow at the outlet (Tyagi, 2012).

The height of the flow and the inflow Froude Number allow us to begin predicting which hydraulic jump inducement system would be necessary. Table 3.1 below shows the flow parameters for a six foot, twelve foot, eighteen foot, and twenty-four foot culvert drop.



Table 3.1: Parameters for the Four Flow Conditions

| Drop  | H    | Q<br>(cfs) | V <sub>u/s</sub><br>(ft/s) | Y <sub>s</sub><br>(in) | Y <sub>toe</sub><br>(in) | Y <sub>1</sub><br>(in) | Y <sub>d/s</sub><br>(in) | Fr <sub>1</sub> | V <sub>toe</sub><br>(ft/s) | V <sub>1</sub><br>(ft/s) | V <sub>d/s</sub><br>(ft/s) | THL<br>(in) |
|-------|------|------------|----------------------------|------------------------|--------------------------|------------------------|--------------------------|-----------------|----------------------------|--------------------------|----------------------------|-------------|
|       | 0.8d | 1.00       | 2.50                       | 2.50                   | 2.50                     |                        | 2.13                     | 2.23            | 5.79                       | 5.79                     | 6.00                       | 0.71        |
| 6 ft  | 1.0d | 1.31       | 2.70                       | 2.83                   | 3.37                     |                        | 2.63                     | 1.98            | 5.95                       | 5.95                     | 6.42                       | 0.65        |
|       | 1.2d | 1.71       | 2.80                       | 4.13                   | 4.00                     |                        | 3.13                     | 1.83            | 6.00                       | 6.00                     | 6.62                       | 0.97        |
|       | 0.8d | 1.18       | 2.96                       | 2.80                   | 3.02                     | 2.75                   | 2.87                     | 2.80            | 7.59                       | 7.59                     | 7.65                       | 3.46        |
| 12 ft | 1.0d | 1.46       | 2.93                       | 2.62                   | 3.50                     | 3.12                   | 3.12                     | 2.61            | 7.54                       | 7.56                     | 7.85                       | 3.80        |
|       | 1.2d | 1.92       | 3.21                       | 2.20                   | 3.50                     | 3.20                   | 3.50                     | 2.88            | 8.19                       | 8.43                     | 8.27                       | 3.67        |
|       | 0.8d | 0.95       | 2.37                       | 2.12                   | 1.75                     | 1.87                   | 1.87                     | 2.50            |                            | 5.59                     | 8.39                       | 1.65        |
| 18 ft | 1.0d | 1.20       | 2.41                       | 2.63                   | 2.25                     | 1.75                   | 1.75                     | 3.13            |                            | 6.78                     | 8.83                       | 1.60        |
|       | 1.2d | 1.53       | 2.56                       | 3.38                   | 2.28                     | 2.32                   | 2.32                     | 3.09            |                            | 7.71                     | 8.97                       | 1.90        |
|       | 0.8d | 0.77       | 1.93                       | 1.50                   | 1.50                     | 1.50                   | 1.50                     | 3.08            |                            | 6.17                     | 4.20                       | 14.83       |
| 24 ft | 1.0d | 1.25       | 2.50                       | 2.00                   | 2.00                     | 1.80                   | 1.90                     | 3.79            |                            | 8.33                     | 7.00                       | 10.01       |
|       | 1.2d | 1.61       | 2.68                       | 2.40                   | 2.20                     | 2.30                   | 2.30                     | 3.39            |                            | 8.41                     | 7.00                       | 10.65       |

For six foot drop, the Froude Number was between 1.8 and 2.2. This means the anticipated hydraulic jump would be classified as a weak jump. With the short length of the steep section, the flow in this experiment had the lowest velocity observed in the study. Pictures of this experiment with its three flow conditions can be seen in Figures 3.2-3.4.

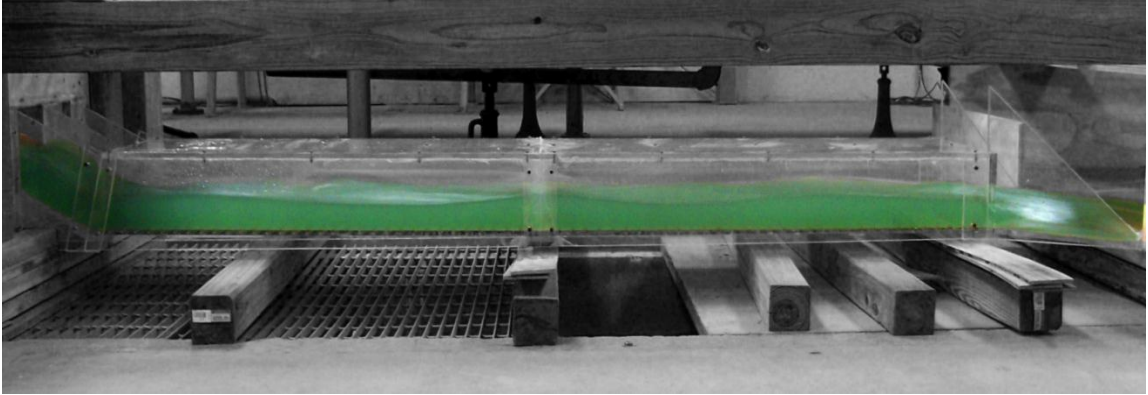


Figure 3.2: 6 Ft Drop A Case

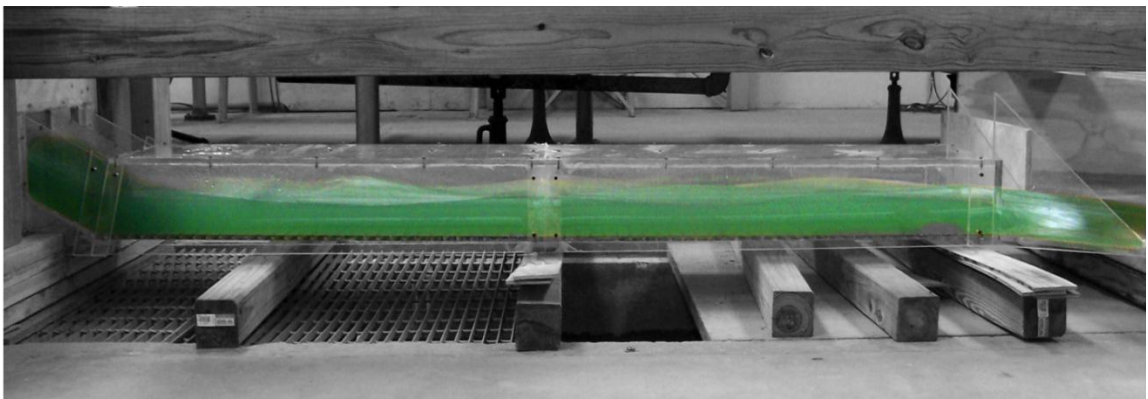


Figure 3.3: 6 Ft Drop B Case

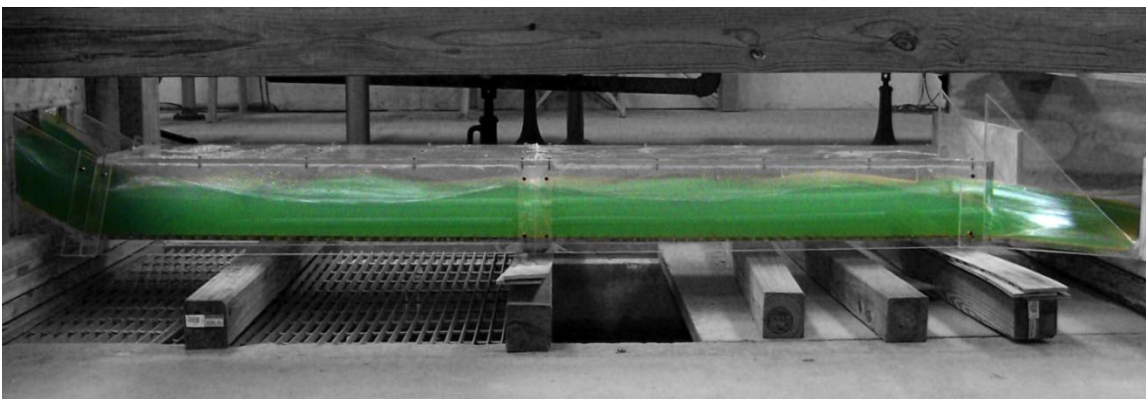


Figure 3.4: 6 Ft Drop C Case

For twelve foot drop, the Froude Number was between 2.6 and 2.9. This means the anticipated hydraulic jump would be classified as a weak jump with some tendency towards oscillating. With the moderate length of the steep section, the flow in this experiment was able to develop some velocity. Pictures of this experiment with its three flow conditions can be seen in Figures 3.5-3.7.

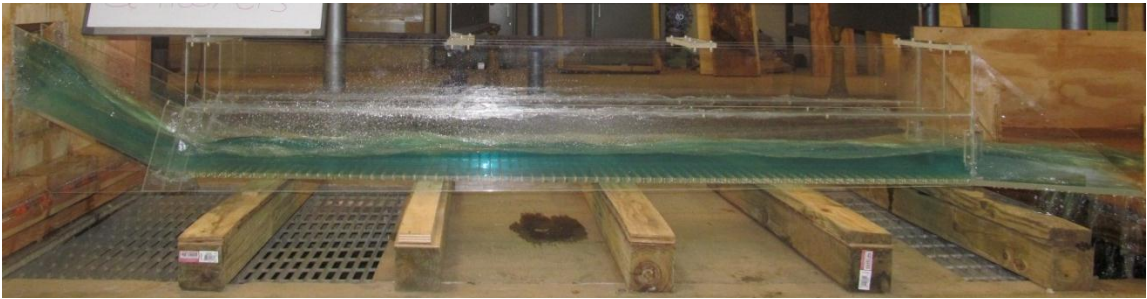


Figure 3.5: 12 Ft Drop A Case

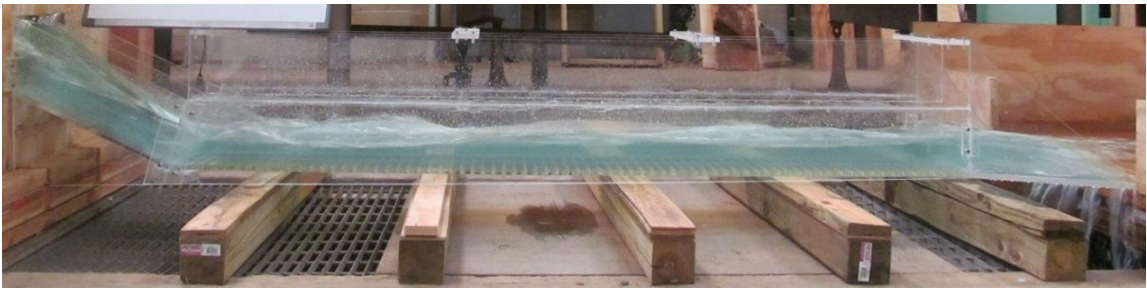


Figure 3.6: 12 Ft Drop B Case

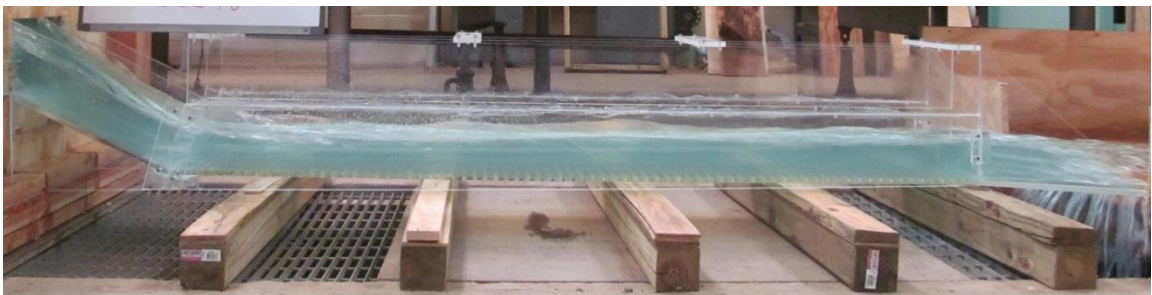


Figure 3.7: 12 Ft Drop C Case

For eighteen foot drop, the Froude Number was between 2.5 and 3.1. This means the anticipated hydraulic jump would be classified as an oscillating jump. With the moderate length of the steep section, the flow in this experiment was at an appreciable velocity similar to the twelve foot drop experiment. Pictures of this experiment with its three flow conditions can be seen in Figures 3.8-3.10.

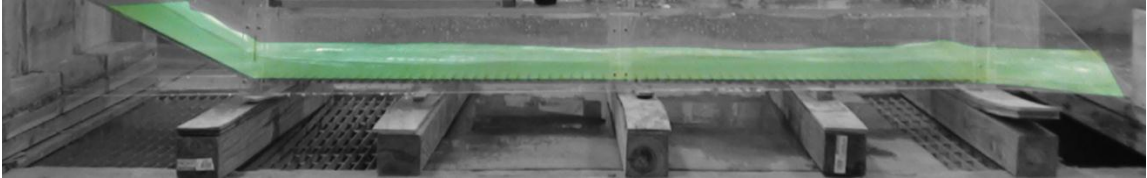


Figure 3.8: 18 Ft Drop A Case

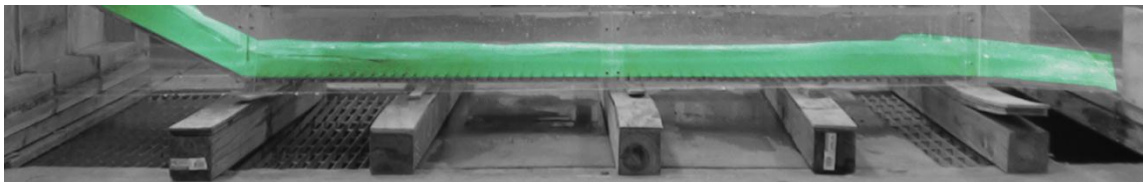


Figure 3.9: 18 Ft Drop B Case

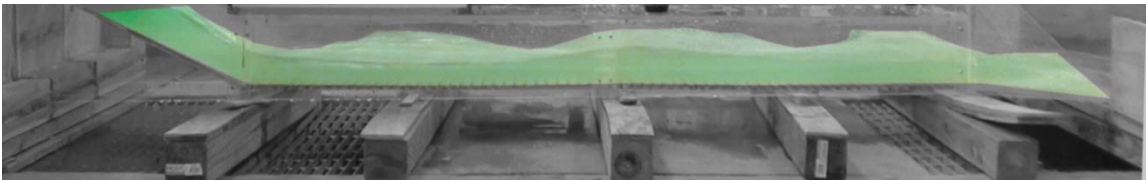


Figure 3.10: 18 Ft Drop C Case

For twenty-four foot drop, the Froude Number was between 3.1 and 3.8. This means the anticipated hydraulic jump would be classified as an oscillating jump. With the long length of the steep section, the velocity in this experiment was consistently the highest observed in this study. Pictures of this experiment with its three flow conditions can be seen in Figures 3.11-3.13.

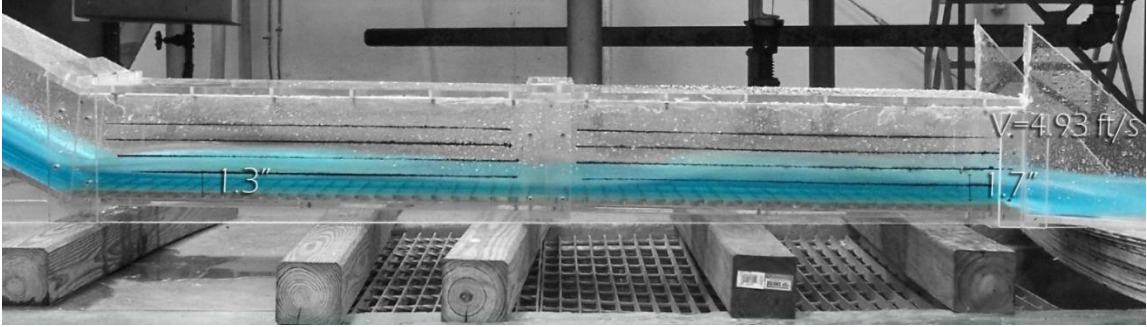


Figure 3.11: 24 Ft Drop A Case

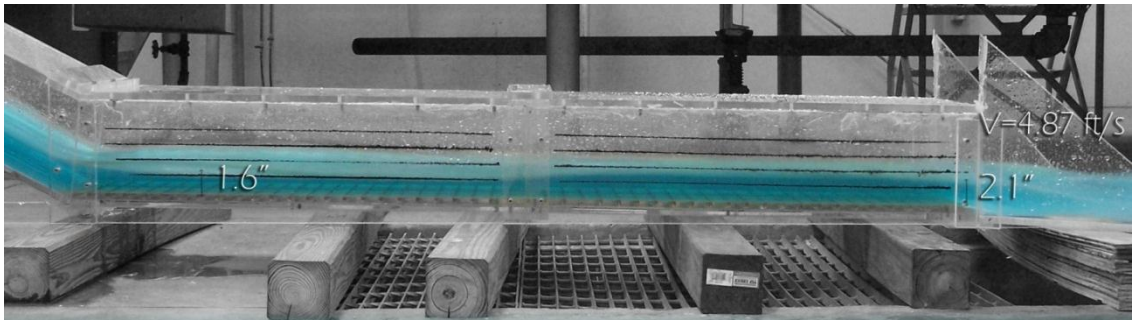


Figure 3.12: 24 Ft Drop B Case

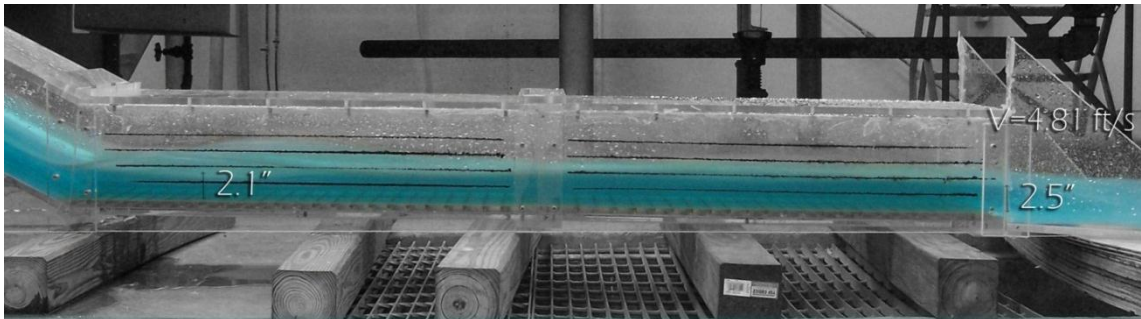


Figure 3.13: 24 Ft Drop C Case

### 3.7 MATHEMATICAL CONSIDERATIONS

#### 3.7.1 FROUDE NUMBER

The Froude Number is defined as velocity of the flow divided by the square root of the acceleration due to gravity times the depth of the flow. As an equation (Chow, 1959):

$$F_{r1} = \frac{V_1}{\sqrt{gY_1}}$$

3.1

The value of the Froude Number shows what kind of hydraulic jump would be expected should it be induced in the culvert.

A Froude Number of 1-1.7 will produce an undular jump, a Froude Number of 1.7-2.5 will produce a weak jump, a Froude Number of 2.5-4.5 will produce an oscillating jump, a Froude Number of 4.5-9.0 will produce a steady jump, and a Froude Number greater than 9.0 will produce a strong jump (Chow, 1959).

The higher the Froude Number, the more energy is dissipated from the jump. This is because more energy must be dissipated at a higher Froude Number to achieve subcritical ( $Fr < 1$ ) flow depth.

### 3.7.2 BERNOULLI EQUATION

The Bernoulli Equation shows the energy present in the culvert. This equation is usually manipulated to compare inflow and outflow scenarios and show the result as percent of energy lost at outflow compared to inflow (Chow, 1959).

The following equation shows the final form of the energy comparison used in this study.

$$\frac{E_2}{E_1} = \frac{(8Fr_1^2 + 1)^{3/2} - 4Fr_1^2 + 1}{8Fr_1^2(2 + Fr_1^2)} \quad 3.2$$

The following equation shows the direct comparison of energies at the inlet and outlet conditions as a difference termed the total head loss.

$$THL = \left( H + \frac{V_{u/s}^2}{2g} + Z \right) - \left( Y_{d/s} + \frac{V_{d/s}^2}{2g} \right) \quad 3.3$$

For the circumstances of this paper, these equations will only show the channel losses of the flow, which are not enough to induce the hydraulic jump and bring the Froude Number to less than one. As experiments that attempt to induce hydraulic jump are conducted in the four channels, these equations become very informative about the jump formed and the energy it dissipates.

### 3.8 DISCUSSION OF RESULTS

All the flow conditions fit into two of the five categories of hydraulic jump, should it be induced: weak jump or oscillating jump. The six and twelve foot drop culverts have Froude Numbers indicative of weak jump, while the twelve, eighteen and twenty-four foot drops have Froude Numbers indicative of oscillating jump.

When the jump is induced the measured height of the jump versus the height of the channel is important to consider. This is shown in the oscillating jumps where if the hydraulic jump becomes confined it is many times necessary to use a two sill system to achieve optimum energy dissipation. When the jump is confined the flow will produce pressure against the ceiling of the culvert. This is likely to happen in standard broken-back culverts with a ceiling height of ten feet.

### 3.9 CONCLUSION

The following conclusions can be made from this information:

- 1) All inflow conditions for the models of interest to this study can be classified as supercritical-turbulent flow.
- 2) For six foot drop broken-back culverts the Froude Number ranges from 1.8 to 2.2 which classifies the induced jump as a weak jump.
- 3) For twelve foot drop broken-back culverts the Froude Number ranges from 2.6 to 2.9 which classifies the induced jump as a weak jump with oscillating jump being seen in some of the higher flow conditions.
- 4) For eighteen foot drop broken-back culverts the Froude Number ranges from 2.5 to 3.1 which classifies the induced jump as an oscillating jump.
- 5) For twenty-four foot drop broken-back culverts the Froude Number ranges from 3.1 to 3.8 which classifies the induced jump as an oscillating jump.

### 3.10 ACKNOWLEDGMENTS

This project was funded by the Federal Highway Administration and sponsored by the Oklahoma Department of Transportation. We would like to thank Mr. Bob Rusch, P.E., Bridge Division Engineer, Oklahoma Department of Transportation for his active participation in incorporating ideas to make this research more practical to field conditions.

In addition, Dr. Greg Hanson, P.E., Dr. Sherry Hunt, Raymond Cox and Kem Kadavy, P.E., Hydraulic Engineers of the U.S. Department of Agriculture, Agricultural Research Service each contributed their ideas in the early stages of this project regarding ways to improve physical construction of the model.

### 3.11 REFERENCES

- Campbell C. S. and others (1985). Flow Regimes in Inclined Open-Channel Flows of Granular Materials. Powder Technology. Elsevier Sequoia.
- Chanson, H. (1996). Free-Surface Flows with Near-Critical Flow Conditions. Canadian Journal of Civil Engineering. CSCE.
- Chow, V.T. (1959). Open-channel Hydraulics. McGraw-Hill, New York, NY, 680 pages.
- Moawad, A. and others (1994). Hydraulic Loading in Culvert Inlets. Canadian Journal of Civil Engineering. CSCE.
- Nettleton, Peter and McCorquodale, John (1989). Radial Flow Stilling Basins with Baffle Blocks. Canadian Journal of Civil Engineering. CSCE.
- Pegram, Geoffry and others (1999). Hydraulics of Skimming Flow on Modeled Stepped Spillways. Journal of Hydraulic Engineering. ASCE.



- Smith, C. D. and Oak, A. G. (1994). Culvert Inlet Efficiency. Canadian Journal of Civil Engineering. CSCE.
- SonTek/YSI, Inc. ADVField/Hydra System Manual (2001).
- Stahl, Helmut and Hager, Willi (1998). Hydraulic Jump in Circular Pipes. Canadian Journal of Civil Engineering. CSCE.
- Tyagi, A.K., Al-Madhhachi, A., and Brown, J. (2010b). Energy Dissipation in Broken-back Culverts under Pressure Flow Conditions. ASCE, Journal Hydraulic Engineering. (submitted for peer review).
- Tyagi, A.K., et al., (2009). “Laboratory Modeling of Energy Dissipation in Broken-back Culverts – Phase I,” Oklahoma Transportation Center, Oklahoma, 82 pp.
- Tyagi, A.K., et al., (2011). “Laboratory Modeling of Energy Dissipation in Broken-back Culverts – Phase II,” Oklahoma Transportation Center, Oklahoma, 80 pp.
- Tyagi, A.K., et al., (2012). Energy Dissipation in Six-Foot Drop Broken Back Culverts under Open Channel Conditions. 5th International Perspective on Water Resources and the Environment Conference, Marrakech, Morocco.
- Tyagi, A.K., Johnson, N. and Ali, A. (2013). Energy Dissipation in 24-foot Drop Broken Back Culverts under Open Channel Conditions. ASCE, Journal Hydraulic Engineering. (Submitted for peer review)
- Tyagi, A.K., Johnson, N. and Ali, A. (2013). Energy Dissipation in Six-Foot Drop Broken Back Culverts under Open Channel Conditions. Journal Hydraulic Engineering. ASCE. (Submitted for peer review)

Tyagi, A. K. and Schwarz, B. (2002). A Prioritizing Methodology for Scour-critical Culverts in Oklahoma. Oklahoma Transportation Center. Oklahoma, 13 pp.

## CHAPTER IV

### ENERGY DISSIPATION IN EIGHTEEN-FOOT DROP BROKEN-BACK CULVERTS UNDER OPEN CHANNEL FLOW CONDITIONS

#### 4.1 ABSTRACT

This paper investigates reduction in degradation downstream of broken-back culverts by forming a hydraulic jump. A model was built in the laboratory focusing on a drop between inlet and outlet of 18 feet. Three flow conditions simulated included 0.8, 1.0 and 1.2 times the culvert depth.

The hydraulic jump created in the culvert is classified as an “oscillating jump.” To locate the jump near the toe, different sill and friction block arrangements were tested. The prototype was 150 feet long. In the broken-back culvert, a slope of 1 (vertical) to 2 (horizontal) was used for ease of construction, with the flat part at a one percent slope. The best option to maximize energy dissipation is to use one 5 foot sill located 43 feet from the outlet. The length of the culvert can be reduced by 40 feet. The calculated energy dissipation of the culvert was 66 percent.

Keywords: Hydraulic jump, energy dissipation, Broken-back culvert, sill, friction block. 18-foot drop

#### 4.2 INTRODUCTION

There are 121 scour-critical culverts on the Interstate System (ISTAT), the National Highway System (NHS), and the State Transportation Program (STP) in Oklahoma according to a research

study conducted by the Oklahoma Transportation Center at Oklahoma State University (Tyagi, 2002). The average replacement cost of these culverts is about \$121M. A survey of culverts in Oklahoma indicates that the drop in flowline between upstream and downstream ends ranges between 6 and 24 feet (Rusch, 2008). In this research, a drop of 18 feet was used in the laboratory model. Advantages of this research are to maximize the energy loss within the culvert, thus minimizing the scour around the culvert and decreasing the degradation downstream in the channel. This reduces the construction and rehabilitation costs of culverts.

The hydraulic jump is a natural phenomenon produced by a sudden rise in water level due to change from supercritical flow to subcritical flow, that is, when there is a sudden decrease in velocity of the flow. This sudden change in the velocity causes the considerable turbulence and loss of energy. Consequently, hydraulic jump in broken-back culverts is generally used as an energy dissipater, and it has been recognized as an effective method for many years. Several investigators have studied hydraulic jump on culvert sloping aprons, Hotchkiss et al. (2005), Tyagi et al. (2010), and others have created expressions for jumps on sloping open rectangular channel [ (Li (1995), Husain et al. (1994), Sholichin and Akib (2010), Demetriou, and Dimitriou, (2008)].

Li (1995) studied how to find the location and length of the hydraulic jump in  $1^\circ$  through  $5^\circ$  slopes of rectangular channels. He did many experiments on laboratory models to get the relationship between upstream flow Froude number and ratio of jump length and sequent depth after jump  $L/y_2$ . Li used the HEC-2 software to locate the heel of a hydraulic jump to get the length of the jump and toe of the jump. The scale between the models and the prototypes was 1:65. Researcher concluded that estimation of sequent depth for a hydraulic jump had to take the channel bed slope into account if the bed slope was greater than  $3^\circ$ , and  $y_2/y_1$ , and  $F_{r1}$ , had a linear relation and could be used to estimate the sequent depth. Li recommended some rules such as using a solid triangular sill which could be arranged at the end of the basin apron to lift the

water and reduce the scour from the leaving flow, and if the  $F_{r1}$  ranged between 4.5 and 9, the tailwater depth was lowered by 5% of the sequent water depth.

Demetriou and Dimitriou (2008) carried out many Laboratory experiments to measure the energy loss efficiency in hydraulic jump within sloped rectangular open channels. The authors used channel inclination angles  $\phi$  between  $2^\circ$  and  $16^\circ$ , and the Froude numbers,  $F_{r1}$ , ranged between 2 and 16. The authors concluded that the dimensionless energy loss was increasing with  $F_{r1}$  for  $\phi$ =constant, while for  $F_{r1}$  =constant this relative energy loss was also increasing with angle  $\phi$ .

Husain et al. (1994) performed many experiments on the sloping floor of open rectangular channels with negative and positive step to predict the length and depth of hydraulic jump and to analyze the sequent depth ratio. They found that the negative step has advantages over the positive with respect to stability and compactness of hydraulic jump. They developed a set of non-dimensional equations in terms of profile coefficient, and they used multiple linear regression analysis on jumps with and without a step. In Froude Numbers between 4 and 12 and slope,  $S$ , between 1 and 10, the length and sequent depth ratio can accurately be predicted.

Numerous studies have examined the characteristics of the hydraulic jump. Bhutto et al. (1989) provided analytical solutions for computing sequent depth and relative energy loss for free hydraulic jump in horizontal and sloping rectangular channels from their experimental studies. They used the ratio of jump length to jump depth and the Froude number to compute the length of free jump on a horizontal bed. Jump factor and shape factor were evaluated experimentally for free jump on a sloping bed. To check the efficiency of the equations, they made comparisons with previous solutions by other researchers and found that the equations they derived could be used instead of previous solutions.

Defina and Susin (2003) investigated the stability of a stationary hydraulic jump situated over sloping topography in a rectangular channel of uniform width with assuming inviscid flow

conditions. On steep slope flow, it was found that hydraulic jump is unstable and if the jump is slightly displaced from its stationary point, it will move further away in the same direction. In the channel with adverse slope, they indicated that a stationary jump can be produced. They calculated the ratio of bed to friction slope such as energy dissipation per unit weight and unit length, and the result was quite large. They found that the actual equilibrium state is weakly perturbed when the theoretical stability condition was imposed by forcing the speed adopted by the jump.

Beirami and Chamani (2006) studied a large variety of hydraulic jumps on horizontal and end sloping ogee standard weirs, which were used to create supercritical flow and slopes of 0.0, -0.025, -0.05, -0.075, and -0.1 to build downstream of the weir. They presented a method to predict the sequent depth ratio that agreed with the results of investigations. Researchers observed that the gravity force component in the jump was opposite to the flow direction, the water surface of the surface roller became undular and unstable. It was found that the negative slope of the basin reduced the sequent depth ratio, whereas a positive slope increased the sequent ratio.

Beirami and Chamani (2010) reported that the energy loss in the classical jump is greater than that in any jump forming on negative or positive slopes.

Hartner et al. (2003) stated that the characteristics of the hydraulic jump depend on Froude number ( $F_{r1}$ ). They added that in order for the hydraulic jump to occur, the flow must be supercritical, i.e. a jump can occur only when the Froude number is greater than 1.0. The hydraulic jump is classified according to its Froude number. When  $F_{r1}$  is between 1.7 and 2.5, the flow is classified as a weak jump: the rise in the water surface will be smooth with less energy dissipation. A  $F_{r1}$  between 2.5 and 4.5 results in an oscillating jump with 15-45% energy dissipation. A steady jump will occur when  $F_{r1}$  ranges from 4.5 to 9.0 and results in energy dissipation from 45% to 70%. When  $F_{r1}$  is above 9.0, a strong jump will occur with energy losses ranging from 70% to 85%.

Hotchkiss et al. (2005) proposed that by controlling the water at the outlet of a culvert, water scour around the culvert can be reduced. The effectiveness of a simple weir near the culvert outlet is compared to that of a culvert having a weir with a drop upstream in the culvert barrel. These two designs are intended to reduce the specific energy of the water at the outlet by inducing a hydraulic jump within the culvert barrel, without the aid of tailwater. The design procedure was proposed after studying the geometry and effectiveness of each jump type in energy reduction. In their research, they found the Froude number ranged from 2.6 to 6.0. It was determined that both outlet forms are effective in reducing the velocity of water and hence the energy and momentum.

Hydraulic Design of Energy Dissipators for Culverts and Channels (2006), from the Federal Highway Administration, provided design information for analyzing and mitigating problems associated with the energy dissipation at culvert outlets and in open channels. It recommends the use of the broken-back culvert design considering it as an internal energy dissipator. The proposed design for a broken-back culvert is limited to the following conditions:

- 1) The slope of the steep section must be less than or equal to 1.4:1 (V: H).
- 2) The hydraulic jump must be completed within the culvert barrel.

The goal of this research was to observe in physical experiments the efficiency of hydraulic jump on broken-back culverts with and without friction blocks between upstream and downstream ends of the culvert and the location of hydraulic jump from the toe of the drop in the culvert. A model was constructed to represent a prototype of a broken-back culvert with a vertical drop of 18 feet. Three different flow conditions were simulated for 0.8, 1.0 and 1.2 times the hydraulic head in the scale model (Tyagi et al., 2009).

#### 4.3 LABORATORY MODEL

The experiments were conducted at the USDA Hydraulic Laboratory, in a prototype representing a 150 foot long broken-back culvert with two barrels 10 x 20 feet and a vertical drop of 18 feet.

The 1 to 20 scale was adopted due to space limitations, and in consideration of the potential need to expand the model depending on where the hydraulic jump occurred. The scale model contains 2 barrels with dimensions of 6 inches wide by 12 inches high and the length of 68.4 inches which represented the open channel flow condition as shown in Figures 4.1 through 4.7. At the upstream end, a reservoir collects the flow discharge. Supercritical inflow is enforced by a steep sloped flume section with a 1 to 2 slope, which has horizontal length of 21.6 inches. At the downstream end of the flume an expansion of the flow section by a wingwall further reduces the downstream velocity. The location of the hydraulic jump is simply controlled by the discharge rate upstream and the sill and friction block location.

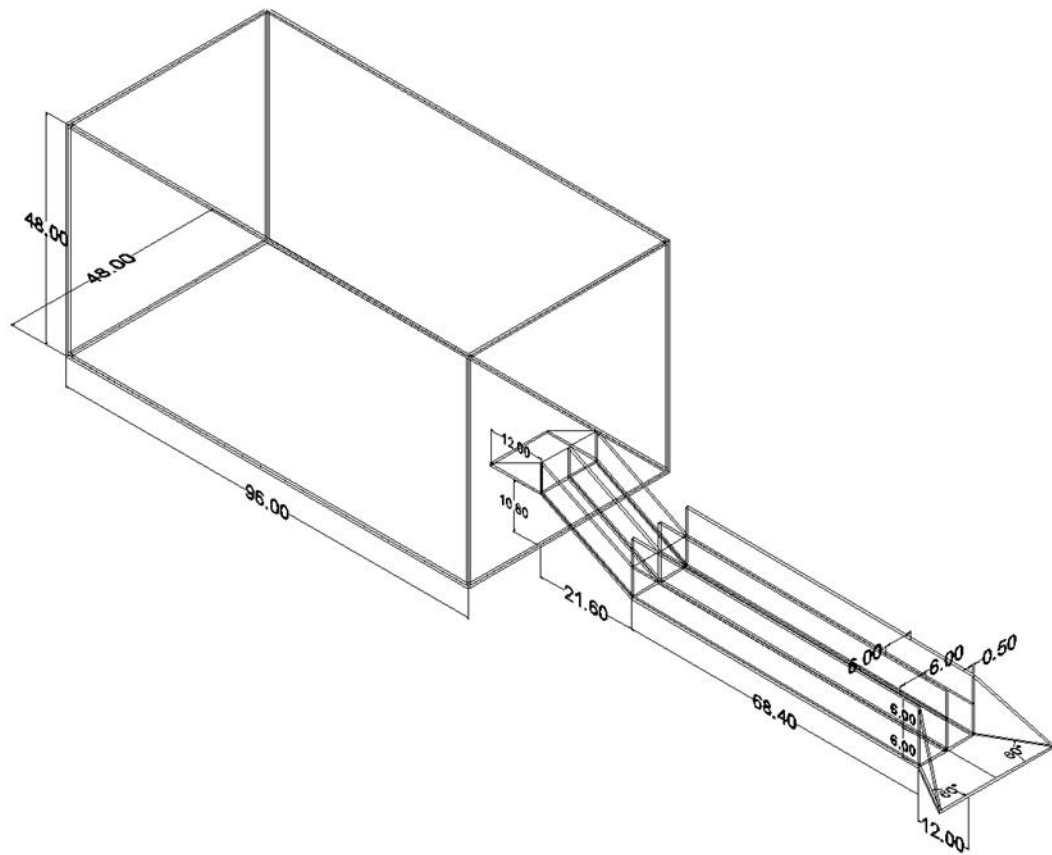


Figure 4.1: Open Channel Flow Conditions Model Isometric



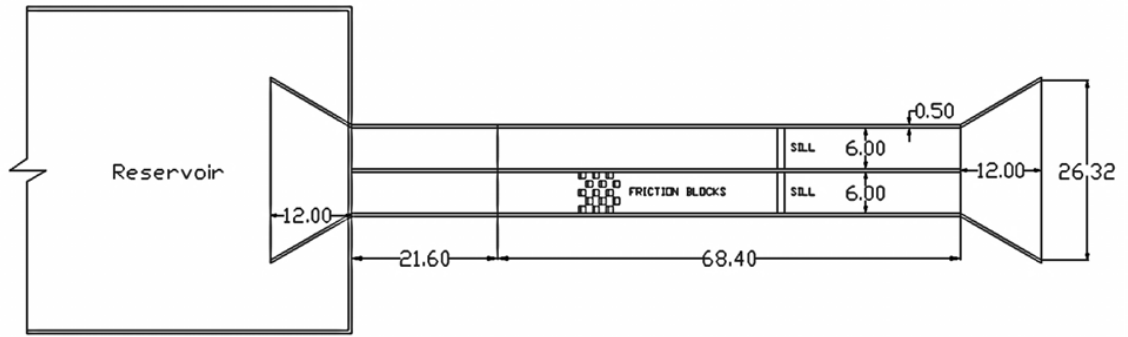


Figure 4.2: Plan View of Model

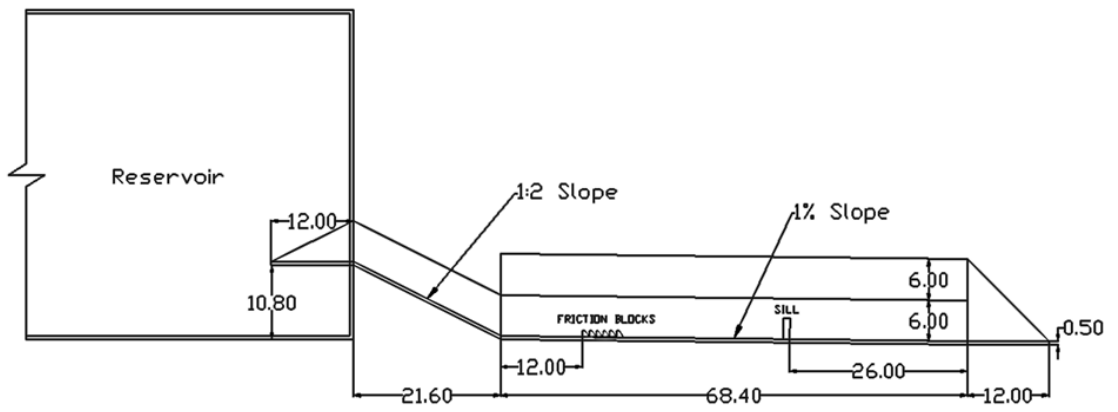


Figure 4.3: Profile View of 1% Slope Model

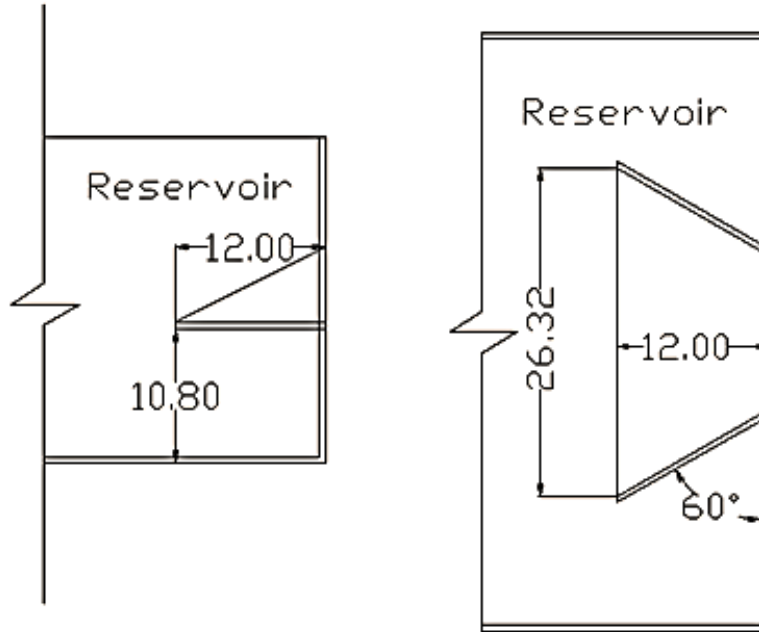


Figure 4.4: Profile and Plan View of Reservoir Inlet (Upstream)

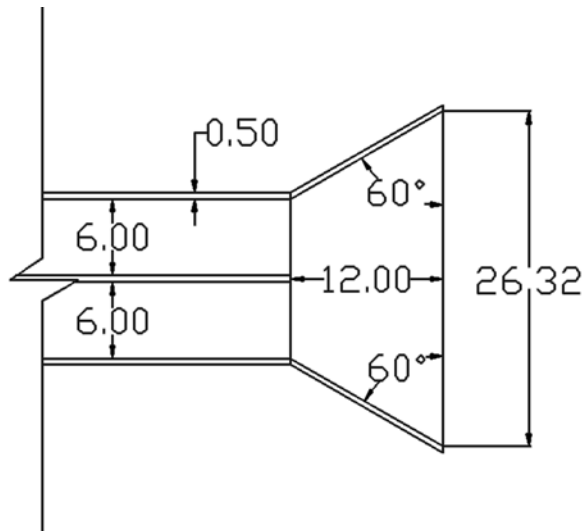


Figure 4.5: Plan View of Culvert Outlet (Downstream)

Plexiglas<sup>®</sup> was used for the flume because it offered visibility as well as durability, and a surface which would more closely simulate the surface of the concrete being modeled (see Figures 4.6 and 4.7). The thickness of the Plexiglas was decided based on weight, rigidity, workability, and ease with which the material would fit into scale. Half-inch Plexiglas proved to be sturdy and was

thick enough to allow connection hardware to be installed in the edges of the plates. This material also fit well into the proposed scale of 1 to 20 which equated one-half inch in the model with one foot in the prototype. The construction methods included creating sections of the model at Oklahoma State University and assembling them at the test facility.

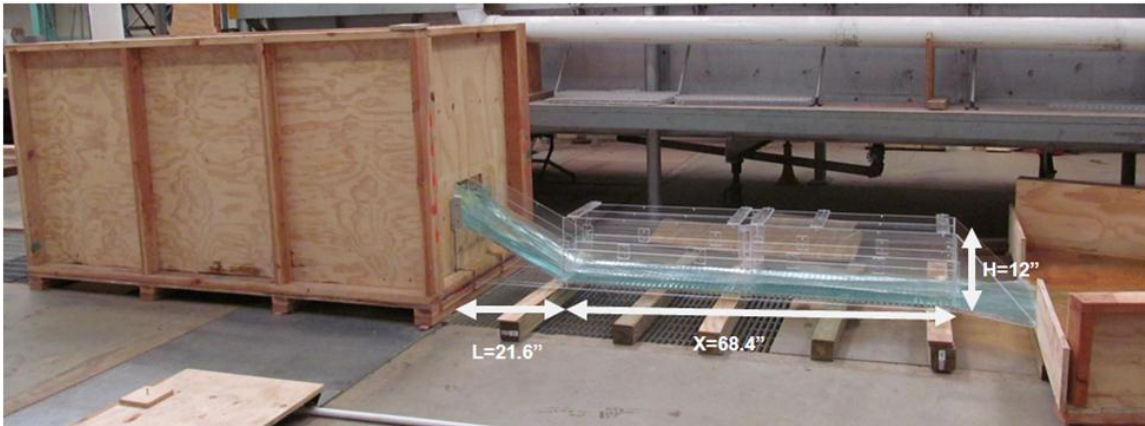


Figure 4.6: Side View of Laboratory Model



Figure 4.7: Front View of Laboratory Model

In addition to the Plexiglas<sup>®</sup> model of the culvert, a reservoir was constructed upstream of the model to collect and calm the fluid entering the model. The reservoir was constructed with plywood because it was not necessary to observe the behavior of the fluid at that stage. Within the reservoir, wing walls at an angle of 60 degrees were constructed to channel flow into the model opening. The base of the wing walls was constructed with plywood and the exposed wing wall models were formed with Plexiglas. The same design was used for the outlet structure of the culvert.

The objective of the test was to determine the effect of sill and friction blocks on the hydraulic jump within the prototype, thus the model was constructed so that different arrangements of sills and friction blocks could be placed and observed (see Figures 4.8, 4.9, and 4.10). Different

heights of sills and flat-faced friction blocks (FFB) were mounted in different configurations on a sheet of Plexiglas the same width as the barrels, and placed in the barrel. Many flat-faced friction blocks (FFB) were examined after testing the efficiency.

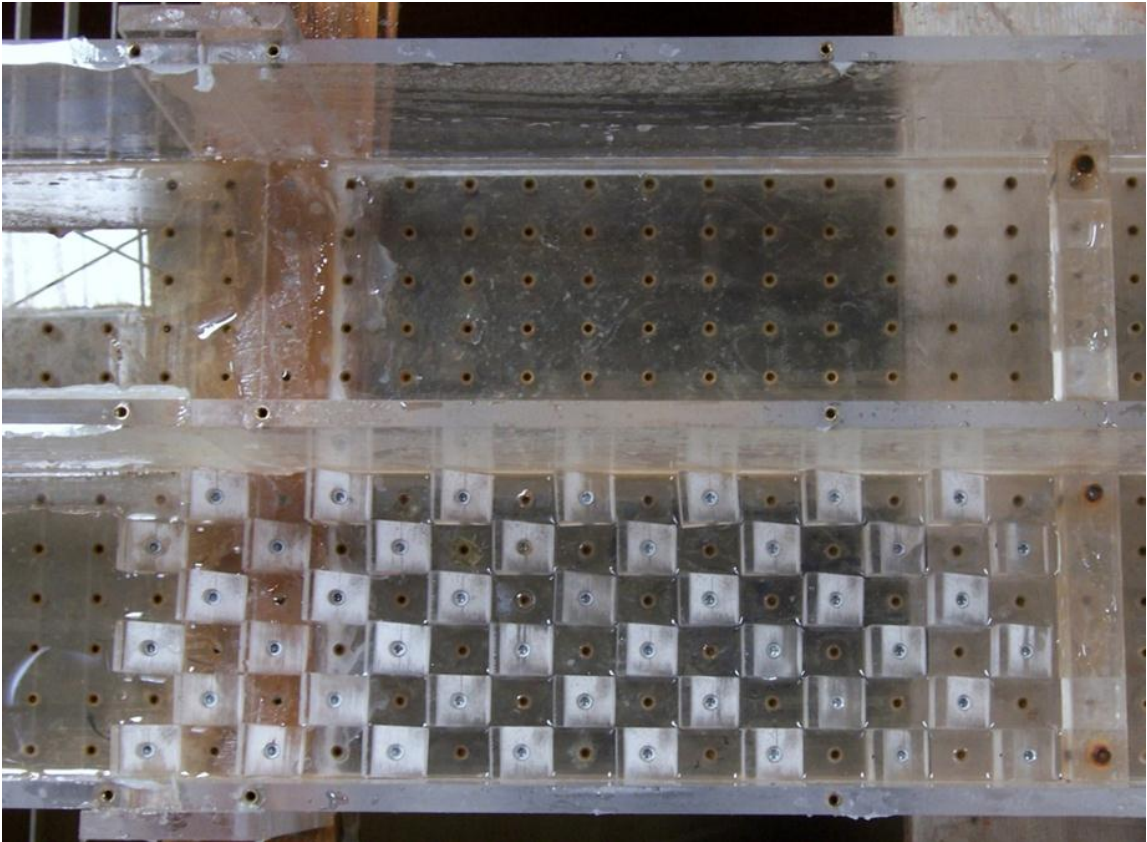


Figure 4.8: Example of Sill and Friction Block Configuration

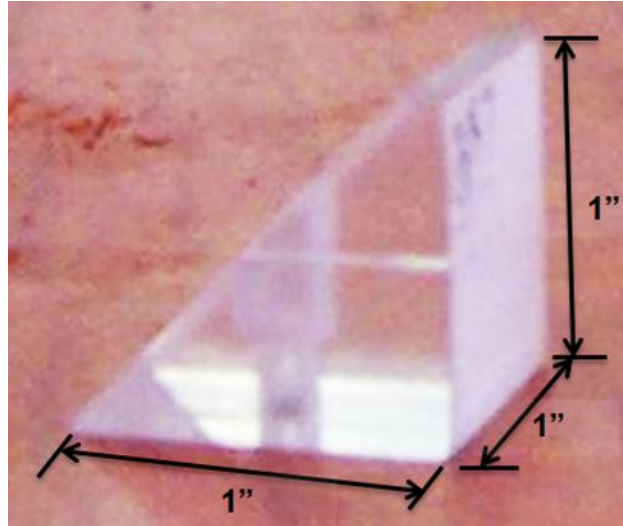


Figure 4.9: Example of Friction Block



Figure 4.10: Typical Sill Dimensions

#### 4.4 DATA COLLECTION AND ANALYSIS

Many experiments were conducted to create energy dissipation within a broken-back culvert. A total of 8 experiments were conducted for this model with variations in length, height, width, and energy dissipaters used. Each experiment tested three scenarios. They were run with upstream heads of  $0.8d$ ,  $1.0d$ , and  $1.2d$  with each depth denoted by A, B, or C, respectively. For example, 5A represents the 5<sup>th</sup> experiment run at  $0.8d$ , 5B represents the 5<sup>th</sup> experiment run at  $1.0d$ , and 5C

represents the 5<sup>th</sup> experiment run at 1.2d. A SonTek side looking 16 Mhz micro-Acoustic Doppler Velocimeter (ADV) was used to measure the velocity at the intake of the structure, after the hydraulic jump, and at the downstream end of the culvert (SonTek/YSI, 2001 and Chanson, 2008). In regions of high velocity and low flow depth (supercritical regime) the ADV does not produce reliable measurement due to wake formation around the emitter and receptors. A Pitot tube was used to measure velocity at these regions. The flow rates for all experiments were measured and used to calculate the velocity at the intake of the structure.

Experiment 1 was performed to investigate the possibility of a hydraulic jump occurring without friction blocks or sills. Different sill heights were used in the experiments. Experiments 2 through 4 were performed with 2, 3, 3.5, and 5-inch sill heights located at the end of the culvert. The reason for increasing the sill heights was to produce a hydraulic jump and try to locate it at the toe of the sloped channel in order to maintain subcritical flow throughout the flat section of the broken-back culvert. In order to get the optimal location of the hydraulic jump with a lower possible sill height, the sill was moved toward the center of the culvert. Therefore Experiment 5 was performed with a 3 inch height sill at 26 inches from the end of the culvert. Once these experiments were chosen as a possible solution, further investigation of energy dissipation was necessary. Different configurations and numbers of friction blocks were utilized in the same sill arrangement. Experiment 6 was performed with fifteen regular flat faced friction blocks.

Five experiments were selected from eight experiments performed in the hydraulic laboratory. These experiments show the model runs without friction blocks, the effect of sills at the end of the model, and with 15, 30, and 45 flat-faced friction blocks. After the effectiveness was evaluated, the number of blocks that showed the best results was 15 blocks.

The total head loss between upstream of structure and downstream of structure was calculated by applying the Bernoulli equation:

$$THL = \left( H + \frac{V_{u/s}^2}{2g} + Z \right) - \left( Y_{d/s} + \frac{V_{d/s}^2}{2g} \right) \quad 4.1$$

Where THL = Total head loss, inches

H = Water depth upstream of the culvert, inches

Z = Drop between upstream and downstream the model was 0.90 feet, representing an 18-foot drop in the prototype.

The loss of energy or energy dissipation in the jump was calculated by taking the difference between the specific energy before the jump and after the jump

$$\Delta E = E_1 - E_2 = \frac{(Y_2 - Y_1)^3}{4Y_1 Y_2} \quad 4.2$$

The efficiency of the jump was calculated by taking the ratio of the specific energy before and after the jump:

$$\frac{E_2}{E_1} = \frac{(8Fr_1^2 + 1)^{3/2} - 4Fr_1^2 + 1}{8Fr_1^2(2 + Fr_1^2)} \quad 4.3$$

The following equation was used to calculate the Froude number ( $F_{r1}$ ) of the hydraulic jump:

$$F_{r1} = \frac{V_1}{\sqrt{gY_1}} \quad 4.4$$

#### 4.5 RESULTS

After careful evaluation, Experiments 1, 5, and 6 were selected from the data analysis portion for an open channel flow conditions. These experiments were selected by examining many factors, including their relatively low downstream velocities, high total hydraulic head losses, acceptable hydraulic jump efficiency, and possible reduction in channel length. These variables are explained in the notation section. These experiments have similar sill arrangements for



Experiments 5 and 6, which consist of a 3-inch sill at 26 inches from the end of the culvert, but Experiment 6 has 15 flat faced friction blocks added. However, Experiment 1 did not have any sills or friction blocks. It was found that these experiments yielded results most applicable to the new construction of culverts due to the increased ceiling height of the culvert. The culvert barrel could be reduced by removing a section at the outlet of the channel where the water surface profile is more uniform.

Experiment 1 was run without any energy dissipation devices in order to evaluate the hydraulic characteristics of the model, including the Froude number and supercritical flow conditions. This experiment did not produce a hydraulic jump for any of the three cases tested as shown in Figures 4.11, 4.12, and 4.13. The results can be found in Table 4.1, below.

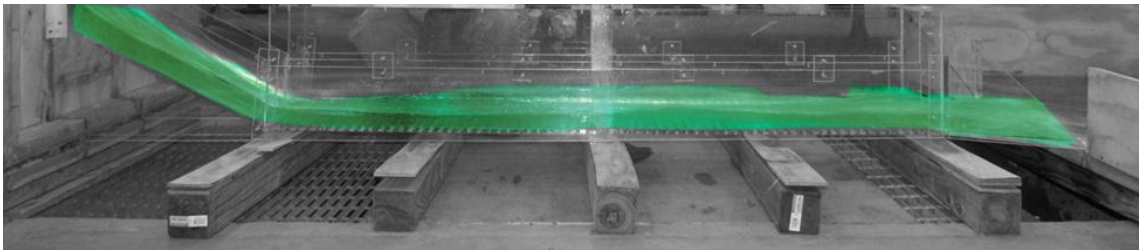


Figure 4.11: Experiment 1A with No Sill or Friction Blocks

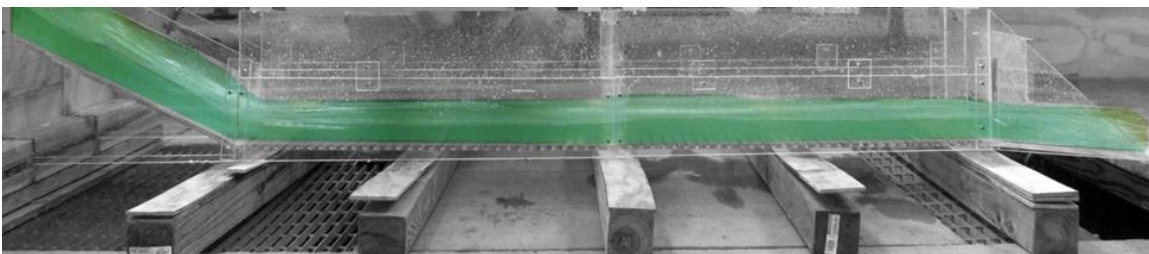


Figure 4.12: Experiment 1B with No Sill or Friction Blocks

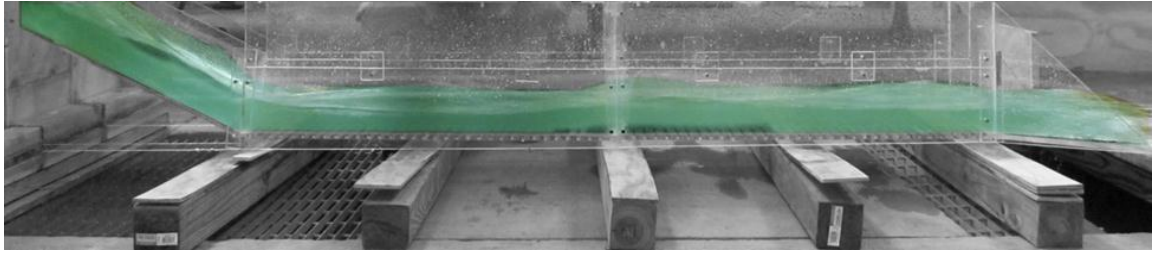


Figure 4.13: Experiment 1C with No Sill or Friction Blocks

Table 4.1: Hydraulic Parameters for Experiment 1.

| CASE            | 0.8d (A) | 1.0d (B) | 1.2d (C) |
|-----------------|----------|----------|----------|
| Q (cfs)         | 0.9481   | 1.2038   | 1.5352   |
| $V_{w/s}$ (fps) | 2.3703   | 2.4076   | 2.5587   |
| $Y_s$ (in)      | 2.12     | 2.63     | 3.38     |
| $Y_t$ (in)      | 1.75     | 2.25     | 2.28     |
| $Y_1$ (in)      | 1.87     | 1.75     | 2.32     |
| $Y_{d/s}$ (in)  | 1.87     | 1.75     | 2.32     |
| $F_{r1}$        | 2.50     | 3.13     | 3.09     |
| $V_1$ (fps)     | 7.7418   | 8.0328   | 8.2241   |

Experiment 5 was run with a 3-inch sill at 26 inches from the end of the culvert utilizing the increased culvert height of 12 inches. A hydraulic jump was observed in all three flow conditions. The results show that the Froude number values ranged from 3.20 to 3.70. This range of Froude number values is indicative of an oscillating type of hydraulic jump. In an oscillating jump, a cyclic jet of water enters the bottom of the jump and then rises to the water surface and back again with no periodicity in cycles as shown in Figures 4.14, 4.15, and 4.16. The energy loss due to hydraulic jump ranges between 3.25 inches to 5.28 inches and the total head loss for the whole culvert ranges between 8.40 inches to 9.70 inches. Additional results can be seen in Table 4.2.

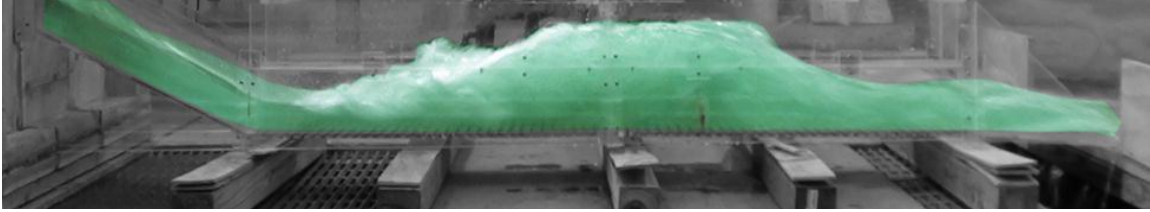


Figure 4.14: Experiment 5A with a 3" Sill at 26" from the End of the Culvert

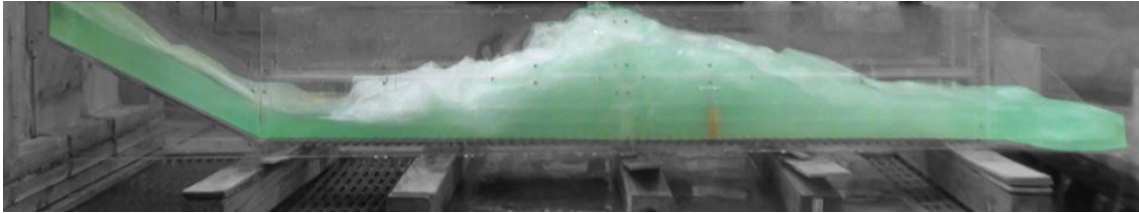


Figure 4.15: Experiment 5B with a 3" Sill at 26" from the End of the Culvert

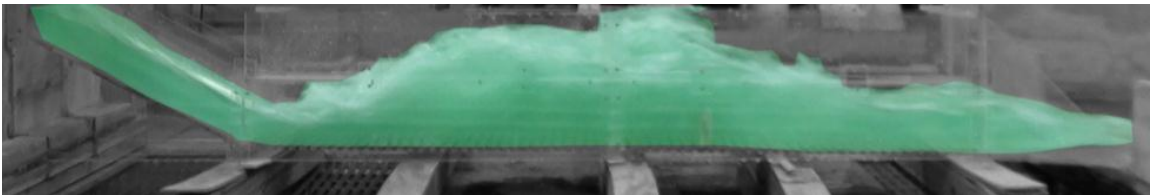


Figure 4.16: Experiment 5C with a 3" Sill at 26" from the End of the Culvert

Table 4.2: Hydraulic Parameters for Experiment 5

| CASE                             | 0.8d (A) | 1.0d (B) | 1.2d (C) |
|----------------------------------|----------|----------|----------|
| Q (cfs)                          | 0.9354   | 1.2838   | 1.5404   |
| $V_{w/s}$ (fps)                  | 2.3385   | 2.5676   | 2.5673   |
| $Y_s$ (in)                       | 2.25     | 2.50     | 3.50     |
| $Y_t$ (in)                       | 1.65     | 1.85     | 2.50     |
| $Y_1$ (in)                       | 1.65     | 2.00     | 2.35     |
| $Y_2$ (in)                       | 7.05     | 8.25     | 9.50     |
| $Y_{d/s}$ (in)                   | 2.25     | 2.75     | 3.75     |
| $F_{r1}$                         | 3.77     | 3.67     | 3.57     |
| $V_{s1}$ (fps)                   | 4.4019   | 5.1118   | 5.4646   |
| $V_{s2}$ (fps)                   | 5.5310   | 7.2333   | 7.5330   |
| $V_1$ (fps)                      | 7.9409   | 8.5118   | 8.9722   |
| $V_2$ (fps)                      | 2.3166   | 3.0646   | 4.0125   |
| $V_{d/s}$ (fps)                  | 4.2572   | 5.6031   | 6.1292   |
| L (in)                           | 17.00    | 20.50    | 21.00    |
| X (in)                           | 42.00    | 42.00    | 42.00    |
| $\Delta E$ (in)                  | 4.0445   | 3.6991   | 4.0932   |
| THL (in)                         | 9.2190   | 9.4284   | 8.4782   |
| $E_2/E_1$                        | 0.6356   | 0.6481   | 0.6613   |
| Prototype Channel Reduction (ft) | 43       | 41       | 40       |

Experiment 6 was run with a 3-inch sill at 26 inches from the end of the culvert with 15 flat-faced friction blocks (FFFB). A hydraulic jump was observed in all three flow conditions as shown in Figures 4.17, 4.18, and 4.19. The results show that the Froude number values ranged from 2.98 to 3.78. These ranges of Froude number values are indicative of an Oscillating type of hydraulic

jump. The energy loss due to hydraulic jump ranges between 1.53 inches to 3.46 inches and the total head loss for the whole culvert ranges between 8.03 inches to 9.60 inches. Additional results can be seen in Table 4.3.

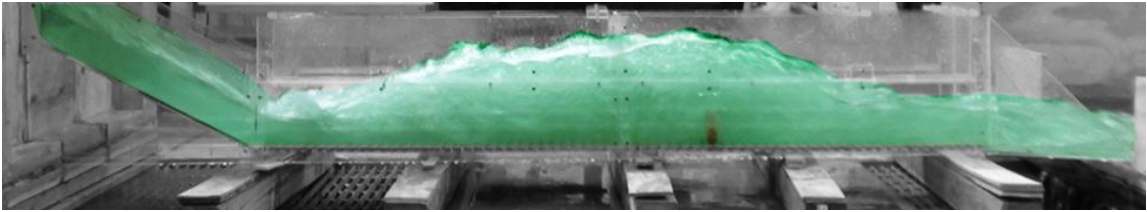


Figure 4.17: Experiment 6A with a 3" Sill at 26" from the End of the Culvert and 15 Flat Faced Friction Blocks

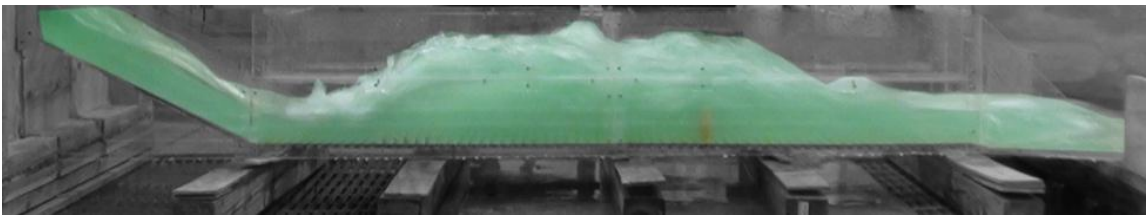


Figure 4.18: Experiment 6B with a 3" Sill at 26" from the End of the Culvert and 15 Flat Faced Friction Blocks

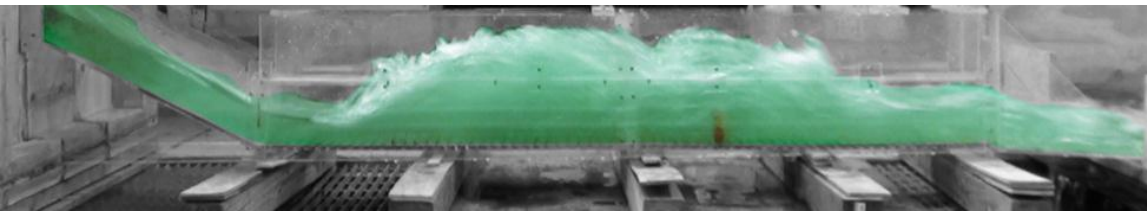


Figure 4.19: Experiment 6C with a 3" Sill at 26" from the End of the Culvert and 15 Flat Faced Friction Blocks

Table 4.3: Hydraulic Parameters for Experiments 6

| CASE                   | 0.8d (A) | 1.0d (B) | 1.2d (C) |
|------------------------|----------|----------|----------|
| Q (cfs)                | 0.9648   | 1.2396   | 1.5430   |
| $V_{w/s}$ (fps)        | 2.4120   | 2.4792   | 2.5717   |
| $Y_s$ (in)             | 2.00     | 2.75     | 3.35     |
| $Y_t$ (in)             | 1.75     | 2.13     | 2.50     |
| $Y_1$ (in)             | 1.75     | 2.13     | 2.35     |
| $Y_2$ (in)             | 6.75     | 7.50     | 8.50     |
| $Y_{d/s}$ (in)         | 2.35     | 2.75     | 3.25     |
| $F_{r1}$               | 3.70     | 3.59     | 3.39     |
| $V_{s1}$ (fps)         | 4.5508   | 4.9115   | 5.4721   |
| $V_{s2}$ (fps)         | 7.0179   | 7.2080   | 5.0467   |
| $V_1$ (fps)            | 8.0250   | 8.5902   | 8.5118   |
| $V_2$ (fps)            | 2.5900   | 3.8417   | 3.6629   |
| $V_{d/s}$ (fps)        | 5.2470   | 5.7356   | 6.1858   |
| L (in)                 | 18.00    | 17.00    | 19.00    |
| X (in)                 | 42.00    | 42.00    | 42.00    |
| $\Delta E$ (in)        | 2.6455   | 2.4234   | 2.9112   |
| THL (in)               | 9.2041   | 9.0653   | 8.8523   |
| $E_2/E_1$              | 0.6445   | 0.6568   | 0.6861   |
| Channel Reduction (ft) | 43       | 41       | 40       |

#### 4.6 CONCLUSION

A laboratory model was constructed to represent a broken-back culvert. The idealized prototype contains a 1 (vertical) to 2 (horizontal) slope, a 36-foot horizontal length of the steep part of the culvert continuing down to a 114-foot mild section. The mild section is built with a slope of 1

percent. The model was made to 1:20 scale. The following dimensions are in terms of the prototype culvert. It was noted that the current practice of not using any energy dissipaters (as in Experiment 1) allowed all the energy to flow through the culvert instead of reducing or dissipating it. The following conclusions can be drawn based on the laboratory experiments for open channel flow conditions:

1. For new culvert construction, Experiment 5 is the best option for open channel flow conditions. This option includes one sill with two small orifices at the bottom for draining the culvert completely located 43 feet from the end of the culvert. The height of the culvert should be at least 16 feet to allow open channel condition in the culvert.
2. If one sill 5.0 feet high is placed in the flat part of the culvert, it results in 66 percent of energy dissipation as seen in Experiment 5C and Figures 4.20 and 4.21.

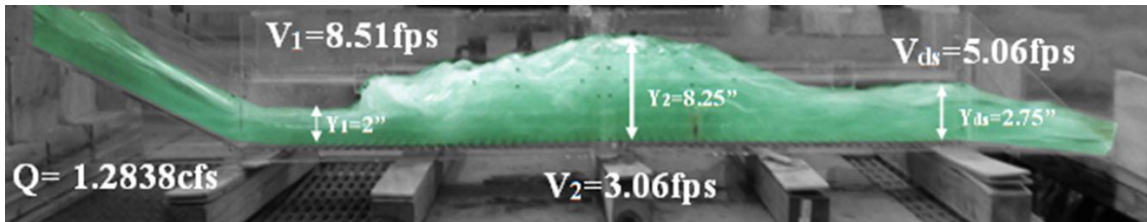


Figure 4.20: Hydraulic Jump Characteristics for Experiment 5B. 1% slope, 1.0d

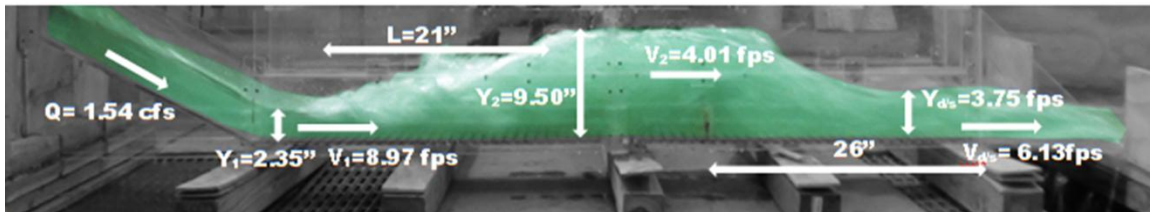


Figure 4.21: Hydraulic Jump Characteristics for Experiment 5C. 1% slope, 1.0d

3. If one sill 5.0 feet high with 15 flat faced friction blocks is placed in the flat part of the culvert starting at initiation of hydraulic jump, energy dissipation of 68 percent occurs as seen in Experiment 6C.

4. The reduction of energy due to friction blocks is marginal. The optimal 5.0-foot sill is the most economical option.
5. Experiment 5 shows an opportunity to reduce the culvert length at the end in the range of 40 to 43 feet. The 33-foot reduction was determined by eliminating the downstream segment of the culvert where the water surface is no longer uniform after the jump shortly after the sill up to the wing-wall. The 43-foot reduction results from truncating the section of the downstream culvert from the sill to the wing-wall. This option is important if there are problems with the right-of-way.
6. The difference of efficiency when flat-faced friction blocks were varied by only 2%. The energy loss ranged between 5.6 feet to 8.8 feet.

#### 4.7 ACKNOWLEDGMENTS

This project was funded by the Federal Highway Administration and sponsored by the Oklahoma Department of Transportation. In addition, Dr. Greg Hanson, P.E., Dr. Sherry Hunt, and Ken Kadavy, P.E., Hydraulic Engineers of the U.S. Department of Agriculture, Agricultural Research Service each contributed their ideas in the early stages of this project regarding ways to improve physical construction of the model. Finally, the work and ideas enacted by student contributors Marizel Rios Motte and Taylor Davis to contribute to the research and data collection.

#### 4.8 NOTATION

The following symbols were used in this paper:

|           |   |   |
|-----------|---|---|
| $E_2/E_1$ | = | Efficiency of hydraulic jump (%)                  |
| $F_{r1}$  | = | Froude Number in supercritical flow               |
| H         | = | Head upstream of culvert ( <i>in</i> )            |
| D         | = | Depth of culvert ( <i>in</i> )                    |
| Q         | = | Flow rate ( $ft^3/s$ )                            |
| THL       | = | Total head loss for entire culvert, ( <i>in</i> ) |



|           |   |   |
|-----------|---|---|
| $V_{d/s}$ | = | Velocity downstream of culvert ( <i>ft/s</i> )                        |
| $V_{u/s}$ | = | Velocity at upstream of culvert ( <i>ft/s</i> )                       |
| $Y_1$     | = | Water depth before hydraulic jump in supercritical flow ( <i>in</i> ) |
| $Y_2$     | = | Water depth after hydraulic jump in subcritical flow ( <i>in</i> )    |
| $Y_{d/s}$ | = | Water depth at downstream of culvert ( <i>in</i> )                    |
| $Z$       | = | the drop between upstream and downstream in the model ( <i>in</i> )   |
| FFFB      | = | Flat-faced friction blocks  |

#### 4.9 REFERENCES

- Bhutto, H., Mirani, S., and Chandio, S. (1989). "Characteristics of free hydraulic jump in rectangular channel." *Mehran University Research Journal of Engineering and Technology*, 8(2), 34 – 44.
- Beirami, M. and Chamani, M. (2006). Hydraulic Jumps in Sloping Channels: Sequent Depth Ratio. *Journal of Hydraulic Engineering, ASCE*. 2006 (132):1061-1068
- Beirami, M. and Chamani, M. (2010). Hydraulic Jumps in Sloping Channels: roller length and energy loss. *Canadian Journal of Civil Engineering*. 2010 (37): 535-543
- Chanson, H. (2008). "Acoustic Doppler Velocimetry (ADV) in the field and in laboratory: practical experiences." *International Meeting on Measurements and Hydraulics of Sewers*, 49-66.
- Chow, V.T. (1959). "Open channel Hydraulics." *McGraw-Hill, USA*, 680 pages.
- Defina, A. and Susin, F., (2003). Stability of a stationary hydraulic jump in an upward sloping channel. *Physics of Fluids*, 15 (12), 3883-3885
- Federal Highway Administration (2006). "The Hydraulic Design of Energy Dissipators for Culverts and Channels."
- Goring, D. and Nikora, V. (2002). "Despiking acoustic doppler velocimeter data." *Journal of Hydraulic Engineering*, 128(1), 117-128
- Hartner, C., Davis, S., and Hale, M. (2003).  
[www.eng.wayne.edu/legacy/forms/4/Hydraulic%20Jump.doc](http://www.eng.wayne.edu/legacy/forms/4/Hydraulic%20Jump.doc) (Dec. 2, 2003).

- Hotchkiss, R. and Larson, E. (2005). "Simple Methods for Energy Dissipation at Culvert Outlets." *Impact of Global Climate Change*. World Water and Environmental Resources Congress.
- Husain D., Alhamid, A., and Negm, A. (1994) Length and depth of hydraulic jump in sloping channels. *Journal of Hydraulic Research*. 32 (6), 899-910
- Rusch, R. (2008). *Personal communication*, Oklahoma Department of Transportation.
- SonTek/YSI, Inc. *ADVField/Hydra System Manual* (2001).
- Sholichin, M. and Akib, S. (2010). Development of drop number performance for estimate hydraulic jump on vertical and sloped structure. *International Journal of the Physical sciences* 5(11), 1678-1687.
- Tyagi, A. K. (2002). "A Prioritizing Methodology for Scour-critical Culverts in Oklahoma." *Oklahoma Transportation Center*. Oklahoma, 13 pp.
- Tyagi, A. K., et al., (2009). "Laboratory Modeling of Energy Dissipation in Broken-Back Culverts-Phase I," Oklahoma Transportation Center, Oklahoma, 82 pp.

## CHAPTER V

### ENERGY DISSIPATION IN EIGHTEEN-FOOT DROP BROKEN-BACK CULVERTS UNDER PRESSURE FLOW CONDITIONS

#### 5.1 ABSTRACT

Hydraulic jump formed in broken-back culverts were investigated experimentally by using energy dissipation devices. This paper investigates the reduction in scour downstream of a broken-back culvert by forming a hydraulic jump inside the culvert. A broken-back culvert in the laboratory represents a 150 foot long culvert. The drop between inlet and outlet was selected as 18 feet, a 1 (vertical) to 2 (horizontal) slope, after the upstream inlet and then continues 114 feet with the mild part at a one percent slope. Three flow conditions were simulated, consisting of 0.8, 1.0 and 1.2 times the culvert depth. The results were analyzed in terms of the inlet Froude number.

The Froude number of the hydraulic jump created in the flat part of the culvert ranges between 2.63 and 4.32 which indicates an “oscillating jump”. To locate the jump near the toe, different sill and friction block arrangements were tested. For new culvert constructions, the best option to maximize energy dissipation under pressure flow condition is to use two sills, one 2.5-foot sill at 62 feet from the end and one 3.33 feet sill at 45 feet from the end of the culvert.

Friction blocks had minimal impact on energy dissipation in the culvert. The length of the culvert can be reduced by 40 to 45 feet. Such a scenario is important where right-of-way problems exist for culvert construction

Keywords: Energy dissipation; Hydraulic jump; Broken-back culvert; Sill; Friction blocks; Six-foot drop; Pressure flow conditions; Efficiency of jump.

## 5.2 INTRODUCTION

Broken-back culverts are capable of dissipating energy, thus lower the effects of water scour, and overall reduction of damage due to water scour. The process of evaluation looks at different parameters that are thought to be related to the damaging effects of scour on broken-back culverts. These parameters include characteristics of hydraulic jump such as Froude number, energy loss, and efficiency of the jump. The Froude number related to the ratio of inertial and gravity forces, is presented by the average flow velocity before the jump ( $V_1$ ) and the

acceleration of gravity wave in shallow water:  $F_{r1} = \frac{V_1}{\sqrt{gY_1}}$ .

In Oklahoma alone, nearly 121 scour-critical culverts on the Interstate System (ISTAT), the National Highway System (NHS), and the State Transportation Program (STP) have been inventoried by the Oklahoma Transportation Center (OTC) at Oklahoma State University (Tyagi, 2002). A survey of culverts in Oklahoma indicates that the drop in flowline between upstream and downstream ends ranges between 6 and 24 feet. In this research, a drop of 18 feet was used in the laboratory model. Results of this research could maximize the energy loss within the culvert, thus minimizing the scour around the culvert and decreasing the degradation downstream in the channel. This reduces the construction and rehabilitation costs of culverts in Oklahoma.

The hydraulic jump is a natural phenomenon of a sudden rise in water level due to change from supercritical flow to subcritical flow, that is, when there is a sudden decrease in velocity of the flow. This sudden change in the velocity causes the considerable turbulence and loss of energy.

Consequently, the hydraulic jump has been recognized as an effective method for energy dissipation for many years.

Many studies have been carried out to examine the characteristics of the hydraulic jump. Ohtsu et al. (1996) evaluated incipient hydraulic jump conditions on flows over vertical sills. They identified two methods of obtaining an incipient jump: (1) increasing the sill height, or (2) increasing the tailwater depth until a surface roller forms upstream of the sill. For wide channels, predicted and experimental data were in agreement, but in the case of narrow channels, incipient jump was affected by channel width.

Hotchkiss et al. (2003) describe the available predictive tools for hydraulic jumps, the performance of the Broken-back Culvert Analysis Program (BCAP) in analyzing the hydraulics of a broken-back culvert, and the current applications and distribution of BCAP. They conducted tests on the broken-back culverts made of Plexiglas to assess the performance of BCAP in predicting headwater rating curves, the locations of hydraulic jumps, and the lengths of hydraulic jumps. They concluded that accounting for the losses within the jump because of the friction in corrugated metal pipes and more accurate predicting of the locations of hydraulic jumps may be improved by predictions of flow hydraulics within the culvert barrel.

Larson (2004), in her Master's thesis entitled *Energy Dissipation in Culverts by Forcing a Hydraulic Jump at the Outlet*, suggests forcing hydraulic jumps to reduce the outlet energy. She considered two design examples to create a hydraulic jump within a culvert barrel: (1) a rectangular weir placed on a flat apron and (2) a vertical drop along with a rectangular weir. These two designs were used to study the reduction in the energy of the flow at the outlet. From these experiments she found that both designs were effective in reduction of outlet velocity, momentum, and energy. These reductions would decrease the need for downstream scour mitigation.

Lowe et al. (2011) indicated that the subcritical sequent depth is a function of the conduit shape, upstream depth, and Froude number. He studied the theoretical determination of subcritical sequent depths for pressure and free-surface jump. Lowe studied the momentum equation which consists of terms for the top width, area, and centroid of flow. Also, it was presented that the general solutions to the sequent depth problem for four prismatic conduits: rectangular, circular, elliptical, and pipe arch. Lowe provided a numerical solution for these shapes, and he neglected the effects of friction and air entrainment. The authors were concentrated on the cost of downstream energy dissipation by forcing a jump to occur within the culvert barrel.

Tyagi et al. (2009) investigated hydraulic jump under pressure and open channel flow conditions in a broken-back culvert with a 24 foot drop. It was found that for pressure flow a two sill solution induced the most desirable jump, and for open channel a single sill close to the middle of the culvert was most desirable. The investigation was funded by the Oklahoma Transportation Center, Research and Innovative Technology Administration, Federal Highway Administration, and Oklahoma Department of Transportation.

Tyagi et al. (2010a) performed many experiments for open channel culvert conditions. Optimum energy dissipation was achieved by placing one sill at 40 feet from the outlet. Friction blocks and other modifications to the sill arrangement were not as effective.

Chamani et al. (2008) studied experimentally energy loss of the vertical drop in the upstream with model of 0.20 m drop; they carried out laboratory experiments to collect data. They developed models by using the theories of the shear layer and fully developed surface to estimate the energy loss. They found similarity between a turbulent surface jet and flow over the drop. The results compared with previous experiments and their experimental data and it was found that the predictions of their model agreed well with the experimental data. Moreover, authors used the predicted values of the energy loss to calculate the downstream depth of flow.

Mignot and Cienfuegos (2010) focused on an experimental investigation of energy dissipation and turbulence production in weak hydraulic jumps. Froude numbers ranged from 1.34 to 1.99. They observed two peak turbulence production regions for the partially developed inflow jump, one in the upper shear layer and the other in the near-wall region. The energy dissipation distribution in the jumps was measured and revealed a similar longitudinal decay of energy dissipation, which was integrated over the flow sections and maximum turbulence production values from the intermediate jump region towards its downstream section. It was found that the energy dissipation and the turbulence production were strongly affected by the inflow development. Turbulent production showed a common behavior for all measured jumps. It appeared that the elevation of maximum Turbulent Kinetic Energy (TKE) and turbulence production in the shear layer were similar.

Alikhani et al. (2010) conducted many experiments to evaluate effects of a continuous vertical end sill in a stilling basin. They measured the effects of sill position on the depth and length of a hydraulic jump without considering the tailwater depth. In the experiments, they used five different sill heights placed at three separate longitudinal distances in their 1:30 scaled model. The characteristics of the hydraulic jump were measured and compared with the classical hydraulic jump under varied discharges. They proposed a new relationship between sill height and position, and sequent depth to basin length ratio. The study concluded that a 30% reduction in basin length could be accomplished by efficiently controlling the hydraulic jump length through sill height.

The aim of this research is to investigate the best option to maximize energy dissipation under pressure channel flow condition, to evaluate the energy dissipation between upstream and downstream ends of the broken-back culvert without and with friction blocks, and to observe in physical experiments the efficiency of hydraulic jump with and without friction blocks between upstream and downstream ends of the culvert and the location of hydraulic jump from the toe of

the drop in the culvert (Tyagi et al., 2009). A scale model was built to represent prototype of a broken-back culvert 150 feet long with two barrels of 10 X 10 feet, and a vertical drop of 18 feet. Simulations of different flow conditions for 0.8, 1.0 and 1.2 times the hydraulic head in the scale model constructed were performed.

### 5.3 THEORY

The nature of the hydraulic jump cannot be accounted for by use of the energy equation because there is a substantial dissipation of energy owing to the turbulence associated with the jump.

However, because momentum is conserved across hydraulic jumps, momentum theory may be applied to determine the jump size and location (Hotchkiss et al. 2003). Momentum theory states that the sum of the external forces acting upon a system equals the change in momentum across that system (Thompson and Kilgore 2006). This principle can successfully be applied to complete or incomplete hydraulic jumps. According to Lowe et al. (2011), using an axis parallel to the channel, a one-dimensional form of the momentum equation may be written:

$$\sum \vec{F}_S = \sum (\vec{M}_S)_{out} - \sum (\vec{M}_S)_{in} \quad 5.1$$

where  $F_S$  = external forces (lbs, N) acting on water within the control volume and  $M_S$  = momentum flux (lbs, N) through the control volume (Lowe et al. 2011).

To solve the momentum equation for pressure flow conditions in the culvert hydraulic jump and then to simplify the solution graphically, the numerous studies that have been done for open channel flow conditions derived from the Belanger equation which expresses the ratio between sequent depths as functions of the upstream Froude number were examined (Chow 1959, Lowe et al. 2011). Chow stated the hydraulic jump will form in the channel if the  $F_{r1}$  of the flow, the flow depth  $Y_1$ , and the depth after hydraulic jump  $Y_2$  satisfy the following equation:

$$\frac{Y_2}{Y_1} = \frac{1}{2} \left( \sqrt{1 + 8F_{r1}^2} - 1 \right) \quad 5.2$$



The following equation was used to calculate the Froude number ( $F_{r1}$ ) of the hydraulic jump in the upstream:

$$F_{r1} = \frac{V_1}{\sqrt{gY_1}} \quad 5.3$$

where  $V_1$  = velocity before hydraulic jump;  $g$  = acceleration due to gravity; and  $Y_1$  = water depth before hydraulic jump.

A complete derivation of momentum theory of incomplete hydraulic jumps can be reviewed in Lowe (2011); the following equations are obtained for sequent depth of incomplete jumps for a rectangular cross-section:

$$Y'_1 = \frac{Y_1}{D} \quad 5.4$$

$$Y'_2 = \frac{1}{2} + \left( F_{r1}^2 + \frac{1}{2} \right) Y_1'^2 - F_{r1}^2 Y_1'^3 \quad 5.5$$

The dimensionless form of the sequent depth;

$$Y'_2 = \frac{Y_2}{D} \quad 5.6$$

where  $Y'_1$ , and  $Y'_2$  are the dimensionless sequent depths before and after the jump, respectively;  $F_{r1}$  is the approach or supercritical Froude number and  $D$  is height of culvert (ft).

According to Lowe (2011) equations to calculate the Froude number in the incomplete hydraulic jump are as follows:

Calculate the  $Y_2$  from  $Y'_2$ , dimensionless flow depth

$$Y_2 = Y'_2 * D \quad 5.7$$

From Equation 5.7, the actual Froude number at upstream supercritical flow can be calculated which the adjusted Froude number is ( $F'_{r1(\text{adjusted})}$ ):

$$F'_{r1(\text{adjusted})} = \sqrt{\frac{\left(\frac{2Y_2}{Y_1} + 1\right)^2 - 1}{8}} \quad 5.8$$

The efficiency of the jump was calculated by taking the ratio of the specific energy before and after the jump (Chow, 1959):

$$\frac{E_2}{E_1} = \frac{(8F_{r1}^2 + 1)^{3/2} - 4F_{r1}^2 + 1}{8F_{r1}^2(2 + F_{r1}^2)} \quad 5.9$$

The efficiency of the jump in the incomplete jump can be calculated by using the adjusted Froude number ( $F'_{r1(\text{adjusted})}$ ):

$$\left(\frac{E_2}{E_1}\right) = \frac{(8F_{r1(\text{adjusted})}^2 + 1)^{3/2} - 4F_{r1(\text{adjusted})}^2 + 1}{8F_{r1(\text{adjusted})}^2(2 + F_{r1(\text{adjusted})}^2)} \quad 5.10$$

where  $E_1$  is energy head before the jump, inches,  $E_2$  is energy head after the jump, inches, and  $F'_{r1(\text{adjusted})}$  is the Froude number before the jump.

The total head loss between upstream and downstream of the structure was calculated by applying the Bernoulli equation:

$$\text{THL} = \left(H + \frac{V_{u/s}^2}{2g} + Z\right) - \left(Y_{d/s} + \frac{V_{d/s}^2}{2g}\right) \quad 5.11$$

where THL is total head loss, inches, H is water depth upstream of the culvert, inches, and Z is the drop between upstream and downstream which in the model was 3.60 inches, representing an 18-foot drop in the prototype.

The loss of energy or energy dissipation in the jump was calculated by taking the difference between the specific energy before the jump and after the jump

$$\Delta E = E_1 - E_2 = \frac{(Y_2 - Y_1)^3}{4Y_1 Y_2} \quad 5.12$$

where  $E_1$  is energy head before the jump, inches and  $E_2$  is energy head after the jump, inches.

## 5.4 EXPERIMENTAL SET UP AND INSTRUMENTATION

### 5.4.1 LABORATORY MODEL

A scale model represented a 150-foot long broken-back culvert with two barrels of 10 x 10 feet each and a vertical drop of 18 feet in the field condition. The 1 to 20 scale was adopted due to space limitations. The scale model contains 2 barrels with dimensions of 6 inches wide by 6 inches high and the length of 68.40 inches which represented the pressure flow condition (see Figures 5.1 through 5.5). At the upstream end, a reservoir collects the flow discharge at three flow rates, depending upon the experiment being conducted. Supercritical inflow is enforced by a steep sloped flume section. At the downstream end of the flume an expansion of the flow section by a wingwall further reduces the downstream velocity. The location of the hydraulic jump is simply controlled by the discharge rate upstream and the sill and/or friction block location.

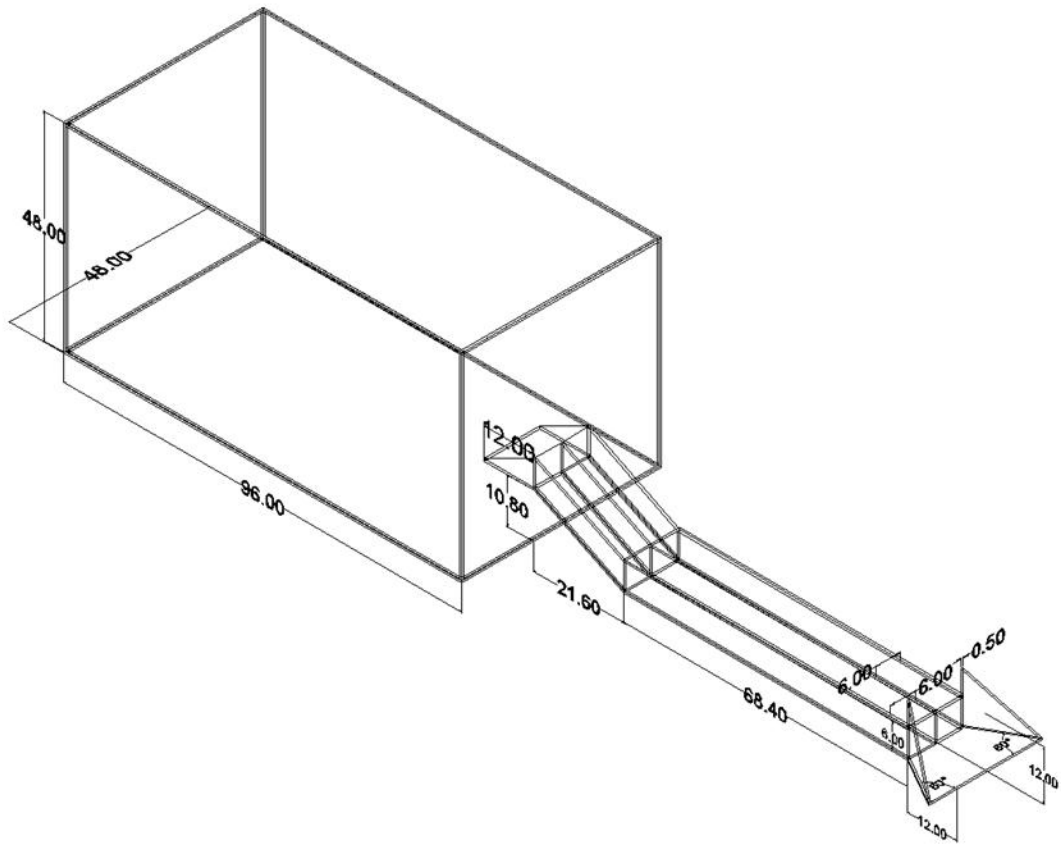


Figure 5.1: Pressure Flow Laboratory Model

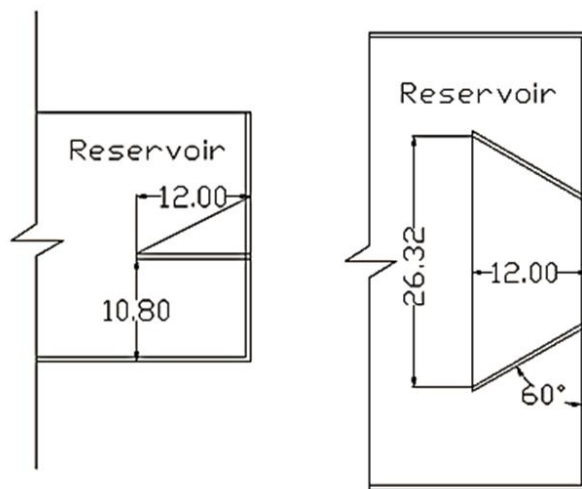


Figure 5.2: Profile and Plan View of Reservoir Inlet (Upstream)

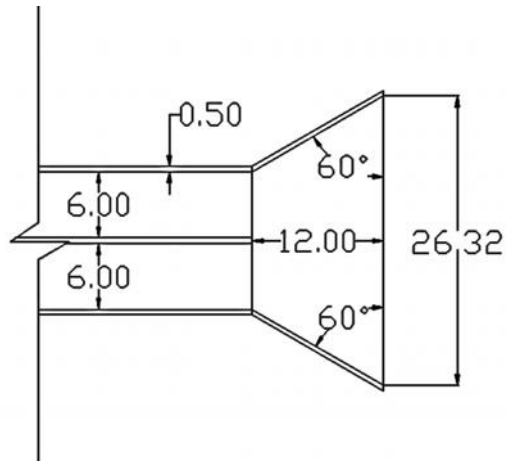


Figure 5.3: Plan View of Culvert Outlet (Downstream)

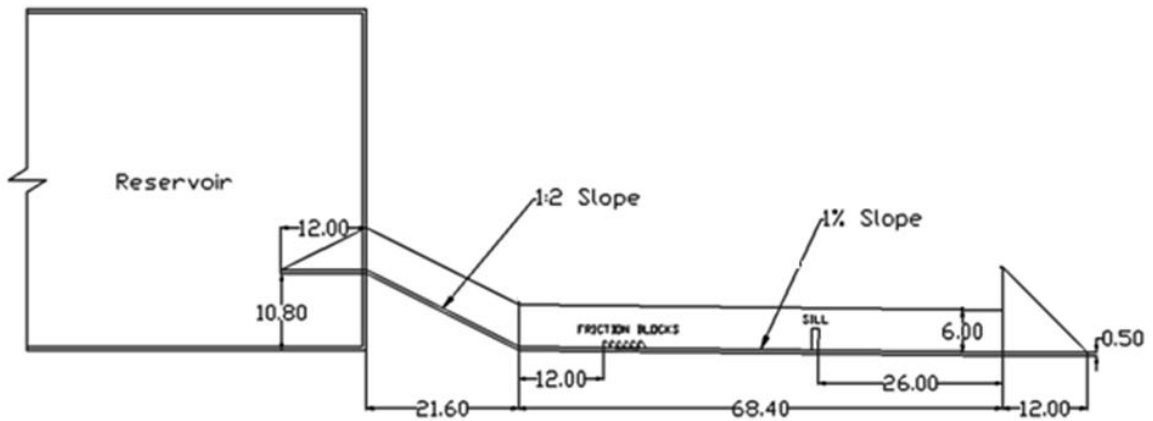


Figure 5.4: Profile View of Laboratory Model

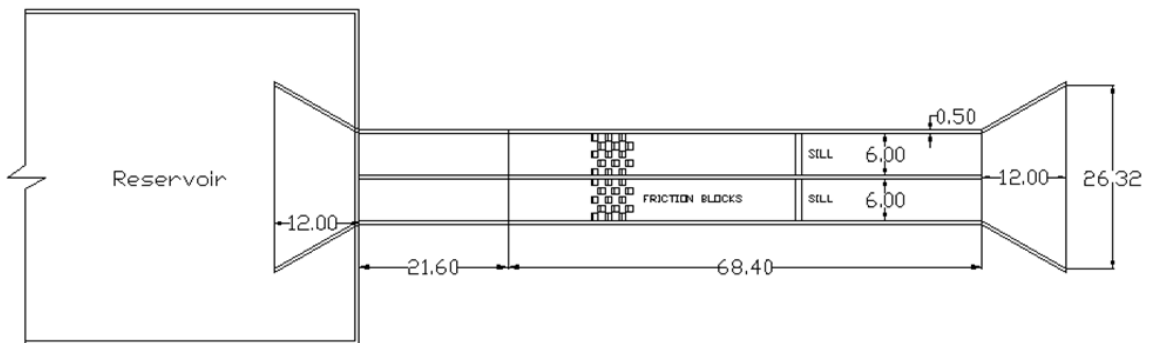


Figure 5.5: Plan View of Laboratory Model

Plexiglas<sup>®</sup> was found preferable because it offered visibility as well as durability, and a surface which would more closely simulate the surface being modeled (see Figures 5.6 and 5.7). The

thickness of the Plexiglas<sup>®</sup> was decided based on weight, rigidity, workability, and the ease with which the material would fit into scale. Half-inch Plexiglas proved to be sturdy and was thick enough to allow connection hardware to be installed in the edges of the plates. This material also fit well into the proposed scale of 1 to 20 which equated one-half inch in the model to one foot in the prototype.

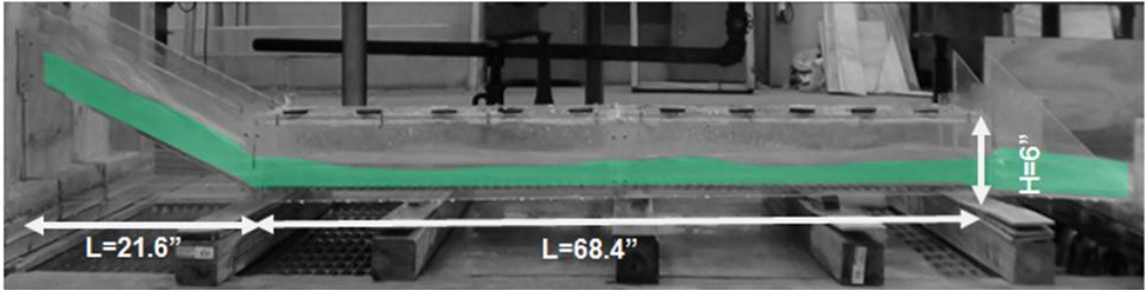


Figure 5.6: Dimensions of Broken-Back Culvert to Apply Pressure Flow Condition



Figure 5.7: Front View of Laboratory Model

In addition to the Plexiglas<sup>®</sup> model of the culvert, a reservoir was constructed upstream of the model to collect and calm the fluid entering the model. The reservoir was constructed with plywood because it was not necessary to observe the behavior of the fluid at that stage. Within the reservoir, wingwalls at an angle of 60 degrees were constructed to channel flow into the model opening. The base of the wingwalls was constructed with plywood and the exposed wingwall models were formed with Plexiglas<sup>®</sup>. The same design was used for the outlet structure of the culvert (see Figures 5.8 and 5.9).

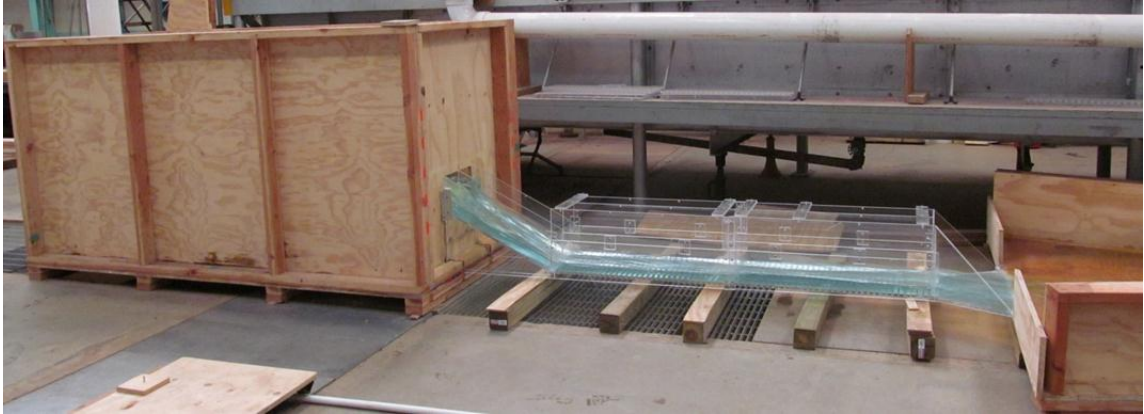


Figure 5.8: Side View of Laboratory Model



Figure 5.9: Downstream Plywood Channel after Wingwall

The objective of the test was to determine the effect of sill and friction blocks on the hydraulic jump within the prototype, therefore the model was constructed so that different arrangements of sills and friction blocks could be placed and observed within the model. Friction blocks were mounted in different arrangements on a sheet of Plexiglas<sup>®</sup> the same width as the barrels, and



placed in the barrel (see Figures 5.10 through 5.13). Flat-faced friction blocks were selected. Sills were located only on the horizontal portion of the model, and the sills contain two small orifices at the bottom to allow the culvert to completely drain. Access holes were cut into the top of these culvert model sections to allow for placement of a velocity meter.



Figure 5.10: Reservoir and Channel Inlet for Culvert Model



Figure 5.11: Typical Sill Dimensions

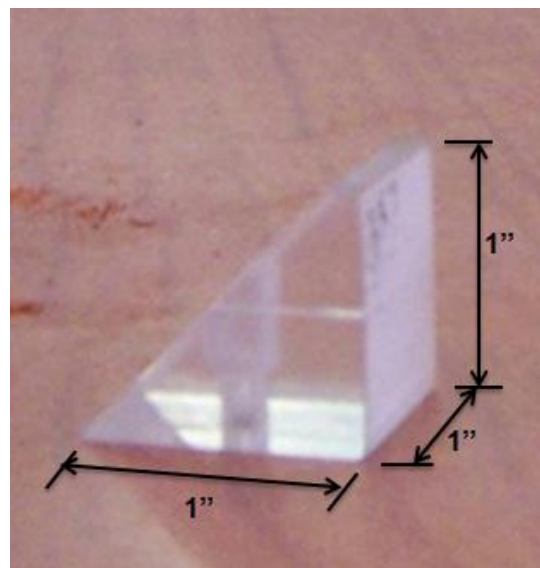


Figure 5.12: Example of Flat Faced Friction Block

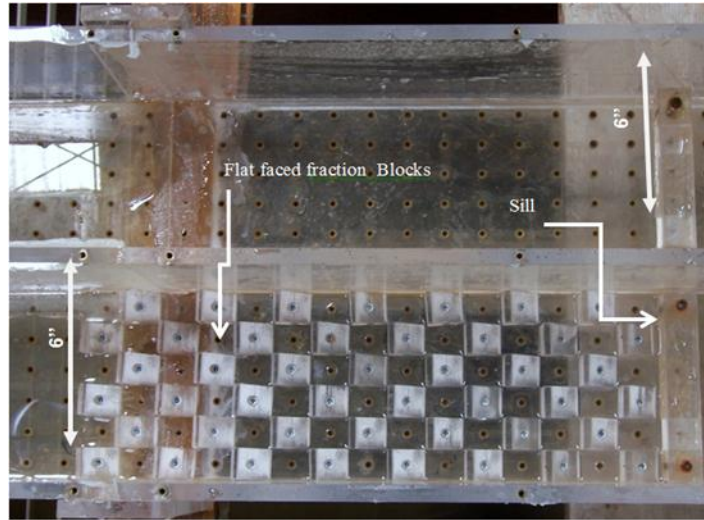


Figure 5.13: Example of Flat Faced Friction Blocks Arranged on Model Bottom

#### 5.4.2 EXPERIMENTAL PROCEDURE AND DATA COLLECTION

Many experiments were conducted to create energy dissipation within a broken-back culvert.

Nine experiments, Experiments 19 through 27, were done for this model with variations in length, height, width, and energy dissipaters used. Each experiment tested three scenarios and they were run with upstream heads of  $0.8d$ ,  $1.0d$ , and  $1.2d$  with each depth denoted by A, B, or C, respectively. For example, 20A represents the 20<sup>th</sup> experiment run at  $0.8d$ , 20B represents the 20<sup>th</sup> experiment run at  $1.0d$ , and 20C represents the 20<sup>th</sup> experiment run at  $1.2d$ . A SonTek 2D-side looking Micro-Acoustic Doppler Velocimeter (ADV) was used to measure the velocity at the intake of the structure, and at the downstream end of the culvert. It is difficult to measure the velocity at the toe before the hydraulic jump because it was necessary to maintain a closed structure to satisfy pressure condition (SonTex/YSI, 2001 and Chanson, 2008). This difficulty precluded us from using the ADV to measure the velocity before the hydraulic jump. Therefore, a Pitot tube was used to measure velocity at the toe before the hydraulic jump.

In these experiments, the length of the hydraulic jump ( $L$ ), the depth before the jump ( $Y_1$ ), the depth after the jump ( $Y_2$ ), the distance from the beginning of the hydraulic jump to the beginning of the sill ( $X$ ), the depth of the water in the inclined channel ( $Y_s$ ), and the depth of the water

downstream of the culvert ( $Y_{d/s}$ ) were measured. All dimensions were measured by using a ruler and point gage. As mentioned above, the velocity before the jump, the velocity at the inlet of structure ( $V_1$ ), the velocity after the jump ( $V_2$ ), and the velocity downstream of the culvert ( $V_{d/s}$ ) were measured by a Pitot tube. The procedure of the experiment is as follows: i) install energy dissipation devices (such as sills or friction blocks) in the model, ii) set point gage to the correct height in the reserve, iii) turn on pump in station, iv) adjust valve and coordinate the opening to obtain the amount of head for the experiment, v) take the reading for flow rate, vi) run the model for 10 minutes before taking measurements vii) measure  $Y_s$ ,  $Y_1$ ,  $Y_2$ ,  $L$ ,  $X$ , and  $Y_{d/s}$ , and viii) measure velocities along the channel  $V_1$ ,  $V_2$ , and  $V_{d/s}$  as shown in Figure 5.14.

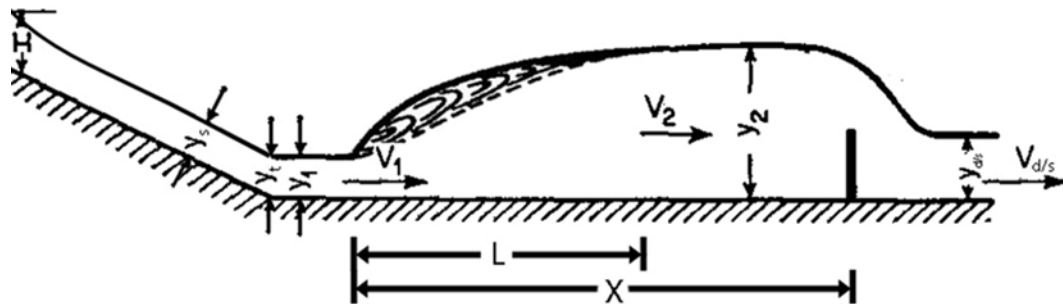


Figure 5.14: Hydraulic Jump Variables in a Broken-Back Culvert

## 5.5 DATA ANALYSIS

Nine experiments were selected from nineteen experiments performed in the hydraulic laboratory. These experiments show model runs without friction blocks, the effect of a sill at the end of the model, and with friction blocks as well as the sill. The flat faced friction blocks are used with sill (see Figure 5.13). After the effectiveness was evaluated, the number of blocks was varied by 15, 30, and 45.

In these experiments, the optimum sill height was determined first, the optimum sill location was found next, and finally the effectiveness of friction blocks in combination with the optimum sill parameters was determined.

Experiment 19 was run without any energy dissipation devices in order to evaluate the hydraulic characteristics of the model, including the Froude number and supercritical flow conditions. This experiment is also an example of the current field practice to allow the kinetic energy of fluid to be transferred downstream without energy reduction. This experiment did not produce a hydraulic jump as shown in Figures 5.15 (case A), 5.16 (case B), and 5.17 (case C). The results can be found in Table 5.1, below.

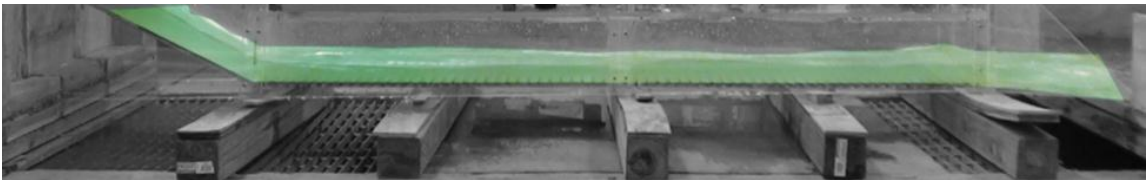


Figure 5.15: Experiment 19A with No Sill or Friction Blocks

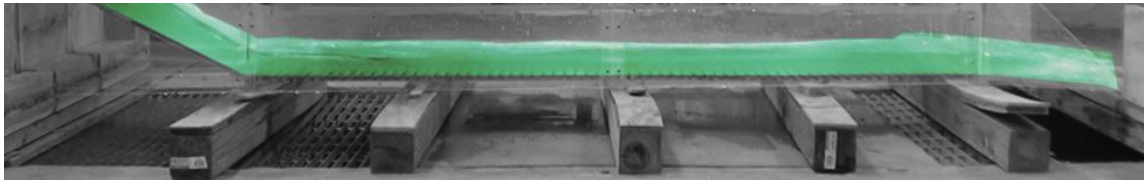


Figure 5.16: Experiment 19B with No Sill or Friction Blocks

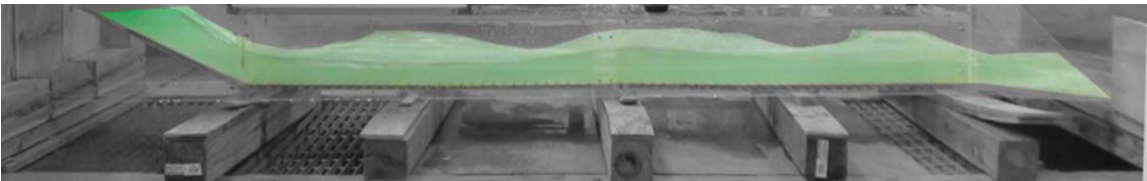


Figure 5.17: Experiment 19C with No Sill or Friction Blocks

Table 5.1: Hydraulic Parameters for Experiments 19

| CASE            | 19A (0.8d) | 19B (1.0d) | 19C (1.2d) |
|-----------------|------------|------------|------------|
| Q (cfs)         | 0.98       | 1.27       | 1.57       |
| $V_{u/s}$ (fps) | 2.44       | 2.53       | 2.62       |
| $Y_1$ (in)      | 1.75       | 2.00       | 2.50       |
| $Y_{d/s}$ (in)  | 1.75       | 2.00       | 2.50       |
| $F_{r1}$        | 3.89       | 3.74       | 3.46       |
| $V_1$ (fps)     | 8.43       | 8.67       | 8.97       |
| THL (in)        | 2.96       | 2.24       | 1.88       |

Experiment 24 was run with two sills: a 1.5-inch sill located at 37 inches from the end of the culvert and a 2-inch sill located at 27 inches from the end of the culvert. Pressure flow is defined by the fluid exerting pressure against the top of the model. A hydraulic jump was observed in all three flow conditions as shown in Figures 5.18 (case A), 5.19 (case B), and 5.20 (case C). The results show that the  $F_{r1}$  values ranged from 3.25 to 4.32. These ranges of  $F_{r1}$  values are indicative of an oscillating hydraulic jump. The total head loss for the whole culvert ranges between 8.32 inches to 9.31 inches. The three cases are considered as incomplete (pressure flow) jump so that Lowe's (2011) technique would be used to calculate  $Y_2$  which meant that  $Y_2$  is greater than the depth of culvert. The energy dissipation due to hydraulic jump ranges between 5.87 inches to 5.95 inches. Additional results can be seen in Table 5.2.



Figure 5.18: Experiment 24A with a 1.5" Sill Located at 37" from the End and a 2" Sill Located at 27" from the End of the Culvert



Figure 5.19: Experiment 24B with a 1.5" Sill Located at 37" from the End and a 2" Sill Located at 27" from the End of the Culvert

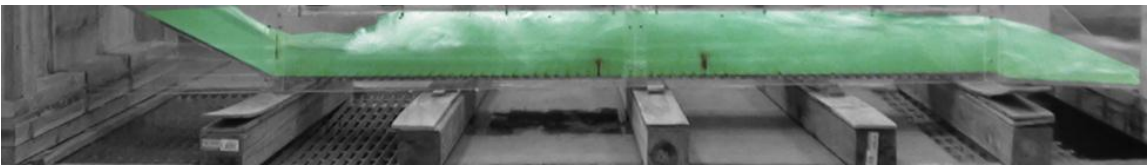


Figure 5.20: Experiment 24C with a 1.5" Sill Located at 37" from the End and a 2" Sill Located at 27" from the End of the Culvert

Table 5.2: Hydraulic Parameters for Experiments 24

| CASE                      | 24A (0.8d) | 24B (1.0d) | 24C (1.2d) |
|---------------------------|------------|------------|------------|
| Q (cfs)                   | 0.95       | 1.25       | 1.60       |
| $V_{w/s}$ (fps)           | 2.38       | 2.50       | 2.66       |
| $Y_1$ (in)                | 1.35       | 2.00       | 2.65       |
| $Y_2$ (in)                | 7.60       | 9.56       | 10.91      |
| $Y_{d/s}$ (in)            | 2.85       | 3.35       | 4.25       |
| $F_{r1}$                  | 4.32       | 3.72       | 3.25       |
| $V_1$ (fps)               | 8.27       | 8.67       | 8.93       |
| $V_2$ (fps)               | 4.18       | 5.91       | 6.75       |
| $V_{d/s}$ (fps)           | 4.91       | 5.56       | 6.02       |
| $\Delta E$ (in)           | 5.94       | 5.64       | 5.87       |
| THL (in)                  | 9.31       | 8.87       | 8.32       |
| $E_2/E_1$                 | 0.57       | 0.64       | 0.71       |
| Culvert<br>Reduction (ft) | 40         | 38         | 30         |

Experiment 25 was run with two sills: a 1.5-inch sill located at 37 inches from the end of the culvert and a 2-inch sill located at 27 inches from the end of the culvert and 15 flat faced friction blocks. An incomplete hydraulic jump was observed in all experiments and three flow conditions as shown in Figures 5.21 (case A), 5.22 (case B), and 5.23 (case C). Therefore, Lowe's method is applied in to calculate  $Y_2$ . The results show that the  $F_{r1}$  values ranged from 2.66 to 3.32. These ranges of  $F_{r1}$  values are indicative of an oscillating hydraulic jump. The total head loss for the whole culvert ranges between 9.04 inches to 9.72 inches. Additional results can be seen in Table 5.3.



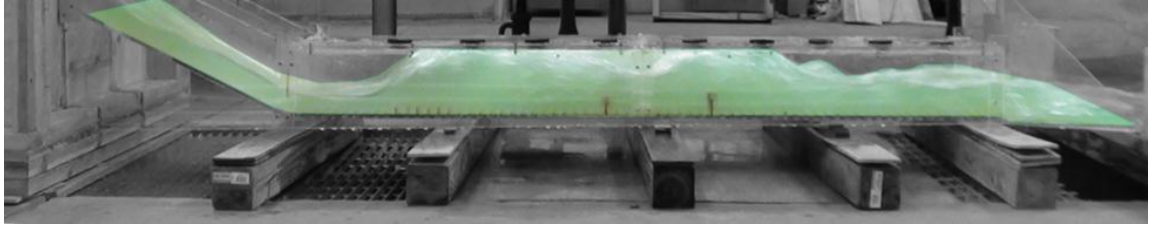


Figure 5.21: Experiment 25A with a 1.5" Sill Located at 37" from the End and a 2" Sill Located at 27" from the End of the Culvert and 15 Flat Faced Friction Blocks

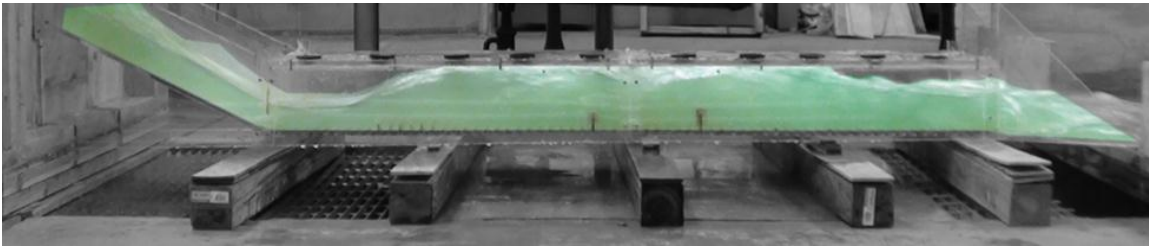


Figure 5.22: Experiment 25B with a 1.5" Sill Located at 37" from the End and a 2" Sill Located at 27" from the End of the Culvert and 15 Flat Faced Friction Blocks

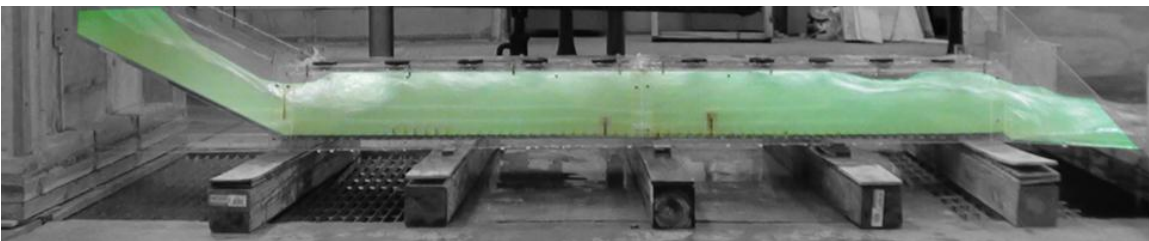


Figure 5.23: Experiment 25C with a 1.5" Sill Located at 37" from the End and a 2" Sill Located at 27" from the End of the Culvert and 15 Flat Faced Friction Blocks

Table 5.3: Hydraulic Parameters for Experiments 25

| CASE                      | 25A (0.8d) | 25B (1.0d) | 25C (1.2d) |
|---------------------------|------------|------------|------------|
| Q (cfs)                   | 0.96       | 1.25       | 1.58       |
| $V_{w/s}$ (fps)           | 2.40       | 2.50       | 2.64       |
| $Y_1$ (in)                | 1.75       | 2.25       | 3.00       |
| $Y_2$ (in)                | 7.39       | 8.93       | 9.88       |
| $Y_{d/s}$ (in)            | 2.75       | 3.25       | 4.00       |
| $F_{r1}$                  | 3.32       | 3.14       | 2.66       |
| $V_1$ (fps)               | 7.33       | 7.94       | 8.11       |
| $V_2$ (fps)               | 3.66       | 5.05       | 5.18       |
| $V_{d/s}$ (fps)           | 4.91       | 5.18       | 5.79       |
| $\Delta E$ (in)           | 3.46       | 3.71       | 2.74       |
| THL (in)                  | 9.42       | 9.72       | 9.04       |
| $E_2/E_1$                 | 0.70       | 0.72       | 0.80       |
| Culvert<br>Reduction (ft) | 40         | 38         | 30         |

## 5.6 RESULTS

After careful evaluation, Experiment 24 was selected from the data analysis portion for pressure flow conditions. This experiment was selected by examining many factors; including its relatively low downstream velocities, high total hydraulic head losses, and possible reduction in channel length. This experiment consists of a 2-inch sill at 27 inches from the end of the culvert and a 1.5-inch sill at 37 inches from the end of the culvert. It was found that this experiment yielded results most applicable to modifying existing culverts with the addition of sills and/or friction blocks.

The culvert barrel could be reduced by reducing a section at the end of the channel where the water surface profile is more uniform, so that the reduction in culvert length could be between 18 inches to 24 inches which is equivalent to 30 ft to 40 ft in the prototype.

Experiment 25 was selected from the data analysis portion for pressure flow conditions. This experiment was selected by examining many factors; including its relatively low downstream velocities, high total hydraulic head losses, and possible reductions in channel length. This experiment has a similar sill arrangement, and it consists of a 2-inch sill at 27 inches from the end of the culvert and a 1.5-inch sill at 37 inches from the end of the culvert with 15 flat faced friction blocks. It was found that this experiment yielded results most applicable to modifying existing culverts with the addition of sills and/or friction blocks. The culvert barrel could be reduced by reducing a section at the end of the channel where the water surface profile is more uniform, so that the reduction in culvert could be between 18 inches to 24 inches which is equivalent to 30 ft to 40 ft in the prototype.

## 5.7 CONCLUSION

Forming a hydraulic jump can be used in reduction of degradation downstream of broken-back culverts. A broken-back culvert is used in areas of high relief and steep topography as it has one or more breaks in profile slope. The advantage of a culvert is to safely pass water underneath the roadways constructed in hilly topography or on the side of a relatively steep hill. A laboratory model was constructed to represent a 150 foot broken-back culvert. The drop between upstream and downstream was 18 feet. The idealized prototype contains a 1 (vertical) to 2 (horizontal) slope, a 36-foot horizontal length of steep part of the culvert continuing down to a 114-foot mild culvert with a 1 percent slope. The prototype for these experiments was a two barrel 10-foot by 10-foot reinforced concrete culvert. The model was made to 1:20 scale. The following dimensions are in terms of the prototype culvert. The following conclusions can be drawn based on the laboratory experiments for pressure flow conditions:

- 1) For retrofitting an existing culvert, Experiment 24 is the best option for pressure flow conditions. Each experiment consists of three flow conditions: 0.8, 1.0 and 1.2 times the

upstream culvert depth of 10 feet. This scenario uses two sills, a 3.33-foot sill at 45 feet from the end of the culvert, and a 2.5-foot sill located 62 feet from the end of the culvert.

- 2) Optimal placement of two sills, 2.5 feet and 3.33 feet high, resulted in 14 feet total head loss and energy dissipation is 71 percent as shown in Experiment 24C.
- 3) For Experiment 24, reductions in culvert length can be made between 30 feet to 40 feet, as seen in Table 2.
- 4) If two sills, one 3.33-foot sill at 45 feet from the end of the culvert and one 2.5-foot sill located 62 feet from the end of the culvert, and 15 flat faced friction blocks are placed in the flat section of the culvert starting at the formation of the hydraulic jump, the THL is 15 feet and energy dissipation of 80 percent as seen in Experiment 25C.
- 5) The reduction of energy due to the region of friction blocks is marginal.

## 5.8 ACKNOWLEDGMENTS

This project was funded by the Federal Highway Administration and sponsored by the Oklahoma Department of Transportation. We would like to thank Mr. Bob Rusch, P.E., Bridge Division Engineer, Oklahoma Department of Transportation for his active participation in incorporating ideas to make this research more practical to field conditions.

In addition, Dr. Greg Hanson, P.E., Dr. Sherry Hunt, Raymond Cox and Kem Kadavy, P.E., Hydraulic Engineers of the U.S. Department of Agriculture, Agricultural Research Service each contributed their ideas in the early stages of this project regarding ways to improve physical construction of the model. Finally, the work and ideas enacted by student contributors Marizel Rios Motte and Taylor Davis to contribute to the research and data collection.

## 5.9 NOTATION

The following symbols were used in this paper:

|            |   |  |
|------------|---|--|
| $E_2/E_1$  | = | Efficiency of hydraulic jump (%);                                      |
| $F_{r1}$   | = | Froude Number in supercritical flow;                                   |
| $H$        | = | Head upstream of culvert ( <i>in</i> );                                |
| $d$        | = | Depth of culvert ( <i>in</i> );  |
| $Q$        | = | Flow rate ( $ft^3/s$ );  |
| THL        | = | Total head loss for entire culvert, ( <i>in</i> );                     |
| $V_{d/s}$  | = | Velocity downstream of culvert ( $ft/s$ );                             |
| $V_{u/s}$  | = | Velocity at upstream of culvert ( $ft/s$ );                            |
| $Y_1$      | = | Water depth before hydraulic jump in supercritical flow ( <i>in</i> ); |
| $Y_2$      | = | Water depth after hydraulic jump in subcritical flow ( <i>in</i> );    |
| $Y_{d/s}$  | = | Water depth at downstream of culvert ( <i>in</i> );                    |
| $Z$        | = | the drop between upstream and downstream in the model ( <i>in</i> );   |
| $\Delta E$ | = | Loss of energy, ( <i>in</i> );   |
| $E_2/E_1$  | = | Efficiency of hydraulic jump (%);                                      |
| BBC        | = | Broken-back culvert;   |
| H.J.       | = | Hydraulic jump;  |
| u.p.       | = | under pressure;  |
| Y          | = | yes; and   |
| N          | = | No.  |

## 5.10 REFERENCES

- Alikhani, A. et al. (2010). Hydraulic jump in stilling basin with vertical end sill. *International Journal of Physical Sciences*. 5(1), 25-29. <http://www.academicjournals.org/IJPS>.
- Chanson, H. (2008). Acoustic Doppler Velocimetry (ADV) in the field and in laboratory: practical experiences. *International Meeting on Measurements and Hydraulics of Sewers*, 49-66.
- Chamani, M., Rajaratnam N., and Beirami M. K. (2008). Turbulent Jet Energy Dissipation at Vertical Drops. *Journal of Hydraulic Engineering*, ASCE, 134(10),
- Chow, V.T. (1959). *Open-channel Hydraulics*. McGraw-Hill, New York, NY, 680 pages.
- Goring, D., Nikora, V. (2002). Despiking Acoustic Doppler Velocimeter data. *Journal Of Hydraulic Engineering*, 128(1), 117-128
- Hotchkiss, R., Flanagan, P. and Donahoo, K. (2003). Hydraulic jumps in broken-back culvert. *Transportation Research Record* (1851), 35 – 44.
- Larson, E. (2004). *Energy dissipation in culverts by forcing a hydraulic jump at the outlet*. Master's Thesis, Washington State University.
- Lowe, N. Hotchkiss, R., and Nelson J. (2010). Air entrainment and sequent depths in horizontal closed conduits. *Challenges of Change*. World Environmental and water Resources Congress 2010, ASCE. 1266-1277.
- Lowe, N. Hotchkiss, R., and Nelson J. (2011). Theoretical Determination of sequent Depths in Closed Conduits. *Journal of Irrigation and drainage engineering*, ASCE. 137(12) 801-810.

- Mignot, E. and Cienfuegos, R. (2010). Energy dissipation and turbulent production in weak hydraulic jumps. *Journal of Hydraulic Engineering*, ASCE, 136 (2), 116-121.
- Ohtsu, I. et al. (1996). Incipient jump conditions for flows over a vertical sill. *Journal of Hydraulic Engineering*, ASCE. 122(8) 465-469. doi: 10.1061/(ASCE)0733-29(1996)122:8(465).
- SonTek/YSI, Inc. *ADVField/Hydra System Manual* (2001).
- Tyagi, A. K. (2002). A Prioritizing Methodology for Scour-critical Culverts in Oklahoma. Oklahoma Transportation Center.
- Tyagi, A. K., et al. (2009), "Laboratory Modeling of Energy Dissipation in Broken-Back Culverts– Phase I," Oklahoma Transportation Center, Oklahoma, 82 pp.
- Tyagi, A. K. et al. (2010a). Energy Dissipation in Broken-back Culverts under Open Channel Flow Conditions. Am. Soc. Civil Engineers International Perspective on Current and Future State of Water Resources, 10 pp.
- Tyagi, A. K., et al. (2009), "Laboratory Modeling of Energy Dissipation in Broken-Back Culverts – Phase II," Oklahoma Transportation Center, Oklahoma, 95 pp.

## CHAPTER VI

### CONCLUSION

Formation of a hydraulic jump can be used in reduction of degradation downstream of broken-back culverts. The advantage of these culverts is that water is safely passed underneath the roadways constructed in hilly topography or on the side of a relatively steep hill. Laboratory models were constructed to represent 150 foot broken-back culverts. The idealized prototype contains a 1 (vertical) to 2 (horizontal) slope followed by a mild section with a 1 percent slope. The prototype for these experiments was a two barrel 10-foot by 10-foot or 10-foot by 20-foot reinforced concrete culvert. The models were made to 1:20 scale. The following conclusions can be drawn from this research:

- 1) All inflow conditions for the models of interest to this study can be classified as supercritical-turbulent flow
- 2) For six foot drop broken-back culverts the Froude Number ranges from 1.8 to 2.2 which classifies the induced jump as a weak jump
- 3) For twelve foot drop broken-back culverts the Froude Number ranges from 2.6 to 2.9 which classifies the induced jump as a weak jump with oscillating jump possible in some of the higher flow conditions
- 4) For eighteen foot drop broken-back culverts the Froude Number ranges from 2.5 to 3.1 which classifies the induced jump as an oscillating jump



- 5) For twenty-four foot drop broken-back culverts the Froude Number ranges from 3.1 to 3.8 which classifies the induced jump as an oscillating jump
- 6) For new culvert construction, Experiment 5 is the best option for open channel flow conditions. This option includes one sill with two small orifices at the bottom for draining the culvert completely located 43 feet from the end of the culvert. The height of the culvert should be at least 16 feet to allow open channel condition in the culvert
- 7) If one sill 5.0 feet high is placed in the flat part of the culvert, it results in 66 percent of energy dissipation
- 8) If one sill 5.0 feet high with 15 flat faced friction blocks is placed in the flat part of the culvert starting at initiation of hydraulic jump, energy dissipation of 68 percent
- 9) The reduction of energy due to friction blocks is marginal, varying by only 2%. The optimal 5.0-foot sill is the most economical option
- 10) The single 5.0 feet high sill scenario shows an opportunity to reduce the culvert length at the end in the range of 40 to 43 feet. This is important if there are problems with the right-of-way
- 11) For retrofitting an existing culvert, Experiment 24 is the best option for pressure flow conditions. This scenario uses two sills, a 3.33-foot sill at 45 feet from the end of the culvert, and a 2.5-foot sill located 62 feet from the end of the culvert
- 12) Optimal placement of two sills, 2.5 feet and 3.33 feet high, resulted in 14 feet total head loss and energy dissipation is 71 percent
- 13) For Experiment 24, reductions in culvert length can be made between 30 feet to 40 feet,
- 14) If two sills, one 3.33-foot sill at 45 feet from the end of the culvert and one 2.5-foot sill located 62 feet from the end of the culvert, and 15 flat faced friction blocks are placed in the flat section of the culvert starting at the formation of the hydraulic jump, the total head loss is 15 feet and energy dissipation of 80 percent
- 15) The reduction of energy due to the region of friction blocks is minimal

## REFERENCES

- Alikhani, A. et al. (2010). Hydraulic jump in stilling basin with vertical end sill. *International Journal of Physical Sciences*. 5(1), 25-29. <http://www.academicjournals.org/IJPS>.
- Beirami, M. and Chamani, M. (2006). Hydraulic Jumps in Sloping Channels: Sequent Depth Ratio. *Journal of Hydraulic Engineering, ASCE*. 2006 (132):1061-1068
- Beirami, M. and Chamani, M. (2010). Hydraulic Jumps in Sloping Channels: roller length and energy loss. *Canadian Journal of Civil Engineering*. 2010 (37): 535-543
- Bhutto, H., Mirani, S., and Chandio, S. (1989). "Characteristics of free hydraulic jump in rectangular channel." *Mehran University Research Journal of Engineering and Technology*, 8(2), 34 – 44.
- Campbell C. S. and others (1985). *Flow Regimes in Inclined Open-Channel Flows of Granular Materials*. Powder Technology. Elsevier Sequoia.
- Chamani, M., Rajaratnam N., and Beirami M. K. (2008). Turbulent Jet Energy Dissipation at Vertical Drops. *Journal of Hydraulic Engineering, ASCE*, 134(10).
- Chanson, H. (1996). *Free-Surface Flows with Near-Critical Flow Conditions*. Canadian Journal of Civil Engineering. CSCE.

- Chanson, H. (2008). "Acoustic Doppler Velocimetry (ADV) in the field and in laboratory: practical experiences." *International Meeting on Measurements and Hydraulics of Sewers*, 49-66.
- Chow, V.T. (1959). "Open channel Hydraulics." *McGraw-Hill, USA*, 680 pages.
- Defina, A. and Susin, F., (2003). Stability of a stationary hydraulic jump in an upward sloping channel. *Physics of Fluids*, 15 (12), 3883-3885.
- Federal Highway Administration (2006). "The Hydraulic Design of Energy Dissipators for Culverts and Channels."
- Goring, D. and Nikora, V. (2002). "Despiking acoustic doppler velocimeter data." *Journal of Hydraulic Engineering*, 128(1), 117-128.
- Hartner, C., Davis, S., and Hale, M. (2003).  
<[www.eng.wayne.edu/legacy/forms/4/Hydraulic%20Jump.doc](http://www.eng.wayne.edu/legacy/forms/4/Hydraulic%20Jump.doc)> (Dec. 2, 2003).
- Hotchkiss, R., Flanagan, P. and Donahoo, K. (2003). Hydraulic jumps in broken-back culvert. *Transportation Research Record* (1851), 35 – 44.
- Hotchkiss, R. and Larson, E. (2005). "Simple Methods for Energy Dissipation at Culvert Outlets." *Impact of Global Climate Change*. World Water and Environmental Resources Congress.
- Husain D., Alhamid, A., and Negm, A. (1994) Length and depth of hydraulic jump in sloping channels. *Journal of Hydraulic Research*. 32 (6), 899-910
- Larson, E. (2004). *Energy dissipation in culverts by forcing a hydraulic jump at the outlet*. Master's Thesis, Washington State University.

- Lowe, N. Hotchkiss, R., and Nelson J. (2010). Air entrainment and sequent depths in horizontal closed conduits. *Challenges of Change*. World Environmental and water Resources Congress 2010, ASCE. 1266-1277.
- Lowe, N. Hotchkiss, R., and Nelson J. (2011). Theoretical Determination of sequent Depths in Closed Conduits. *Journal of Irrigation and drainage engineering, ASCE*. 137(12) 801-810.
- Moawad, A. and others (1994). Hydraulic Loading in Culvert Inlets. *Canadian Journal of Civil Engineering*. CSCE.
- Mignot, E. and Cienfuegos, R. (2010). Energy dissipation and turbulent production in weak hydraulic jumps. *Journal of Hydraulic Engineering, ASCE*, 136 (2), 116-121.
- Nettleton, Peter and McCorquodale, John (1989). Radial Flow Stilling Basins with Baffle Blocks. *Canadian Journal of Civil Engineering*. CSCE.
- Ohtsu, I. et al. (1996). Incipient jump conditions for flows over a vertical sill. *Journal of Hydraulic Engineering, ASCE*. 122(8) 465-469. doi: 10.1061/(ASCE)0733-29(1996)122:8(465).
- Pegram, Geoffry and others (1999). Hydraulics of Skimming Flow on Modeled Stepped Spillways. *Journal of Hydraulic Engineering*. ASCE.
- Rusch, R. (2008). *Personal communication*, Oklahoma Department of Transportation.
- Sholichin, M. and Akib, S. (2010). Development of drop number performance for estimate hydraulic jump on vertical and sloped structure. *International Journal of the Physical Sciences* 5(11), 1678-1687.

- Smith, C. D. and Oak, A. G. (1994). Culvert Inlet Efficiency. Canadian Journal of Civil Engineering. CSCE.
- SonTek/YSI, Inc. *ADVField/Hydra System Manual* (2001).
- Stahl, Helmut and Hager, Willi (1998). Hydraulic Jump in Circular Pipes. Canadian Journal of Civil Engineering. CSCE.
- Tyagi, A. K. and Schwarz, B. (2002). A Prioritizing Methodology for Scour-critical Culverts in Oklahoma. Oklahoma Transportation Center. Oklahoma, 13 pp.
- Tyagi, A.K., et al., (2009). “Laboratory Modeling of Energy Dissipation in Broken-back Culverts – Phase I,” Oklahoma Transportation Center, Oklahoma, 82 pp.
- Tyagi, A. K. et al. (2010a). Energy Dissipation in Broken-back Culverts under Open Channel Flow Conditions. Am. Soc. Civil Engineers International Perspective on Current and Future State of Water Resources, 10 pp.
- Tyagi, A.K., et al., (2011). “Laboratory Modeling of Energy Dissipation in Broken-back Culverts – Phase II,” Oklahoma Transportation Center, Oklahoma, 80 pp.
- Tyagi, A.K., Johnson, N. Ali, A. and Brown, J. (2012). Energy Dissipation in Six-Foot Drop Broken Back Culverts under Open Channel Conditions. 5th International Perspective on Water Resources and the Environment Conference, Marrakech, Morocco.
- Tyagi, A.K., Al-Madhhachi, A., and Brown, J. (2013b). Energy Dissipation in Broken-back Culverts under Pressure Flow Conditions. ASCE, Journal Hydraulic Engineering. (submitted for peer review).

Tyagi, A.K., Johnson, N. and Ali, A. (2013). Energy Dissipation in 24-foot Drop Broken Back Culverts under Open Channel Conditions. ASCE, Journal Hydraulic Engineering.  
(Submitted or peer review)

## APPENDIX

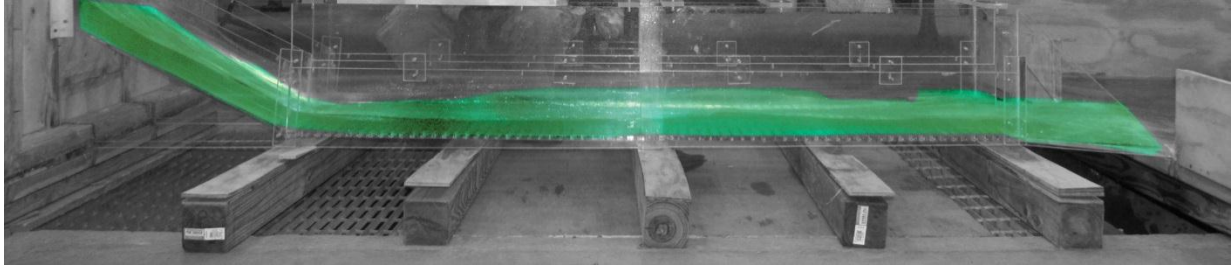


Figure A1: Experiment 1A for 1% Slope

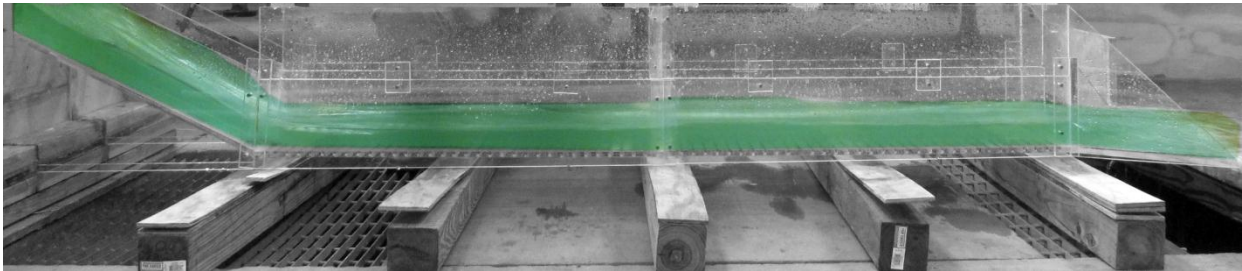


Figure A2: Experiment 1B for 1% Slope

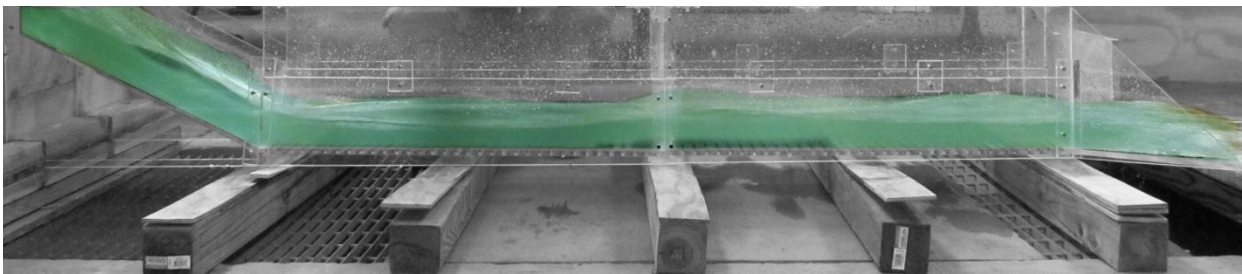


Figure A3: Experiment 1C for 1% Slope

Table A1: Experiment 1 for 1% Slope Using Open Channel Flow Condition with No Sill in the Culvert

| H.J. | Run | H    | $W_{temp}$ | Q      | $V_{u/s}$ | $Y_s$ | $Y_{toe}$ | $Y_1$ | $Y_2$ | $Y_{d/s}$ | Fr1 | $V_1$            | $V_2$ | $V_{d/s}$        | L | X | $\Delta E$ | THL    | $E_2/E_1$ |
|------|-----|------|------------|--------|-----------|-------|-----------|-------|-------|-----------|-----|------------------|-------|------------------|---|---|------------|--------|-----------|
| N    | 1A  | 0.8d | -          | 0.9481 | 2.3703    | 2.12  | 1.75      | -     | -     | 1.87      | 3.5 | 7.7412<br>P-tube | -     | 8.3943<br>P-tube | - | - | -          | 1.6469 | -         |
| N    | 1B  | 1.0d | -          | 1.2038 | 2.4076    | 2.63  | 2.25      | -     | -     | 1.75      | 3.7 | 8.0328<br>P-tube | -     | 8.8292<br>P-tube | - | - | -          | 2.2551 | -         |
| N    | 1C  | 1.2d | -          | 1.5352 | 2.5587    | 3.38  | 2.28      | -     | -     | 2.32      | 3.3 | 8.2241<br>P-tube | -     | 8.9722<br>P-tube | - | - | -          | 1.8999 | -         |



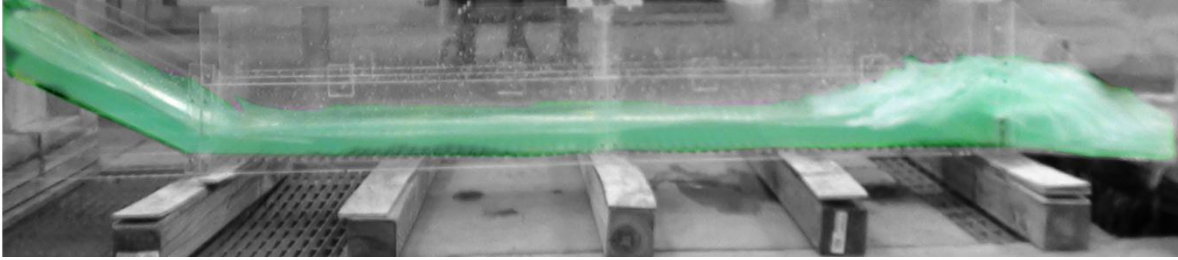


Figure A4: Experiment 2A for 1% Slope

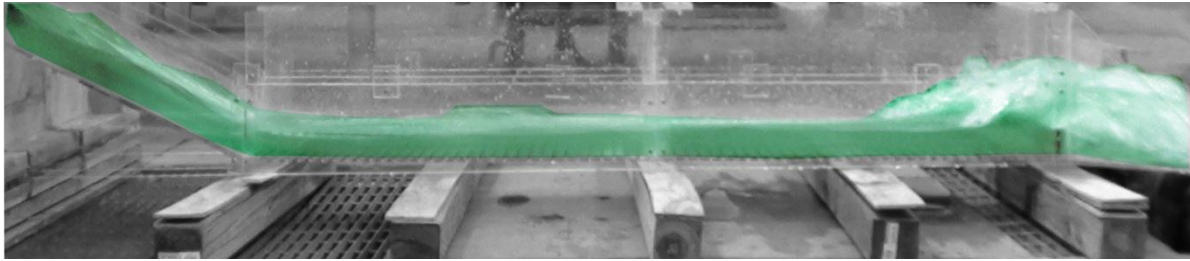


Figure A5: Experiment 2B for 1% Slope

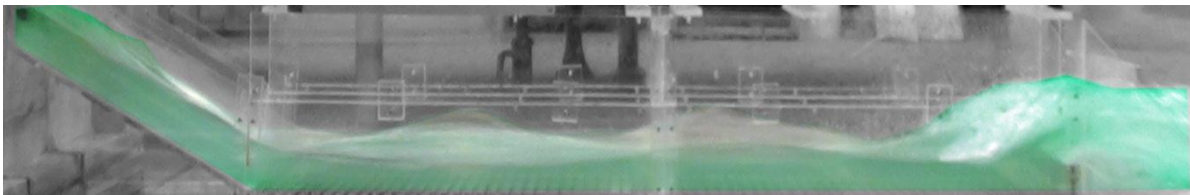


Figure A6: Experiment 2C for 1% Slope

Table A2: Experiment 2 for 1% Slope Using Open Channel Flow Condition with a 2" End Sill

| H.J. | Run | H    | $W_{temp}$ | Q      | $V_{u/s}$ | $Y_s$ | $Y_{toe}$ | $Y_1$ | $Y_2$ | $Y_{d/s}$ | Fr1 | $V_1$            | $V_2$ | $V_{d/s}$   | L    | X  | $\Delta E$ | THL     | $E_2/E_1$ |
|------|-----|------|------------|--------|-----------|-------|-----------|-------|-------|-----------|-----|------------------|-------|-------------|------|----|------------|---------|-----------|
| Y    | 2A  | 0.8d | -          | 0.9565 | 2.3913    | 2.00  | 1.65      | 1.70  | 5.50  | 5.50      | 3.9 | 8.3526<br>P-tube | -     | -<br>P-tube | 9.00 | 15 | 1.4672     | 11.1655 | 0.6190    |
| Y    | 2B  | 1.0d | -          | 1.2332 | 2.4664    | 3.00  | 2.13      | 2.00  | 6.00  | 6.00      | 3.7 | 8.5902<br>P-tube | -     | -<br>P-tube | 8.50 | 12 | 1.3333     | 11.9335 | 0.6438    |
| Y    | 2C  | 1.2d | -          | 1.5558 | 2.5930    | 3.35  | 3.37      | 3.37  | 8.00  | 8.00      | 2.9 | 8.8214<br>P-tube | -     | -<br>P-tube | 6.00 | 13 | 0.9204     | 11.2529 | 0.7537    |

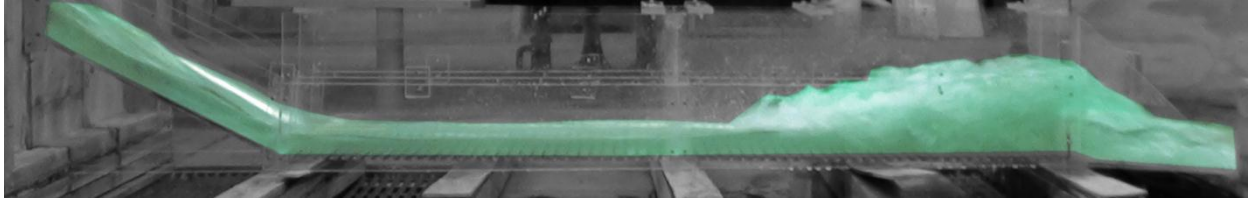


Figure A7: Experiment 3A for 1% Slope

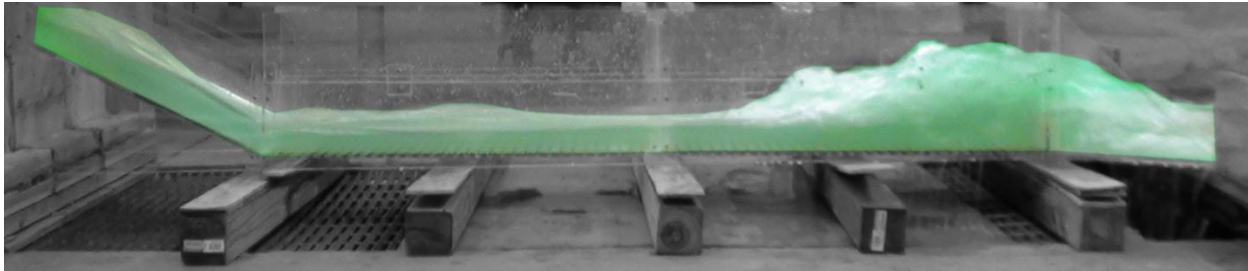


Figure A8: Experiment 3B for 1% Slope

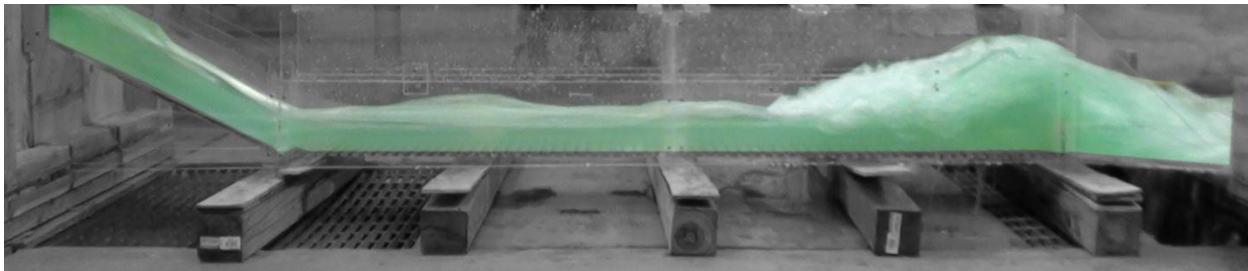


Figure A9: Experiment 3C for 1% Slope

Table A3: Experiment 3 for 1% Slope Using Open Channel Flow Condition with a 3" End Sill

| H.J. | Run | H    | $W_{temp}$ | Q      | $V_{u/s}$ | $Y_s$ | $Y_{toe}$ | $Y_1$ | $Y_2$ | $Y_{d/s}$ | Fr1 | $V_1$            | $V_2$  | $V_{d/s}$        | L     | X  | $\Delta E$ | THL    | $E_2/E_1$ |
|------|-----|------|------------|--------|-----------|-------|-----------|-------|-------|-----------|-----|------------------|--------|------------------|-------|----|------------|--------|-----------|
| Y    | 3A  | 0.8d | -          | 0.9225 | 2.3063    | 2.35  | 1.65      | 2.00  | 6.75  | 6.75      | 3.7 | 8.4643<br>P-tube | 5.3080 | 2.2573<br>P-tube | 13.00 | 26 | 1.9847     | 8.8916 | 0.6508    |
| Y    | 3B  | 1.0d | -          | 1.2588 | 2.5176    | 2.75  | 2.00      | 2.35  | 7.50  | 7.50      | 3.5 | 8.9122<br>P-tube | 5.1801 | 2.9155<br>P-tube | 20.00 | 25 | 1.9375     | 8.8972 | 0.6644    |
| Y    | 3C  | 1.2d | -          | 1.5937 | 2.6562    | 3.50  | 3.35      | 3.00  | 8.00  | 8.00      | 3.2 | 9.1205<br>P-tube | 5.8377 | 3.1413<br>P-tube | 16.00 | 20 | 1.3021     | 9.4759 | 0.7111    |

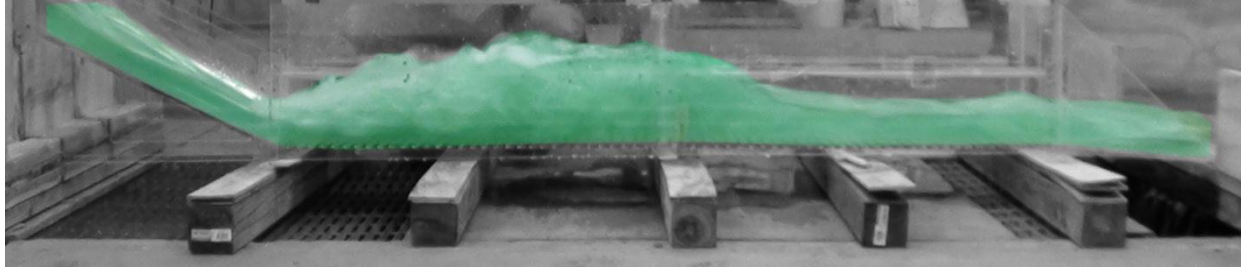


Figure A10: Experiment 4A for 1% Slope

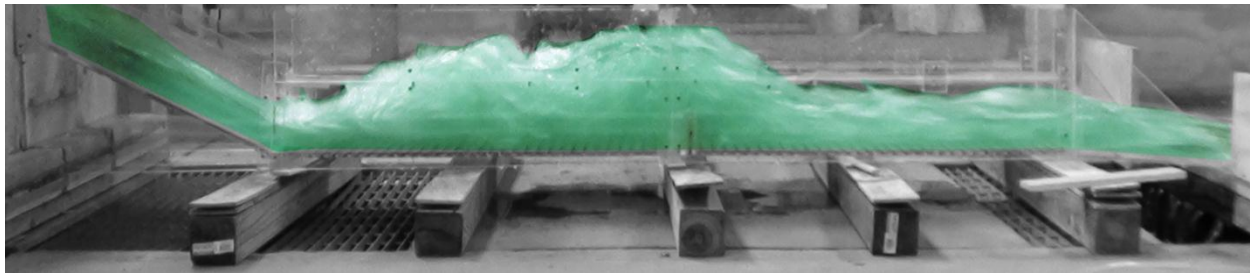


Figure A11: Experiment 4B for 1% Slope

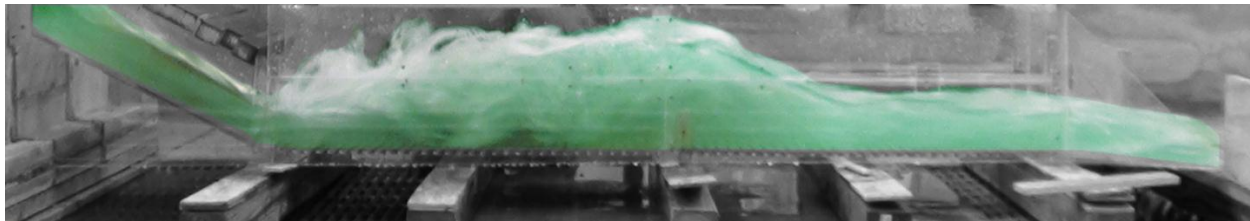


Figure A12: Experiment 4C for 1% Slope

Table A4: Experiment 4 for 1% Slope Using Open Channel Flow Condition with a 3” Sill 33” from the End

| H.J. | Run | H    | $W_{temp}$ | Q      | $V_{u/s}$ | $Y_s$ | $Y_{toe}$ | $Y_1$ | $Y_2$ | $Y_{d/s}$ | Fr1 | $V_1$            | $V_2$  | $V_{d/s}$        | L     | X  | $\Delta E$ | THL    | $E_2/E_1$ |
|------|-----|------|------------|--------|-----------|-------|-----------|-------|-------|-----------|-----|------------------|--------|------------------|-------|----|------------|--------|-----------|
| Y    | 4A  | 0.8d | -          | 0.9730 | 2.4325    | 2.62  | 2.35      | 2.35  | 8.00  | 2.75      | 3.1 | 7.6833<br>P-tube | 3.2762 | 5.1801<br>P-tube | 14.00 | 36 | 2.3984     | 8.9525 | 0.7342    |
| Y    | 4B  | 1.0d | -          | 1.2428 | 2.4856    | 2.50  | 2.50      | 2.75  | 8.75  | 3.00      | 3.0 | 8.1904<br>P-tube | 4.8317 | 5.5791<br>P-tube | 16.00 | 35 | 2.2442     | 9.1512 | 0.7410    |
| Y    | 4C  | 1.2d | -          | 1.5584 | 1.5584    | 3.62  | 3.25      | 3.25  | 9.00  | 3.87      | 2.9 | 8.5432<br>P-tube | 4.7758 | 6.0187<br>P-tube | 16.50 | 34 | 1.6249     | 8.6371 | 0.7601    |

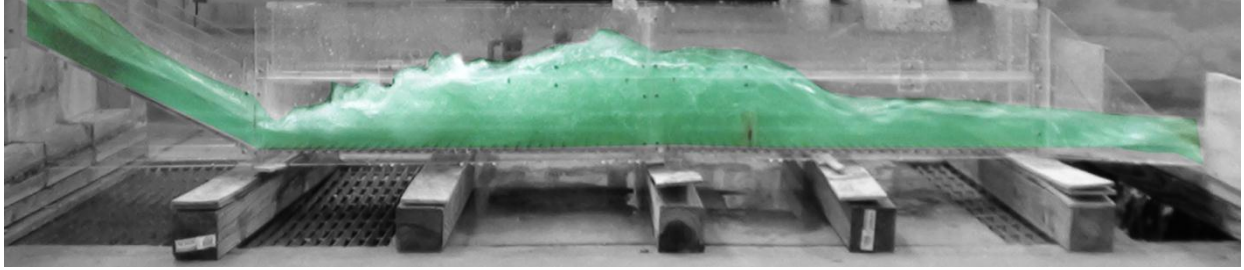


Figure A13: Experiment 5A for 1% Slope

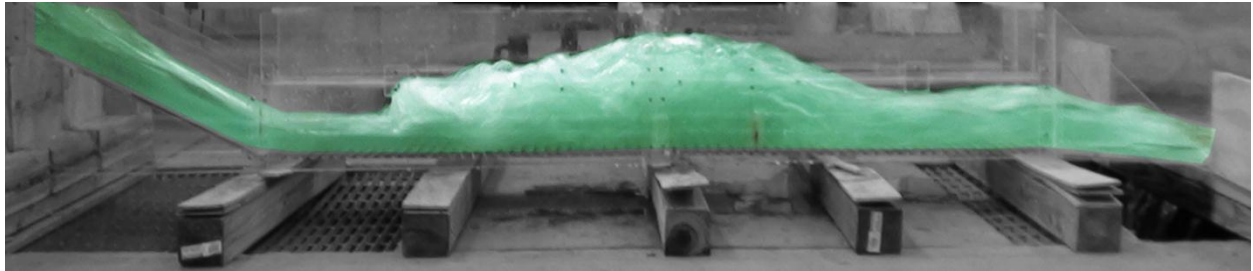


Figure A14: Experiment 5B for 1% Slope

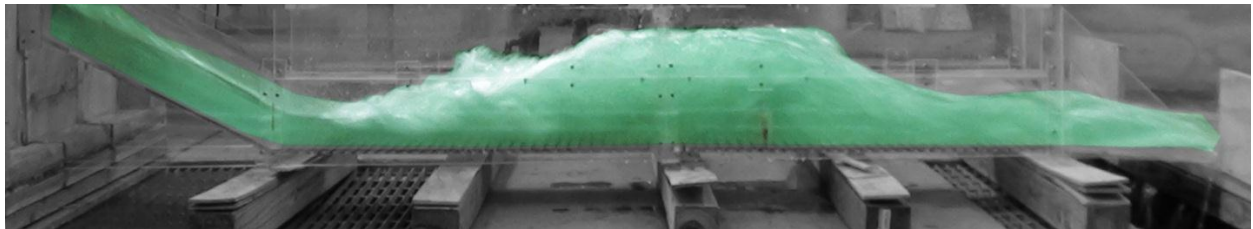


Figure A15: Experiment 5C for 1% Slope

Table A5: Experiment 5 for 1% Slope Using Open Channel Flow Condition with a 3” Sill 26” from the End

| H.J. | Run | H    | $W_{temp}$ | Q      | $V_{u/s}$ | $Y_s$ | $Y_{toe}$ | $Y_1$ | $Y_2$ | $Y_{d/s}$ | Fr1 | $V_1$            | $V_2$  | $V_{d/s}$        | L     | X  | $\Delta E$ | THL    | $E_2/E_1$ |
|------|-----|------|------------|--------|-----------|-------|-----------|-------|-------|-----------|-----|------------------|--------|------------------|-------|----|------------|--------|-----------|
| Y    | 5A  | 0.8d | -          | 0.9354 | 2.3385    | 2.25  | 1.65      | 1.65  | 7.50  | 2.25      | 3.8 | 7.9409<br>P-tube | 2.3166 | 5.2572<br>P-tube | 17.00 | 40 | 4.0445     | 9.2190 | 0.6356    |
| Y    | 5B  | 1.0d | -          | 1.2838 | 2.5676    | 2.50  | 1.85      | 2.00  | 8.25  | 2.75      | 3.7 | 8.5118<br>P-tube | 3.0646 | 5.6031<br>P-tube | 20.50 | 32 | 3.6991     | 9.4284 | 0.6481    |
| Y    | 5C  | 1.2d | -          | 1.5404 | 1.5673    | 3.50  | 2.50      | 2.35  | 9.50  | 3.75      | 3.6 | 8.9722<br>P-tube | 4.0125 | 6.1292<br>P-tube | 21.00 | 37 | 4.0932     | 8.4782 | 0.6613    |

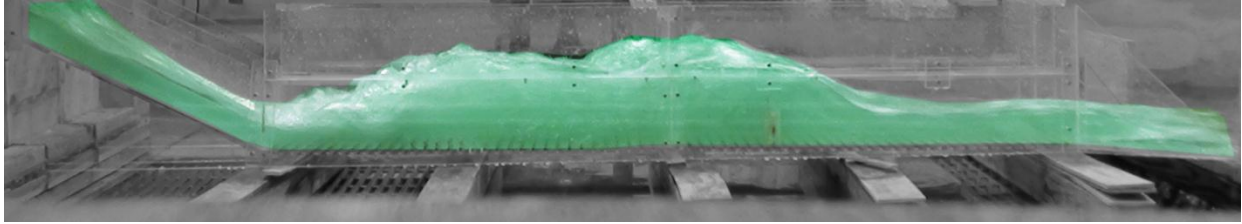


Figure A16: Experiment 6A for 1% Slope

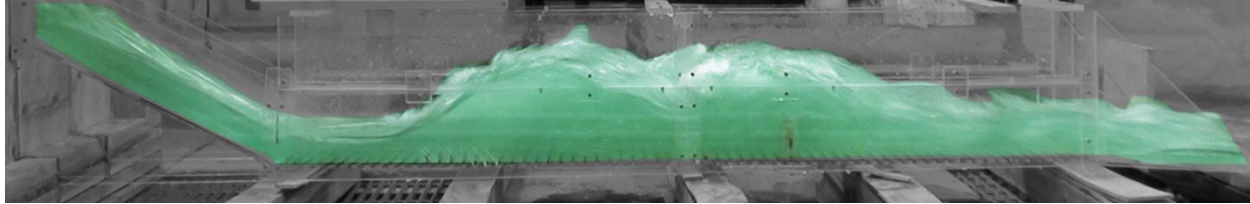


Figure A17: Experiment 6B for 1% Slope

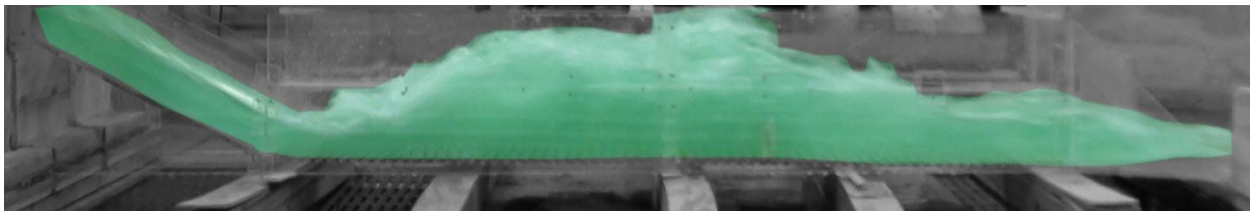


Figure A18: Experiment 6C for 1% Slope

Table A6: Experiment 6 for 1.0% Slope Using Open Channel Flow Condition with a 3" Sill at 26" from the End and 15 Flat Faced Friction Blocks at 12" from the Toe

| H.J. | Run | H    | W <sub>temp</sub> | Q      | V <sub>w/s</sub> | Y <sub>s</sub> | Y <sub>toe</sub> | Y <sub>1</sub> | Y <sub>2</sub> | Y <sub>d/s</sub> | Fr1 | V <sub>1</sub>   | V <sub>2</sub> | V <sub>d/s</sub> | L     | X  | ΔE     | THL    | E <sub>2</sub> /E <sub>1</sub> |
|------|-----|------|-------------------|--------|------------------|----------------|------------------|----------------|----------------|------------------|-----|------------------|----------------|------------------|-------|----|--------|--------|--------------------------------|
| Y    | 6A  | 0.8d | -                 | 0.9648 | 2.4120           | 2.00           | 1.75             | 1.75           | 6.75           | 2.35             | 3.7 | 8.0250<br>P-tube | 2.5900         | 5.2470<br>P-tube | 18.00 | 42 | 2.6455 | 9.2041 | 0.6445                         |
| Y    | 6B  | 1.0d | -                 | 1.2396 | 2.4792           | 2.75           | 2.13             | 2.13           | 7.50           | 2.75             | 3.6 | 8.5902<br>P-tube | 3.8417         | 5.7356<br>P-tube | 17.00 | 33 | 2.4234 | 9.0653 | 0.6586                         |
| Y    | 6C  | 1.2d | -                 | 1.5430 | 2.5717           | 3.35           | 2.50             | 2.35           | 7.00           | 3.25             | 3.4 | 8.5118<br>P-tube | 3.6629         | 6.1858<br>P-tube | 19.00 | 36 | 1.5280 | 8.8523 | 0.6861                         |

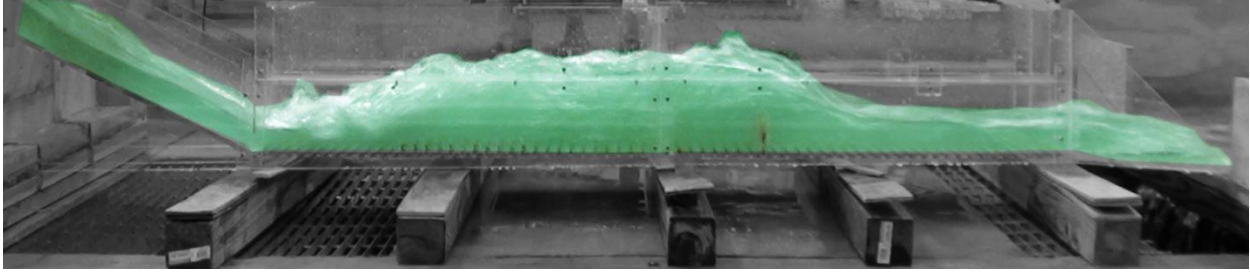


Figure A19: Experiment 7A for 1% Slope

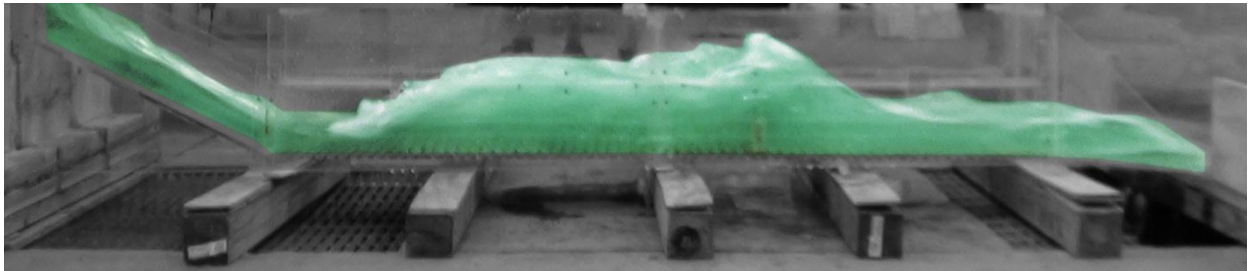


Figure A20: Experiment 7B for 1% Slope

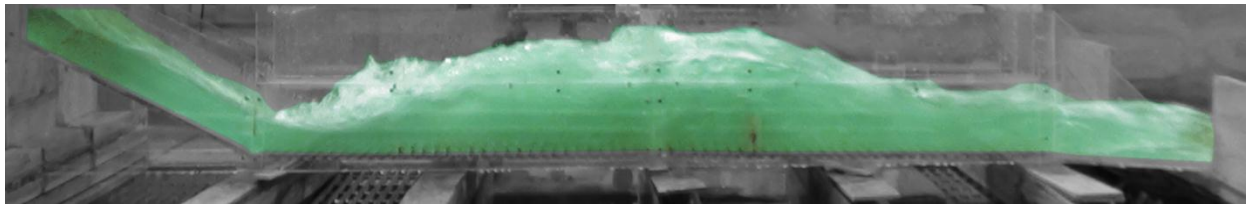


Figure A21: Experiment 7C for 1% Slope

Table A7: Experiment 7 for 1.0% Slope Using Open Channel Flow Condition with a 3” Sill at 26” from the End with 30 Flat Faced Friction Blocks at 12” from the Toe

| H.J. | Run | H    | W <sub>temp</sub> | Q      | V <sub>u/s</sub> | Y <sub>s</sub> | Y <sub>toe</sub> | Y <sub>1</sub> | Y <sub>2</sub> | Y <sub>d/s</sub> | Fr1 | V <sub>1</sub>   | V <sub>2</sub> | V <sub>d/s</sub> | L     | X  | ΔE     | THL    | E <sub>2</sub> /E <sub>1</sub> |
|------|-----|------|-------------------|--------|------------------|----------------|------------------|----------------|----------------|------------------|-----|------------------|----------------|------------------|-------|----|--------|--------|--------------------------------|
| Y    | 7A  | 0.8d | -                 | 0.9648 | 2.4120           | 2.00           | 1.75             | 1.75           | 6.50           | 2.35             | 3.8 | 8.1904<br>P-tube | 2.4626         | 5.3080<br>P-tube | 17.00 | 42 | 2.3554 | 9.0841 | 0.6338                         |
| Y    | 7B  | 1.0d | -                 | 1.2364 | 2.4728           | 2.63           | 2.13             | 2.13           | 9.00           | 3.50             | 3.5 | 8.4580<br>P-tube | 4.0985         | 5.7915<br>P-tube | 19.00 | 36 | 4.2285 | 8.1894 | 0.6645                         |
| Y    | 7C  | 1.2d | -                 | 1.5837 | 2.6395           | 3.25           | 2.75             | 2.63           | 7.50           | 3.50             | 3.3 | 8.7081<br>P-tube | 4.3340         | 6.4906<br>P-tube | 19.00 | 40 | 1.4639 | 7.9482 | 0.7000                         |

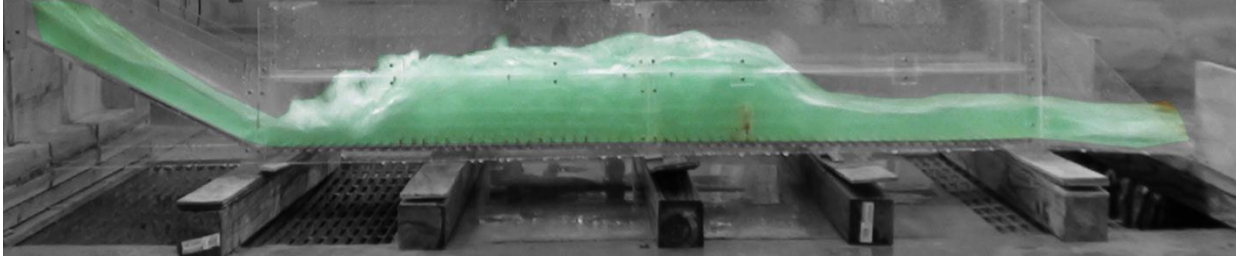


Figure A22: Experiment 8A for 1% Slope

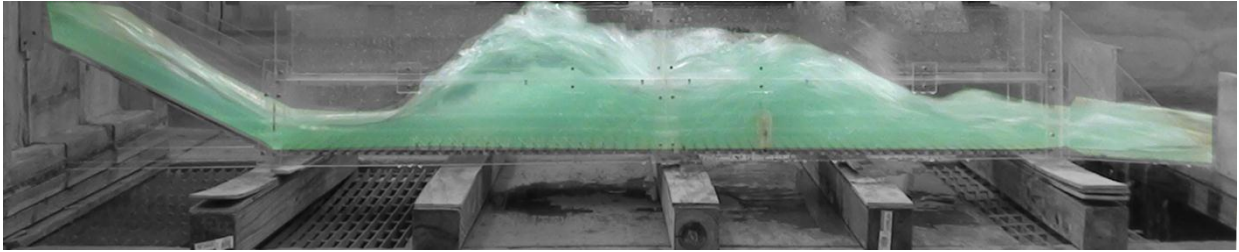


Figure A23: Experiment 8B for 1% Slope

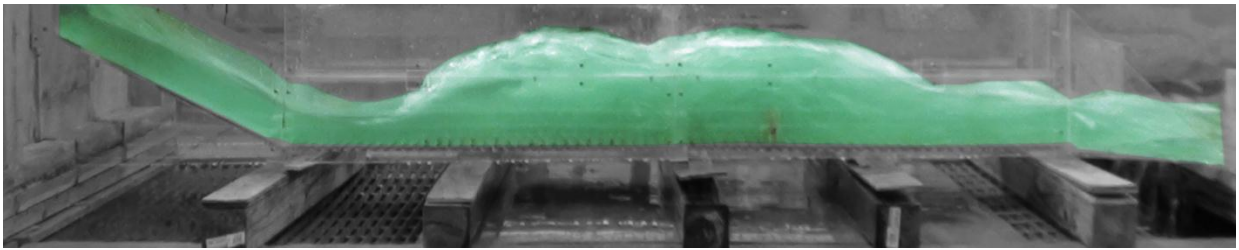


Figure A24: Experiment 8C for 1% Slope

Table A8: Experiment 8 for 1.0% Slope Using Open Channel Flow Condition with a 3” Sill at 26” from the End with 45 Flat Faced Friction Blocks at 12” from the Toe

| H.J. | Run | H    | W <sub>temp</sub> | Q      | V <sub>u/s</sub> | Y <sub>s</sub> | Y <sub>toe</sub> | Y <sub>1</sub> | Y <sub>2</sub> | Y <sub>d/s</sub> | Fr <sub>1</sub> | V <sub>1</sub>   | V <sub>2</sub> | V <sub>d/s</sub> | L     | X  | ΔE     | THL    | E <sub>2</sub> /E <sub>1</sub> |
|------|-----|------|-------------------|--------|------------------|----------------|------------------|----------------|----------------|------------------|-----------------|------------------|----------------|------------------|-------|----|--------|--------|--------------------------------|
| Y    | 8A  | 0.8d | -                 | 0.9606 | 2.4015           | 1.85           | 1.75             | 1.75           | 7.00           | 2.25             | 3.7             | 8.1081<br>P-tube | 2.8373         | 5.2470<br>P-tube | 18.00 | 39 | 2.9531 | 9.2646 | 0.6385                         |
| Y    | 8B  | 1.0d | -                 | 1.2619 | 2.5238           | 2.85           | 2.13             | 2.13           | 7.85           | 3.00             | 3.5             | 8.2719<br>P-tube | 4.1763         | 5.7915<br>P-tube | 17.00 | 34 | 2.7982 | 8.7369 | 0.6749                         |
| Y    | 8C  | 1.2d | -                 | 1.5987 | 2.6645           | 3.13           | 2.75             | 2.65           | 9.50           | 3.50             | 3.3             | 8.8214<br>P-tube | 3.0646         | 6.2805<br>P-tube | 22.00 | 33 | 3.1918 | 8.4729 | 0.6958                         |

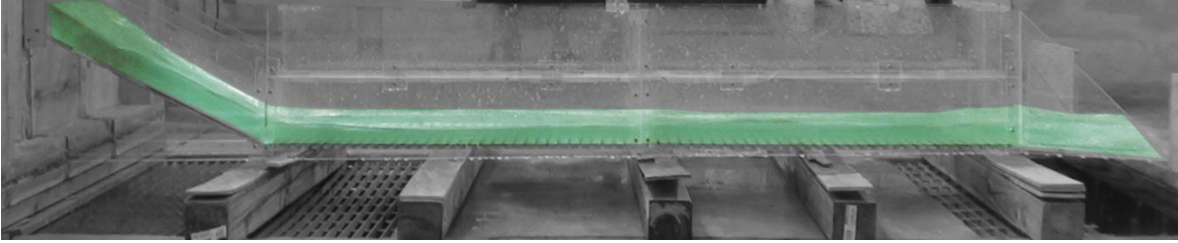


Figure A25: Experiment 9A for 0.6% Slope

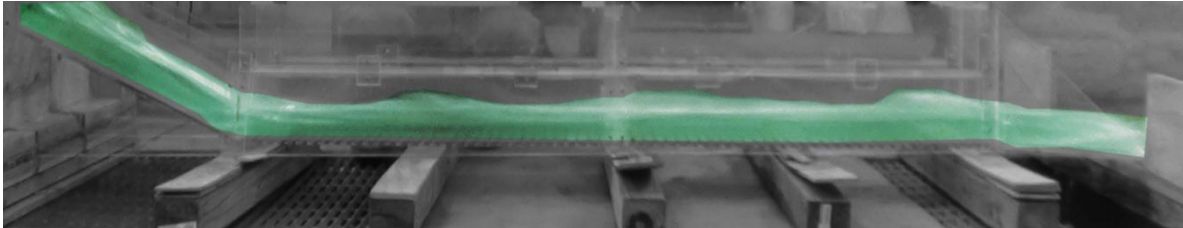


Figure A26: Experiment 9B for 0.6% Slope

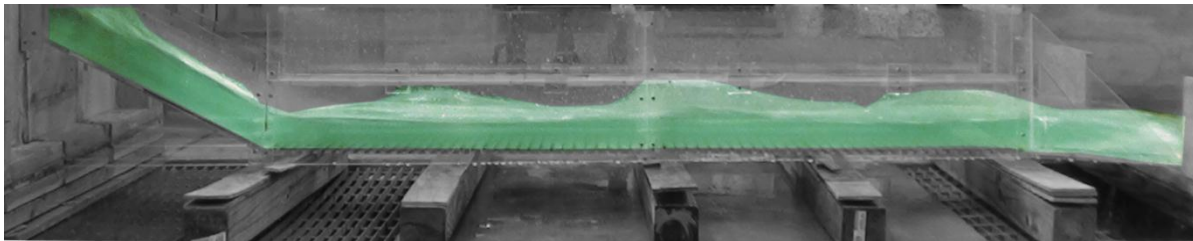


Figure A27: Experiment 9C for 0.6% Slope

Table A9: Experiment 9 for 0.6% Slope Using Open Channel Flow Condition with No Sill in the Culvert

| H.J. | Run | H    | $W_{temp}$ | Q      | $V_{u/s}$ | $Y_s$ | $Y_{loc}$ | $Y_1$ | $Y_2$ | $Y_{d/s}$ | Fr1 | $V_1$            | $V_2$ | $V_{d/s}$        | L | X | $\Delta E$ | THL    | $E_2/E_1$ |
|------|-----|------|------------|--------|-----------|-------|-----------|-------|-------|-----------|-----|------------------|-------|------------------|---|---|------------|--------|-----------|
| N    | 9A  | 0.8d | -          | 0.9852 | 2.4630    | 2.13  | 1.85      | -     | -     | 1.65      | 4.1 | 8.2719<br>P-tube | -     | 8.1412<br>P-tube | - | - | -          | 2.7304 | -         |
| N    | 9B  | 1.0d | -          | 1.2364 | 2.4728    | 2.62  | 2.38      | -     | -     | 2.00      | 3.9 | 8.9722<br>P-tube | -     | 8.5118<br>P-tube | - | - | -          | 2.4393 | -         |
| N    | 9C  | 1.2d | -          | 1.6622 | 2.7703    | 3.35  | 3.00      | -     | -     | 2.35      | 3.7 | 9.1937<br>P-tube | -     | 8.9722<br>P-tube | - | - | -          | 2.0801 | -         |



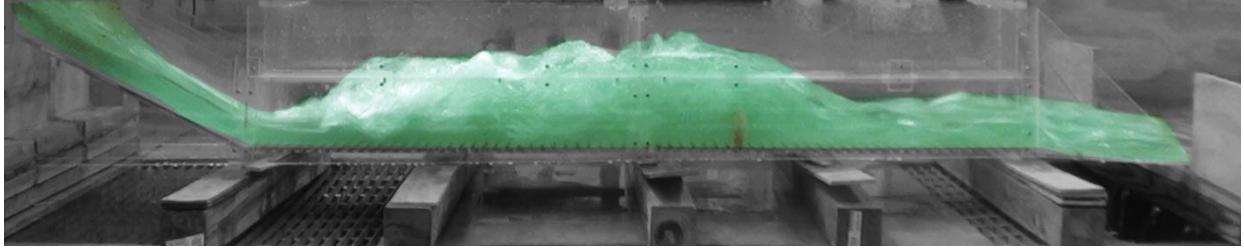


Figure A28: Experiment 10A for 0.6% Slope

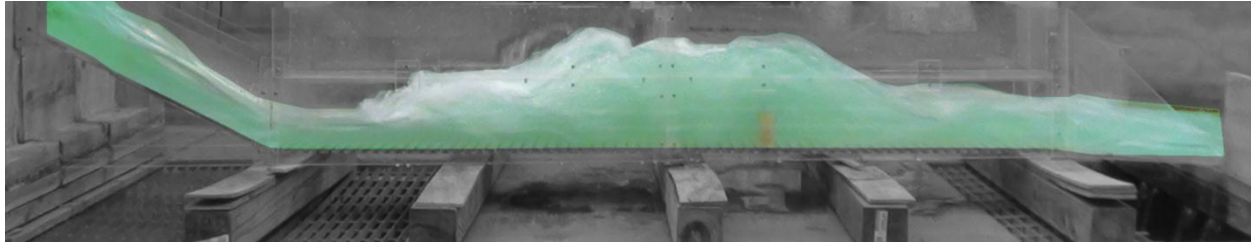


Figure A29: Experiment 10B for 0.6% Slope

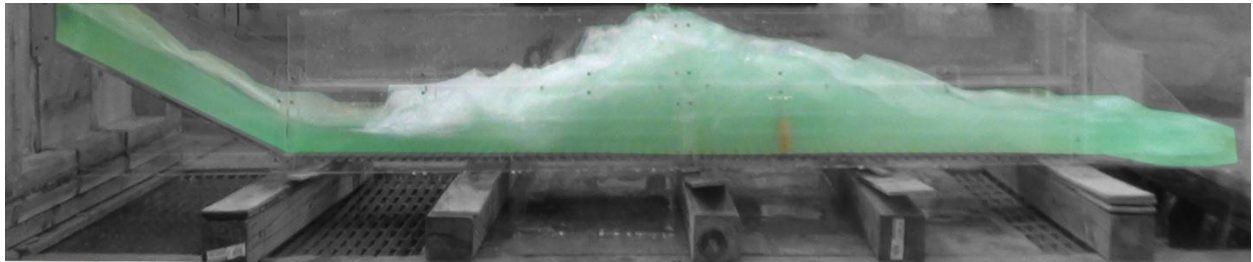


Figure A30: Experiment 10C for 0.6% Slope

Table A10: Experiment 10 for 0.6% Slope Using Open Channel Flow Condition with a 3" Sill at 26" from the End

| H.J. | Run | H    | W <sub>temp</sub> | Q      | V <sub>u/s</sub> | Y <sub>s</sub> | Y <sub>toe</sub> | Y <sub>1</sub> | Y <sub>2</sub> | Y <sub>d/s</sub> | Fr <sub>1</sub> | V <sub>1</sub>   | V <sub>2</sub> | V <sub>d/s</sub> | L     | X  | ΔE     | THL    | E <sub>2</sub> /E <sub>1</sub> |
|------|-----|------|-------------------|--------|------------------|----------------|------------------|----------------|----------------|------------------|-----------------|------------------|----------------|------------------|-------|----|--------|--------|--------------------------------|
| Y    | 10A | 0.8d | -                 | 0.9973 | 2.4933           | 2.13           | 1.75             | 1.65           | 8.25           | 2.35             | 3.9             | 8.1904<br>P-tube | 2.5900         | 5.2470<br>P-tube | 19.00 | 40 | 5.2800 | 9.2783 | 0.6202                         |
| Y    | 10B | 1.0d | -                 | 1.2460 | 2.4920           | 2.75           | 2.13             | 2.13           | 8.75           | 3.13             | 3.5             | 8.2719<br>P-tube | 3.1509         | 5.6031<br>P-tube | 21.00 | 34 | 3.8916 | 8.9772 | 0.6749                         |
| Y    | 10C | 1.2d | -                 | 1.6086 | 2.6810           | 3.13           | 2.85             | 2.50           | 9.50           | 3.75             | 3.2             | 8.3526<br>P-tube | 4.1763         | 6.0187<br>P-tube | 23.00 | 35 | 3.6105 | 8.8393 | 0.7076                         |

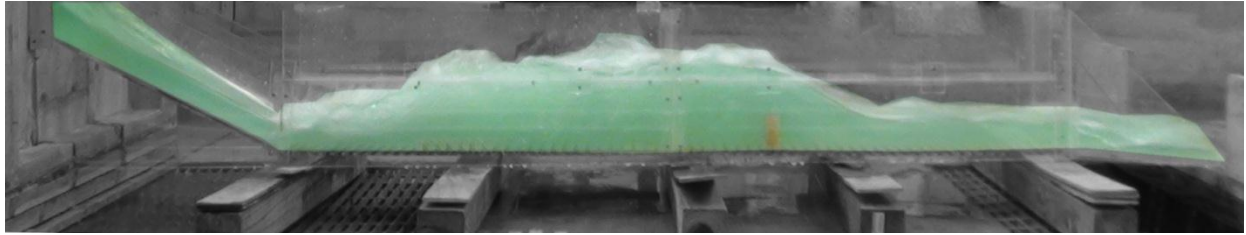


Figure A31: Experiment 11A for 0.6% Slope

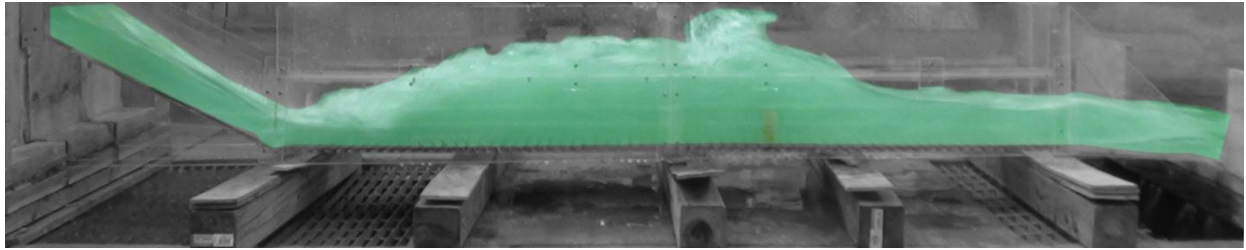


Figure A32: Experiment 11B for 0.6% Slope

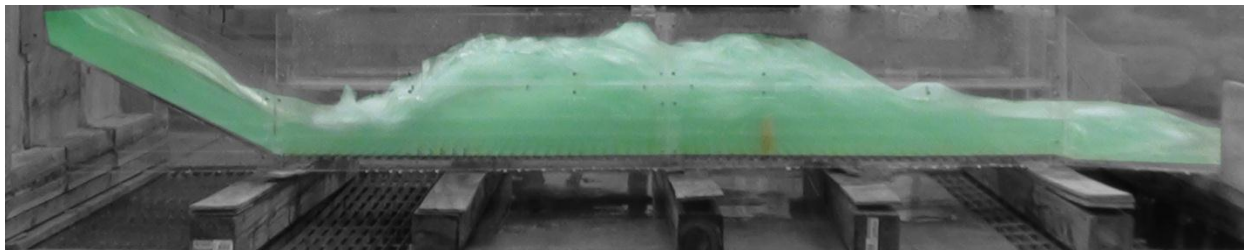


Figure A33: Experiment 11C for 0.6% Slope

Table A11: Experiment 11 for 0.6% Slope Using Open Channel Flow Condition with a 3” Sill at 26” from the End and 15 Flat Faced Friction Blocks at 12” from the Toe

| H.J. | Run | H    | W <sub>temp</sub> | Q      | V <sub>u/s</sub> | Y <sub>s</sub> | Y <sub>toe</sub> | Y <sub>1</sub> | Y <sub>2</sub> | Y <sub>d/s</sub> | Fr1 | V <sub>1</sub>   | V <sub>2</sub> | V <sub>d/s</sub> | L     | X  | ΔE     | THL    | E <sub>2</sub> /E <sub>1</sub> |
|------|-----|------|-------------------|--------|------------------|----------------|------------------|----------------|----------------|------------------|-----|------------------|----------------|------------------|-------|----|--------|--------|--------------------------------|
| Y    | 11A | 0.8d | -                 | 0.9648 | 2.4120           | 2.00           | 1.85             | 1.85           | 7.50           | 2.50             | 3.5 | 7.7286<br>P-tube | 2.5900         | 5.2470<br>P-tube | 18.50 | 42 | 3.2498 | 9.0541 | 0.6737                         |
| Y    | 11B | 1.0d | -                 | 1.2776 | 2.5552           | 2.85           | 2.35             | 2.25           | 8.25           | 3.25             | 3.3 | 8.1412<br>P-tube | 3.6629         | 5.5550<br>P-tube | 19.50 | 39 | 2.9091 | 9.0166 | 0.6951                         |
| Y    | 11C | 1.2d | -                 | 1.5887 | 2.6478           | 3.25           | 2.85             | 2.65           | 9.25           | 3.50             | 3.2 | 8.5118<br>P-tube | 3.8417         | 6.3443<br>P-tube | 21.50 | 37 | 2.9321 | 8.3064 | 0.7124                         |

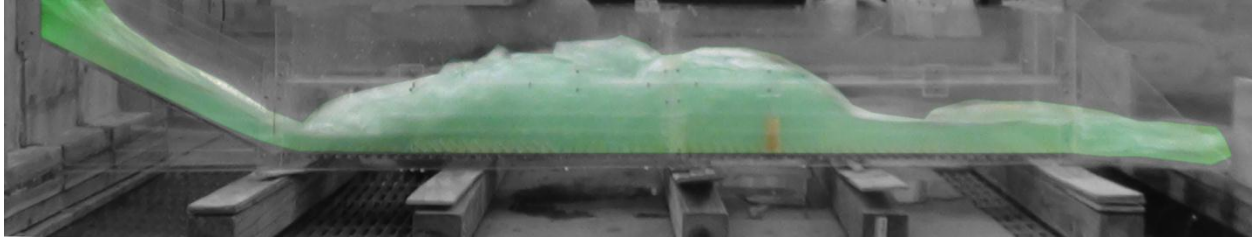


Figure A34: Experiment 12A for 0.6% Slope

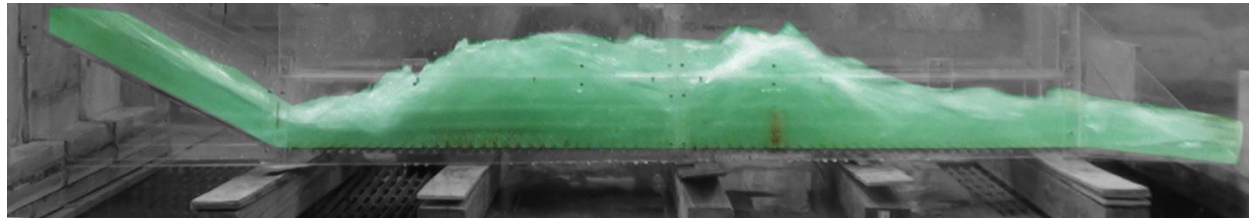


Figure A35: Experiment 12B for 0.6% Slope

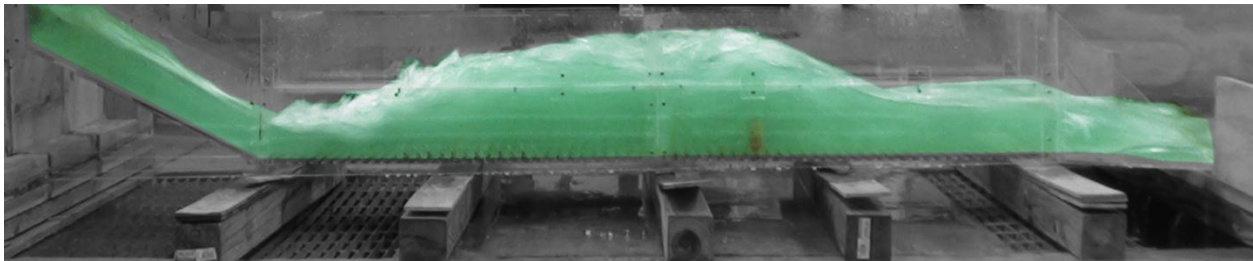


Figure A36: Experiment 12C for 0.6% Slope

Table A12: Experiment 12 for 0.6% Slope Using Open Channel Flow Condition with a 3” Sill at 26” from the End with 30 Flat Faced Friction Blocks at 12” from the Toe

| H.J. | Run | H    | $W_{temp}$ | Q      | $V_{u/s}$ | $Y_s$ | $Y_{toe}$ | $Y_1$ | $Y_2$ | $Y_{d/s}$ | Fr1 | $V_1$            | $V_2$  | $V_{d/s}$        | L     | X  | $\Delta E$ | THL    | $E_2/E_1$ |
|------|-----|------|------------|--------|-----------|-------|-----------|-------|-------|-----------|-----|------------------|--------|------------------|-------|----|------------|--------|-----------|
| Y    | 12A | 0.8d | -          | 0.9771 | 2.4428    | 2.00  | 1.85      | 1.85  | 7.50  | 2.50      | 3.6 | 7.9409<br>P-tube | 2.3166 | 5.2470<br>P-tube | 18.00 | 39 | 3.2498     | 9.0819 | 0.6611    |
| Y    | 12B | 1.0d | -          | 1.2619 | 2.5238    | 2.63  | 2.50      | 2.13  | 7.50  | 3.25      | 3.5 | 8.2881<br>P-tube | 3.6629 | 5.5550<br>P-tube | 16.00 | 40 | 2.4234     | 8.9826 | 0.6740    |
| Y    | 12C | 1.2d | -          | 1.6550 | 2.7583    | 3.50  | 3.00      | 2.55  | 9.75  | 3.75      | 3.2 | 8.3943<br>P-tube | 4.0125 | 6.2377<br>P-tube | 22.50 | 40 | 3.7531     | 8.4177 | 0.7099    |

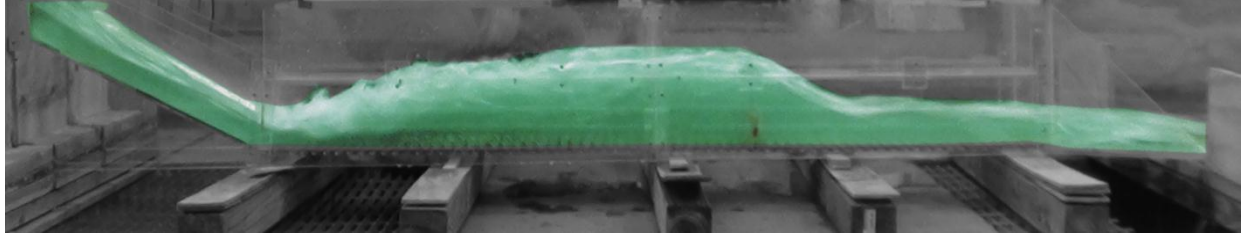


Figure A37: Experiment 13A for 0.6% Slope

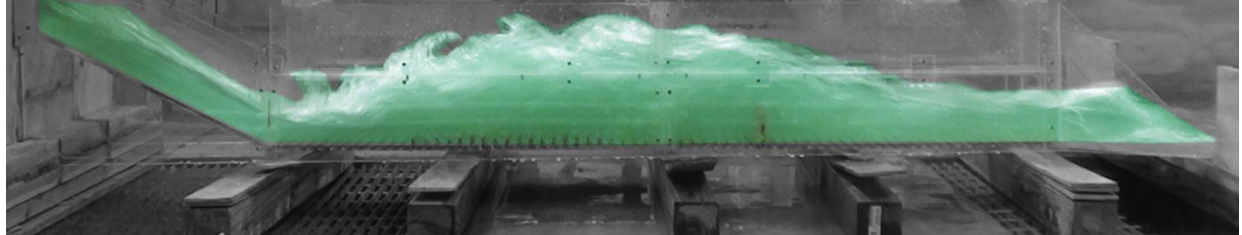


Figure A38: Experiment 13B for 0.6% Slope

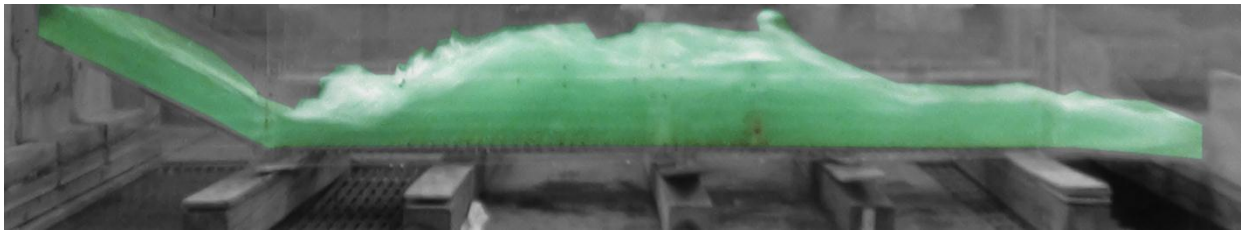


Figure A39: Experiment 13C for 0.6% Slope

Table A13: Experiment 13 for 0.6% Slope Using Open Channel Flow Condition with a 3” Sill at 26” from the End with 45 Flat Faced Friction Blocks at 12” from the Toe

| H.J. | Run | H    | W <sub>temp</sub> | Q      | V <sub>u/s</sub> | Y <sub>s</sub> | Y <sub>toe</sub> | Y <sub>1</sub> | Y <sub>2</sub> | Y <sub>d/s</sub> | Fr1 | V <sub>1</sub>   | V <sub>2</sub> | V <sub>d/s</sub> | L     | X  | ΔE     | THL    | E <sub>2</sub> /E <sub>1</sub> |
|------|-----|------|-------------------|--------|------------------|----------------|------------------|----------------|----------------|------------------|-----|------------------|----------------|------------------|-------|----|--------|--------|--------------------------------|
| Y    | 13A | 0.8d | -                 | 0.9268 | 2.3170           | 1.87           | 2.00             | 2.00           | 7.50           | 2.62             | 3.4 | 7.8149<br>P-tube | 2.3166         | 5.1801<br>P-tube | 14.00 | 42 | 2.7729 | 8.9803 | 0.6867                         |
| Y    | 13B | 1.0d | -                 | 1.2588 | 2.5176           | 2.75           | 2.13             | 2.00           | 8.00           | 3.25             | 3.6 | 8.3526<br>P-tube | 3.2762         | 5.7915<br>P-tube | 19.00 | 40 | 3.3750 | 8.4811 | 0.6557                         |
| Y    | 13C | 1.2d | -                 | 1.5862 | 2.6437           | 3.35           | 2.75             | 2.50           | 9.00           | 3.50             | 3.2 | 8.3526<br>P-tube | 4.0125         | 6.3443<br>P-tube | 21.00 | 39 | 3.0514 | 8.3023 | 0.7076                         |

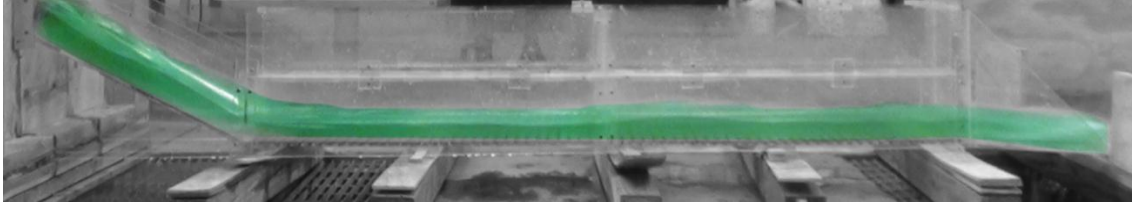


Figure A40: Experiment 14A for 0.3% Slope

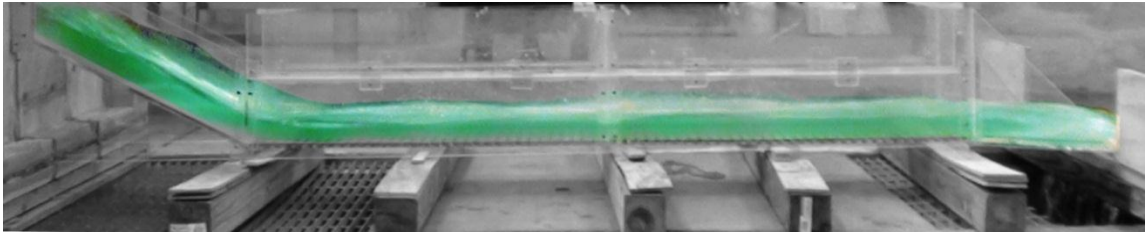


Figure A41: Experiment 14B for 0.3% Slope

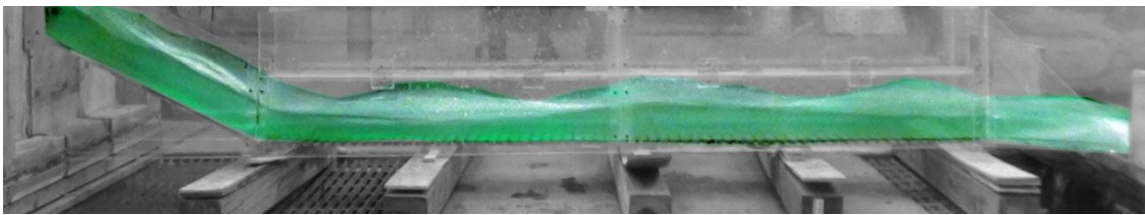


Figure A42: Experiment 14C for 0.3% Slope

Table A14: Experiment 14 for 0.3% Slope Using Open Channel Flow Condition with No Sill in the Culvert

| H.J. | Run | H    | $W_{temp}$ | Q      | $V_{u/s}$ | $Y_s$ | $Y_{toe}$ | $Y_1$ | $Y_2$ | $Y_{d/s}$ | Fr1 | $V_1$            | $V_2$ | $V_{d/s}$        | L | X | $\Delta E$ | THL    | $E_2/E_1$ |
|------|-----|------|------------|--------|-----------|-------|-----------|-------|-------|-----------|-----|------------------|-------|------------------|---|---|------------|--------|-----------|
| N    | 14A | 0.8d | -          | 0.9852 | 2.4630    | 2.00  | 1.85      | -     | -     | 1.75      | 4.1 | 8.7081<br>P-tube | -     | 8.0250<br>P-tube | - | - | -          | 2.9804 | -         |
| N    | 14B | 1.0d | -          | 1.2202 | 2.4404    | 2.65  | 2.25      | -     | -     | 2.00      | 4.0 | 8.8669<br>P-tube | -     | 8.1904<br>P-tube | - | - | -          | 3.4097 | -         |
| N    | 14C | 1.2d | -          | 1.5787 | 2.6312    | 3.50  | 2.75      | -     | -     | 2.35      | 3.5 | 9.1645<br>P-tube | -     | 8.8669<br>P-tube | - | - | -          | 2.2900 | -         |

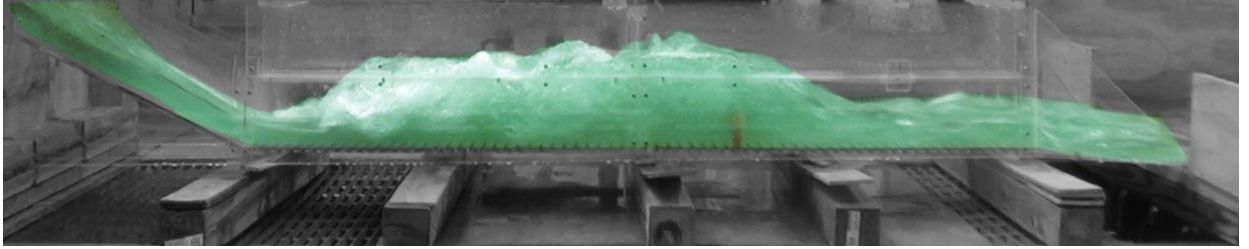


Figure A43: Experiment 15A for 0.3% Slope

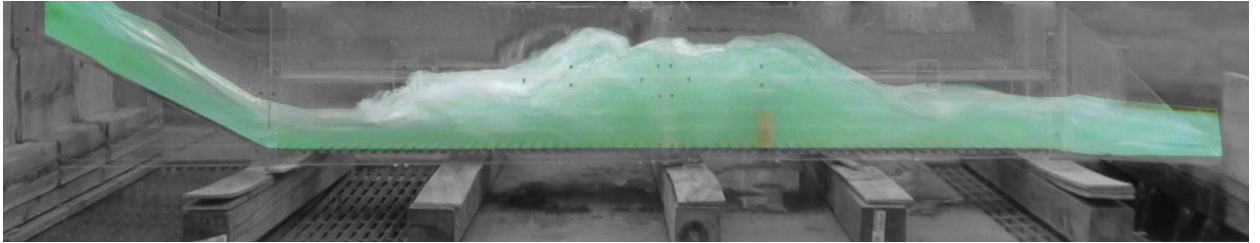


Figure A44: Experiment 15B for 0.3% Slope

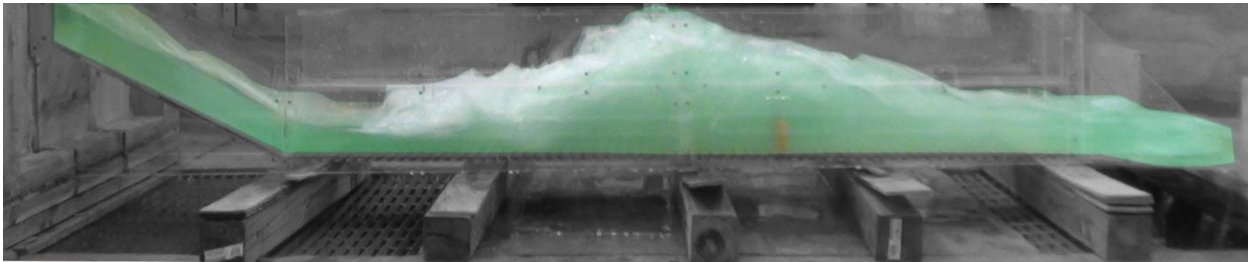


Figure A45: Experiment 15C for 0.3% Slope

Table A15: Experiment 15 for 0.3% Slope Using Open Channel Flow Condition with a 3" Sill at 26" from the End

| H.J. | Run | H    | $W_{temp}$ | Q      | $V_{u/s}$ | $Y_s$ | $Y_{toe}$ | $Y_1$ | $Y_2$ | $Y_{d/s}$ | Fr1 | $V_1$            | $V_2$  | $V_{d/s}$        | L     | X  | $\Delta E$ | THL    | $E_2/E_1$ |
|------|-----|------|------------|--------|-----------|-------|-----------|-------|-------|-----------|-----|------------------|--------|------------------|-------|----|------------|--------|-----------|
| Y    | 15A | 0.8d | -          | 0.9354 | 2.3385    | 2.25  | 2.00      | 2.00  | 8.00  | 2.75      | 3.5 | 8.0250<br>P-tube | 2.9757 | 5.0913<br>P-tube | 15.00 | 40 | 3.3750     | 9.0390 | 0.6744    |
| Y    | 15B | 1.0d | -          | 1.2202 | 2.4404    | 2.65  | 2.13      | 2.13  | 8.50  | 3.00      | 3.4 | 8.1904<br>P-tube | 3.0646 | 5.6031<br>P-tube | 20.50 | 40 | 3.5691     | 9.0597 | 0.6795    |
| Y    | 15C | 1.2d | -          | 1.5606 | 2.6015    | 3.25  | 2.65      | 2.50  | 9.50  | 3.25      | 3.3 | 8.4326<br>P-tube | 3.4749 | 5.7915<br>P-tube | 24.00 | 41 | 3.6105     | 9.7611 | 0.7032    |

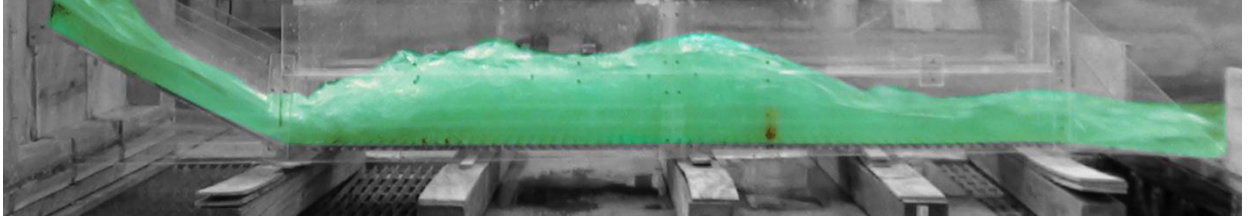


Figure A46: Experiment 16A for 0.3% Slope

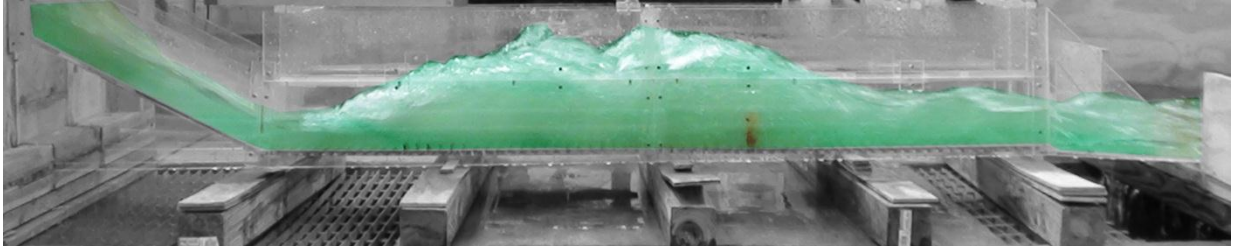


Figure A47. Experiment 16B for 0.3% Slope

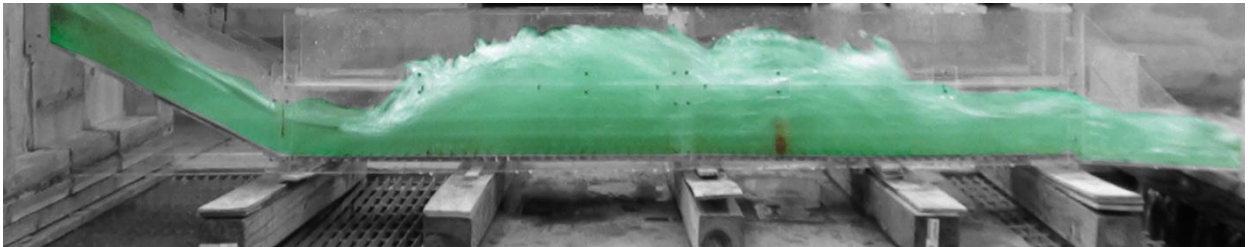


Figure A48: Experiment 16C for 0.3% Slope

Table A16: Experiment 16 for 0.3% Slope Using Open Channel Flow Condition with a 3'' Sill at 26'' from the End with 15 Flat Faced Friction Blocks at 12'' from the Toe

| H.J. | Run | H    | W <sub>temp</sub> | Q      | V <sub>u/s</sub> | Y <sub>s</sub> | Y <sub>toe</sub> | Y <sub>1</sub> | Y <sub>2</sub> | Y <sub>d/s</sub> | Fr1 | V <sub>1</sub>   | V <sub>2</sub> | V <sub>d/s</sub> | L     | X  | ΔE     | THL    | E <sub>2</sub> /E <sub>1</sub> |
|------|-----|------|-------------------|--------|------------------|----------------|------------------|----------------|----------------|------------------|-----|------------------|----------------|------------------|-------|----|--------|--------|--------------------------------|
| Y    | 16A | 0.8d | -                 | 0.9648 | 2.4120           | 2.00           | 2.00             | 2.00           | 7.50           | 2.50             | 3.3 | 7.5955<br>P-tube | 2.3166         | 5.3080<br>P-tube | 18.00 | 42 | 2.7729 | 8.9341 | 0.6999                         |
| Y    | 16B | 1.0d | -                 | 1.2396 | 2.4792           | 2.75           | 2.50             | 2.13           | 8.25           | 3.00             | 3.5 | 8.2719<br>P-tube | 3.1509         | 5.4329<br>P-tube | 20.00 | 38 | 3.2611 | 9.4453 | 0.6749                         |
| Y    | 16C | 1.2d | -                 | 1.5762 | 2.6270           | 3.50           | 2.75             | 2.65           | 9.75           | 3.75             | 3.2 | 8.4643<br>P-tube | 3.9109         | 6.3443<br>P-tube | 22.50 | 36 | 3.4631 | 8.0359 | 0.7149                         |

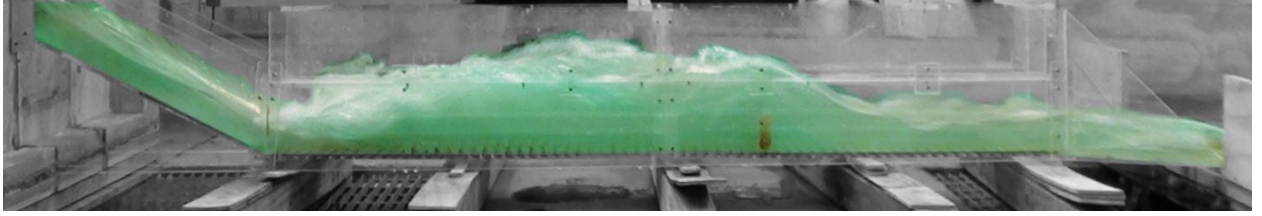


Figure A49: Experiment 17A for 0.3% Slope

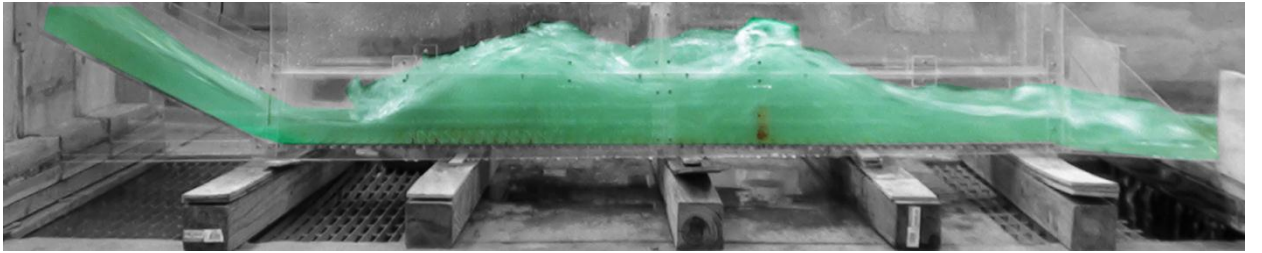


Figure A50: Experiment 17B for 0.3% Slope

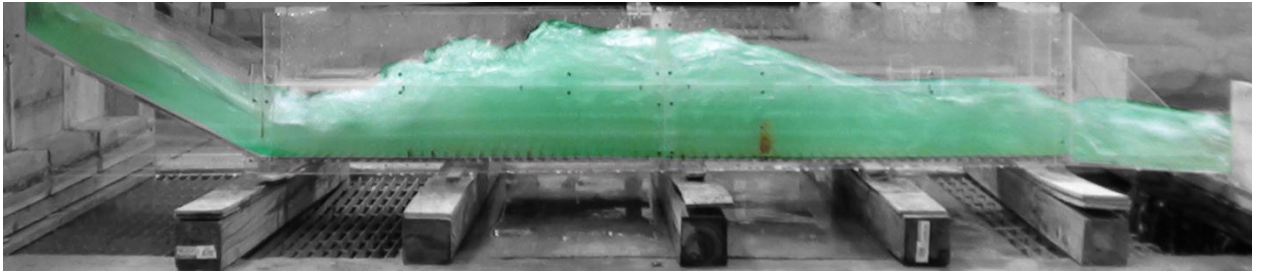


Figure A51: Experiment 17C for 0.3% Slope

Table A17: Experiment 17 for 0.3% Slope Using Open Channel Flow Condition with a 3" Sill at 26" from the End with 30 Flat Faced Friction Blocks at 12" from the Toe

| H.J. | Run | H    | $W_{temp}$ | Q      | $V_{u/s}$ | $Y_s$ | $Y_{toe}$ | $Y_1$ | $Y_2$ | $Y_{d/s}$ | Fr1 | $V_1$            | $V_2$  | $V_{d/s}$        | L     | X  | $\Delta E$ | THL    | $E_2/E_1$ |
|------|-----|------|------------|--------|-----------|-------|-----------|-------|-------|-----------|-----|------------------|--------|------------------|-------|----|------------|--------|-----------|
| Y    | 17A | 0.8d | -          | 0.9812 | 2.4530    | 2.00  | 1.75      | 1.75  | 7.75  | 2.35      | 3.7 | 7.9746<br>P-tube | 2.3166 | 5.3080<br>P-tube | 17.00 | 42 | 3.9816     | 9.1212 | 0.6462    |
| Y    | 17B | 1.0d | -          | 1.2460 | 2.4920    | 2.75  | 2.25      | 2.25  | 8.00  | 3.50      | 3.4 | 8.3526<br>P-tube | 3.4749 | 5.4329<br>P-tube | 15.00 | 34 | 2.6404     | 8.9572 | 0.6831    |
| Y    | 17C | 1.2d | -          | 1.6037 | 2.6728    | 3.50  | 2.75      | 2.50  | 10.00 | 3.63      | 3.3 | 8.4326<br>P-tube | 4.1763 | 6.0631<br>P-tube | 22.00 | 42 | 4.2188     | 8.8512 | 0.7032    |



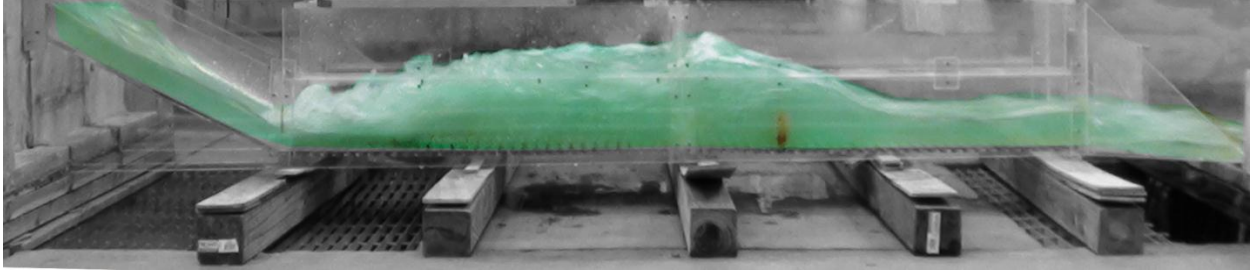


Figure A52: Experiment 18A for 0.3% Slope

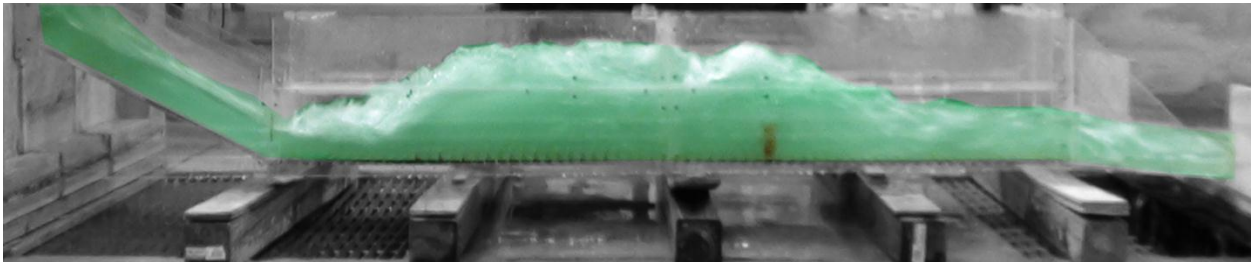


Figure A53: Experiment 18B for 0.3% Slope

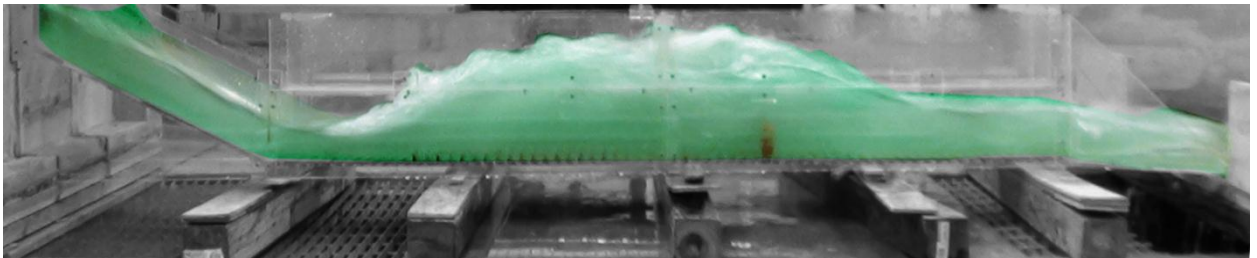


Figure A54: Experiment 18C for 0.3% Slope

Table A18: Experiment 18 for 0.3% Slope Using Open Channel Flow Condition with a 3” Sill at 26” from the End with 45 Flat Faced Friction Blocks at 12” from the Toe

| H.J. | Run | H    | W <sub>temp</sub> | Q      | V <sub>u/s</sub> | Y <sub>s</sub> | Y <sub>toe</sub> | Y <sub>1</sub> | Y <sub>2</sub> | Y <sub>d/s</sub> | Fr1 | V <sub>1</sub>   | V <sub>2</sub> | V <sub>d/s</sub> | L     | X  | ΔE     | THL    | E <sub>2</sub> /E <sub>1</sub> |
|------|-----|------|-------------------|--------|------------------|----------------|------------------|----------------|----------------|------------------|-----|------------------|----------------|------------------|-------|----|--------|--------|--------------------------------|
| Y    | 18A | 0.8d | -                 | 0.9565 | 2.3913           | 2.25           | 2.13             | 2.00           | 7.25           | 2.63             | 3.3 | 7.6833<br>P-tube | 2.0062         | 5.3080<br>P-tube | 17.00 | 42 | 2.4949 | 9.9855 | 0.6946                         |
| Y    | 18B | 1.0d | -                 | 1.2651 | 2.5302           | 2.85           | 2.25             | 2.13           | 8.50           | 3.00             | 3.5 | 8.3526<br>P-tube | 3.8417         | 5.5550<br>P-tube | 20.00 | 39 | 3.5691 | 9.2429 | 0.6704                         |
| Y    | 18C | 1.2d | -                 | 1.5762 | 2.6270           | 3.25           | 2.75             | 2.50           | 9.50           | 3.50             | 3.3 | 8.4326<br>P-tube | 4.0125         | 6.2377<br>P-tube | 22.00 | 37 | 3.6105 | 8.5359 | 0.7032                         |

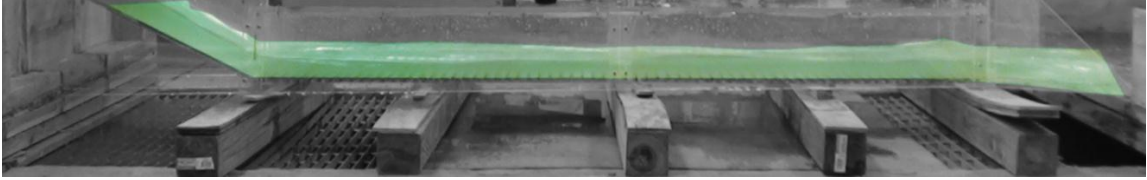


Figure A55: Experiment 19A for 1% Slope

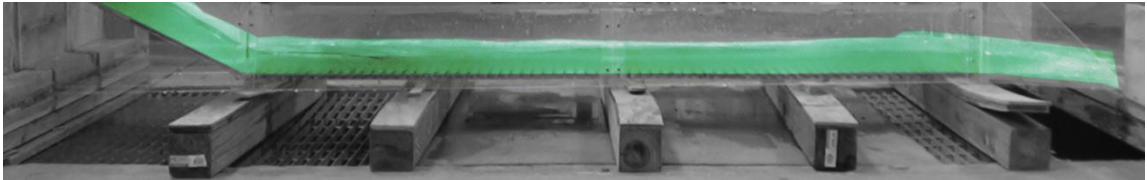


Figure A56: Experiment 19B for 1% Slope

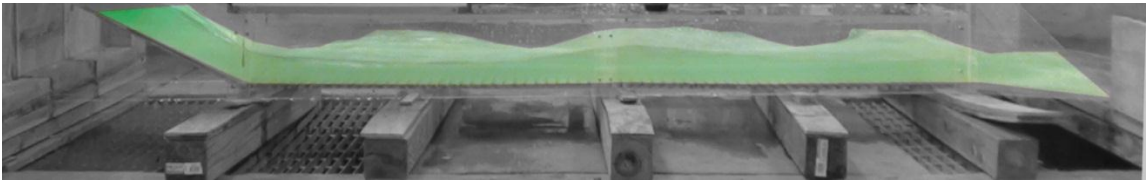


Figure A57: Experiment 19C for 1% Slope

Table A19: Experiment 19 for 1.0% Slope Horizontal Channel Using Pressure Flow Condition without any Friction Blocks

| H.J. | Run | H    | $W_{temp}$ | Q      | $V_{u/s}$ | $Y_s$ | $Y_{toe}$ | $Y_1$ | $Y_2$ | $Y_{d/s}$ | Fr1 | $V_1$            | $V_2$ | $V_{d/s}$        | L | X | $\Delta E$ | THL    | $E_2/E_1$ |
|------|-----|------|------------|--------|-----------|-------|-----------|-------|-------|-----------|-----|------------------|-------|------------------|---|---|------------|--------|-----------|
| N    | 19A | 0.8d | -          | 0.9771 | 2.4428    | 2.13  | 1.85      | 1.75  | 1.75  | 1.75      | 3.9 | 8.4326<br>P-tube | -     | 8.0250<br>P-tube | - | - | -          | 2.9619 | -         |
| N    | 19B | 1.0d | -          | 1.2656 | 2.5312    | 2.75  | 2.25      | 2.00  | 2.13  | 2.00      | 3.7 | 8.6679<br>P-tube | -     | 8.5902<br>P-tube | - | - | -          | 2.2438 | -         |
| N    | 19C | 1.2d | -          | 1.5736 | 2.6227    | 2.83  | 2.75      | 2.50  | 2.50  | 2.50      | 3.5 | 8.9722<br>P-tube | -     | 8.9422<br>P-tube | - | - | -          | 1.8817 | -         |

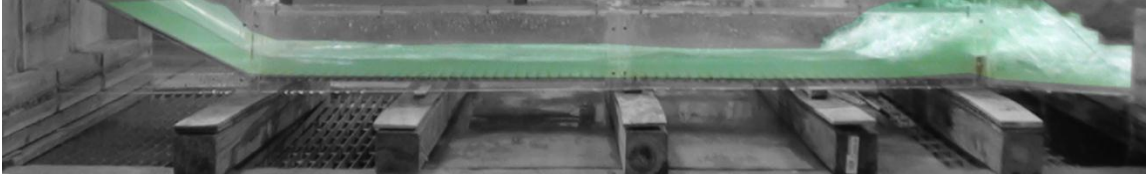


Figure A58: Experiment 20A for 1% Slope

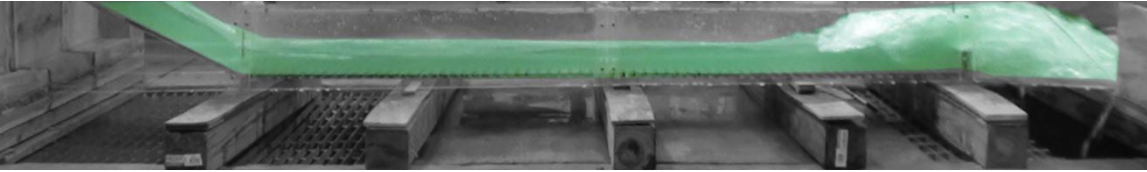


Figure A59: Experiment 20B for 1% Slope

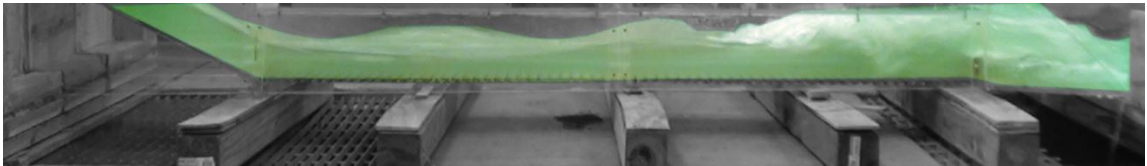


Figure A60: Experiment 20C for 1% Slope

Table A20: Experiment 20 for 1.0% Slope Using Pressure Flow Condition with a 2” End Sill

| H.J. | Run | H    | W <sub>temp</sub> | Q      | V <sub>u/s</sub> | Y <sub>s</sub> | Y <sub>toe</sub> | Y <sub>1</sub> | Y <sub>2</sub> | Y <sub>d/s</sub> | Fr1 | V <sub>1</sub>   | V <sub>2</sub> | V <sub>d/s</sub> | L     | X     | ΔE     | THL    | E <sub>2</sub> /E <sub>1</sub> |
|------|-----|------|-------------------|--------|------------------|----------------|------------------|----------------|----------------|------------------|-----|------------------|----------------|------------------|-------|-------|--------|--------|--------------------------------|
| Y    | 20A | 0.8d | -                 | 0.9893 | 2.4733           | 2.00           | 1.75             | 1.75           | 8.61           |                  | 3.8 | 8.2719<br>P-tube | 6.6539         | 6.6539<br>P-tube | 11.00 | 12.00 | 5.3609 | 8.4898 | 0.6303                         |
| Y    | 20B | 1.0d | -                 | 1.2524 | 2.5048           | 2.75           | 2.13             | 2.00           | 9.25           |                  | 3.6 | 8.3526<br>P-tube | 7.3258         | 7.3258<br>P-tube | 11.00 | 14.00 | 5.1449 | 7.9691 | 0.6570                         |
| Y    | 20C | 1.2d | -                 | 1.5837 | 2.6395           | 3.50           | 2.85             | 3.13           | 12.39          |                  | 3.1 | 9.0763<br>P-tube | 7.6833         | 7.6833<br>P-tube | 15.00 | 18.00 | 5.1137 | 8.2982 | 0.7233                         |

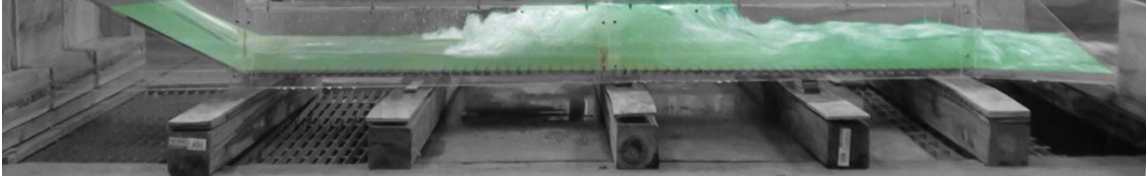


Figure A61: Experiment 21A for 1% Slope

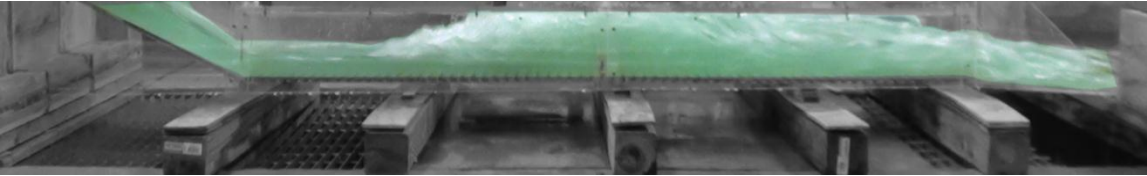


Figure A62: Experiment 21B for 1% Slope

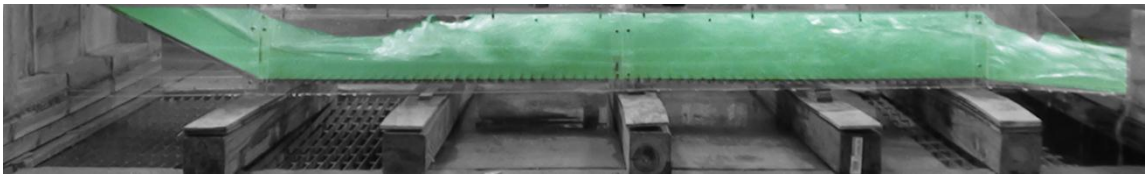


Figure A63: Experiment 21C for 1% Slope

Table A21: Experiment 21 for 1.0% Slope Using Pressure Flow Condition with a 2” Sill at 34” from the End

| H.J. | Run | H    | W <sub>temp</sub> | Q      | V <sub>u/s</sub> | Y <sub>s</sub> | Y <sub>toe</sub> | Y <sub>1</sub> | Y <sub>2</sub> | Y <sub>d/s</sub> | Fr1 | V <sub>1</sub>   | V <sub>2</sub> | V <sub>d/s</sub> | L     | X     | ΔE     | THL    | E <sub>2</sub> /E <sub>1</sub> |
|------|-----|------|-------------------|--------|------------------|----------------|------------------|----------------|----------------|------------------|-----|------------------|----------------|------------------|-------|-------|--------|--------|--------------------------------|
| Y    | 21A | 0.8d | -                 | 0.9812 | 2.4530           | 2.00           | 1.85             | 1.50           | 7.22           | 3.00             | 3.7 | 7.5067<br>P-tube | 5.6031         | 4.9847<br>P-tube | 14.00 | 16.00 | 4.3245 | 9.0912 | 0.6396                         |
| Y    | 21B | 1.0d | -                 | 1.2460 | 2.4920           | 2.75           | 2.13             | 1.85           | 9.30           | 3.25             | 3.9 | 8.6679<br>P-tube | 6.0631         | 5.4968<br>P-tube | 14.50 | 22.00 | 6.0001 | 9.0772 | 0.6214                         |
| Y    | 21C | 1.2d | -                 | 1.5887 | 2.6478           | 3.50           | 2.65             | 2.13           | 8.67           | 3.50             | 3.2 | 7.6833<br>P-tube | 7.3258         | 6.1292<br>P-tube | 16.00 | 34.00 | 3.7924 | 8.8064 | 0.7112                         |

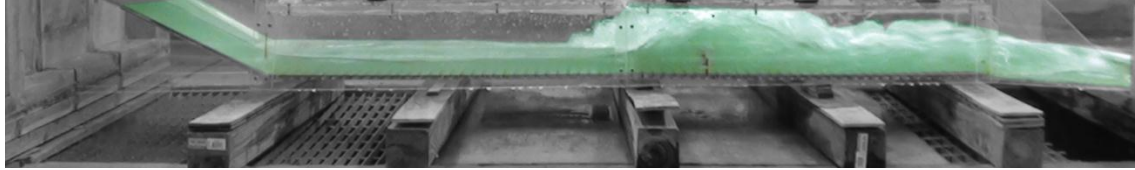


Figure A64: Experiment 22A for 1% Slope

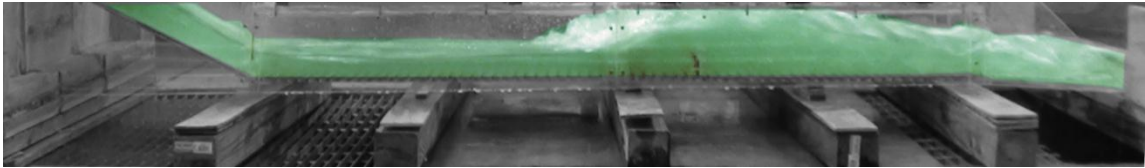


Figure A65: Experiment 22B for 1% Slope

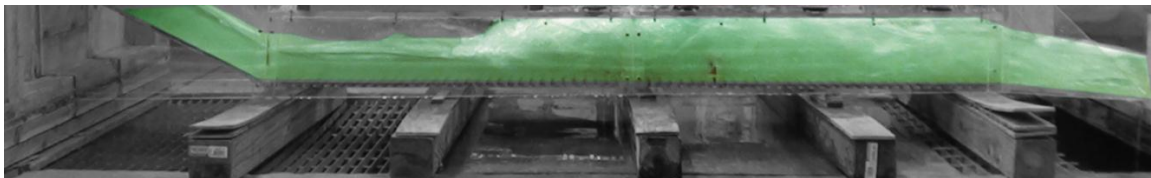


Figure A66: Experiment 22C for 1% Slope

Table A22: Experiment 22 for 1.0% Slope Using Pressure Flow Condition with a 2.5” Sill at 26” from the End

| H.J. | Run | H    | W <sub>temp</sub> | Q      | V <sub>u/s</sub> | Y <sub>s</sub> | Y <sub>loc</sub> | Y <sub>1</sub> | Y <sub>2</sub> | Y <sub>d/s</sub> | Fr <sub>1</sub> | V <sub>1</sub>   | V <sub>2</sub> | V <sub>d/s</sub> | L     | X     | ΔE     | THL    | E <sub>2</sub> /E <sub>1</sub> |
|------|-----|------|-------------------|--------|------------------|----------------|------------------|----------------|----------------|------------------|-----------------|------------------|----------------|------------------|-------|-------|--------|--------|--------------------------------|
| Y    | 22A | 0.8d | -                 | 0.9648 | 2.4120           | 1.85           | 1.75             | 1.50           | 7.81           | 2.75             | 4.0             | 8.0683<br>P-tube | 5.3080         | 4.9143<br>P-tube | 6.00  | 6.00  | 5.3690 | 9.4341 | 0.6061                         |
| Y    | 22B | 1.0d | -                 | 1.2524 | 2.5048           | 2.85           | 2.13             | 2.00           | 9.50           | 3.25             | 3.7             | 8.5589<br>P-tube | 6.6539         | 5.3080<br>P-tube | 9.50  | 14.00 | 5.5471 | 9.4691 | 0.6456                         |
| Y    | 22C | 1.2d | -                 | 1.6086 | 2.6810           | 3.25           | 2.75             | 2.50           | 10.69          | 4.00             | 3.4             | 8.6989<br>P-tube | 5.9062         | 5.5065<br>P-tube | 12.00 | 25.00 | 5.1389 | 9.6893 | 0.6904                         |

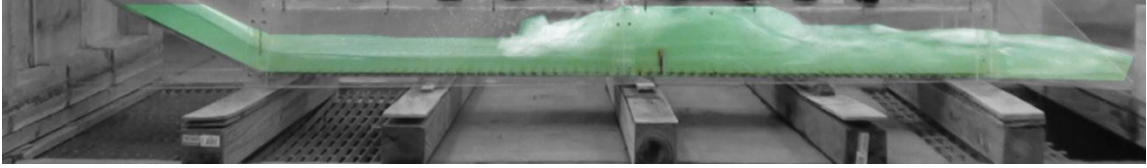


Figure A67: Experiment 23A for 1% Slope

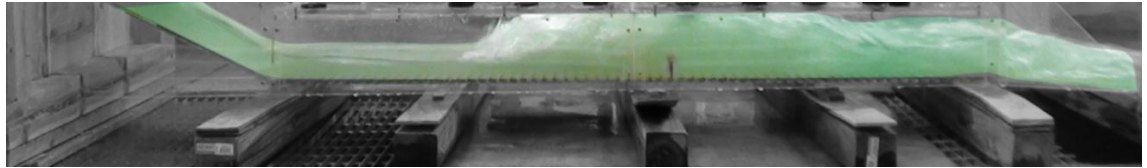


Figure A68: Experiment 23B for 1% Slope

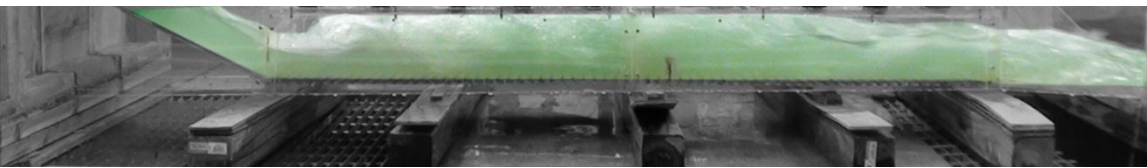


Figure A69: Experiment 23C for 1% Slope

Table A23: Experiment 23 for 1.0% Slope Using Pressure Flow Condition with a 2” Sill at 30” from the End

| H.J. | Run | H    | W <sub>temp</sub> | Q      | V <sub>u/s</sub> | Y <sub>s</sub> | Y <sub>toe</sub> | Y <sub>1</sub> | Y <sub>2</sub> | Y <sub>d/s</sub> | Fr <sub>1</sub> | V <sub>1</sub>   | V <sub>2</sub> | V <sub>d/s</sub> | L     | X     | ΔE     | THL    | E <sub>2</sub> /E <sub>1</sub> |
|------|-----|------|-------------------|--------|------------------|----------------|------------------|----------------|----------------|------------------|-----------------|------------------|----------------|------------------|-------|-------|--------|--------|--------------------------------|
| Y    | 23A | 0.8d | -                 | 0.9606 | 2.4015           | 2.00           | 1.75             | 1.50           | 7.77           | 2.75             | 4.0             | 8.0250<br>P-tube | 2.3166         | 5.1018<br>P-tube | 10.50 | 14.00 | 5.2842 | 9.0746 | 0.6086                         |
| Y    | 23B | 1.0d | -                 | 1.2524 | 2.5048           | 2.85           | 2.13             | 2.85           | 10.99          | 3.50             | 3.1             | 8.4643<br>P-tube | 2.8373         | 5.5550<br>P-tube | 13.50 | 21.00 | 4.3092 | 8.7191 | 0.7340                         |
| Y    | 23C | 1.2d | -                 | 1.6086 | 2.6810           | 3.35           | 2.75             | 2.50           | 10.65          | 4.00             | 3.3             | 8.6679<br>P-tube | 4.6332         | 6.5524<br>P-tube | 14.00 | 35.00 | 5.0803 | 7.3393 | 0.6921                         |



Figure A70: Experiment 24A for 1% Slope

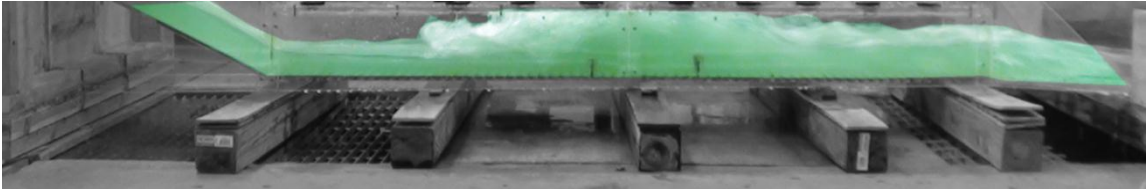


Figure A71. Experiment 24B for 1% Slope

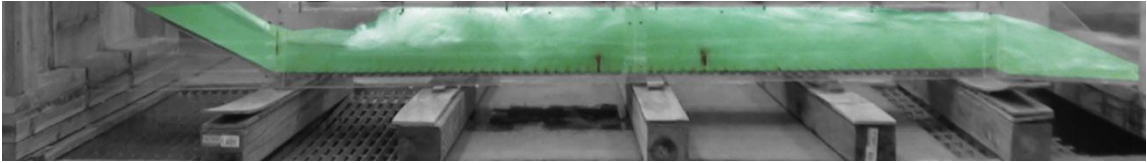


Figure A72: Experiment 24C for 1% Slope

Table A24: Experiment 24 for 1.0% Slope Using Pressure Flow Condition and a 1.5” Sill at 37” from the End and 2” Sill at 27” from the End

| H.J. | Run | H    | W <sub>temp</sub> | Q      | V <sub>u/s</sub> | Y <sub>s</sub> | Y <sub>toe</sub> | Y <sub>1</sub> | Y <sub>2</sub> | Y <sub>d/s</sub> | Fr1 | V <sub>1</sub>   | V <sub>2</sub> | V <sub>d/s</sub> | L     | X     | ΔE     | THL    | E <sub>2</sub> /E <sub>1</sub> |
|------|-----|------|-------------------|--------|------------------|----------------|------------------|----------------|----------------|------------------|-----|------------------|----------------|------------------|-------|-------|--------|--------|--------------------------------|
| Y    | 24A | 0.8d | -                 | 0.9523 | 2.3808           | 1.85           | 1.75             | 1.35           | 7.65           | 2.85             | 4.3 | 8.2719<br>P-tube | 4.1763         | 4.9143<br>P-tube | 11.00 | 22.00 | 6.0529 | 9.3061 | 0.5707                         |
| Y    | 24B | 1.0d | -                 | 1.2524 | 2.5048           | 2.85           | 2.50             | 2.00           | 9.63           | 3.35             | 3.7 | 8.6679<br>P-tube | 5.9062         | 5.5550<br>P-tube | 12.00 | 26.00 | 5.7660 | 8.8691 | 0.6396                         |
| Y    | 24C | 1.2d | -                 | 1.5987 | 2.6645           | 3.25           | 2.85             | 2.65           | 11.29          | 4.25             | 3.3 | 8.9272<br>P-tube | 6.7540         | 6.0187<br>P-tube | 13.50 | 33.00 | 5.3909 | 8.3229 | 0.6919                         |

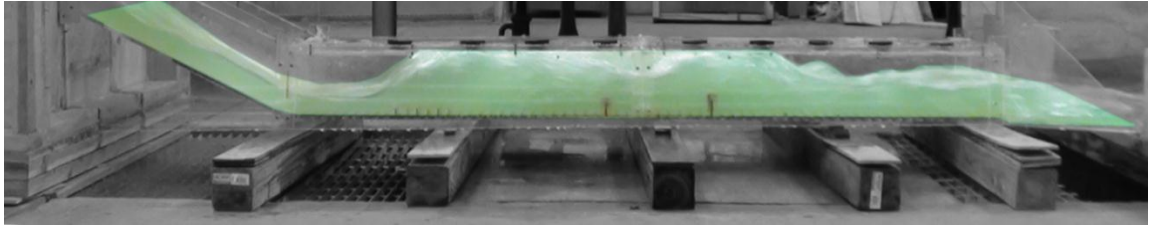


Figure A73: Experiment 25A for 1% Slope

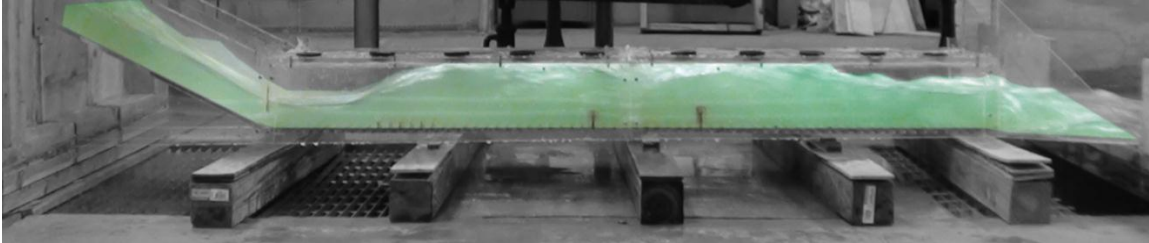


Figure A74. Experiment 25B for 1% Slope

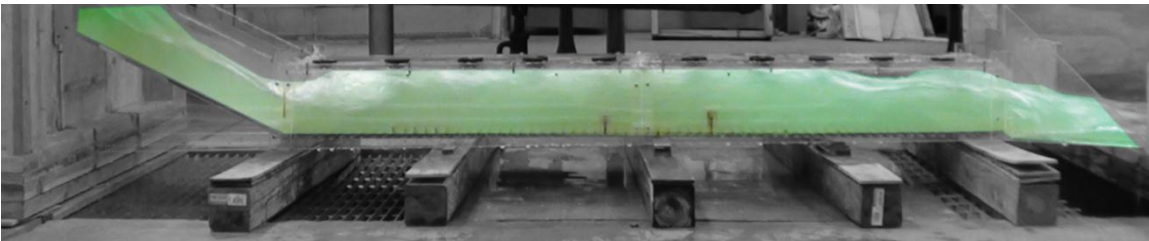


Figure A75. Experiment 25C for 1% Slope

Table A25: Experiment 25 for 1% Slope Using Pressure Flow Condition with 15 Flat Faced Friction Blocks and a 1.5" Sill at 37" from the End and a 2" Sill at 27" from the End

| H.J. | Run | H    | W <sub>temp</sub> | Q      | V <sub>u/s</sub> | Y <sub>s</sub> | Y <sub>toe</sub> | Y <sub>1</sub> | Y <sub>2</sub> | Y <sub>d/s</sub> | Fr <sub>1</sub> | V <sub>1</sub>   | V <sub>2</sub> | V <sub>d/s</sub> | L     | X     | ΔE     | THL    | E <sub>2</sub> /E <sub>1</sub> |
|------|-----|------|-------------------|--------|------------------|----------------|------------------|----------------|----------------|------------------|-----------------|------------------|----------------|------------------|-------|-------|--------|--------|--------------------------------|
| Y    | 25A | 0.8d | -                 | 0.9606 | 2.4015           | 1.85           | 1.75             | 1.75           | 7.54           | 2.75             | 3.4             | 7.3258<br>P-tube | 3.6629         | 4.9143<br>P-tube | 7.50  | 35.50 | 3.6737 | 9.4246 | 0.6873                         |
| Y    | 25B | 1.0d | -                 | 1.2524 | 2.5048           | 2.85           | 2.13             | 2.25           | 9.22           | 3.25             | 3.2             | 7.9409<br>P-tube | 5.0489         | 5.1801<br>P-tube | 8.00  | 33.00 | 4.0804 | 9.7191 | 0.7085                         |
| Y    | 25C | 1.2d | -                 | 1.5812 | 2.6353           | 3.25           | 3.00             | 3.00           | 10.72          | 4.00             | 2.9             | 8.1081<br>P-tube | 5.1801         | 5.7915<br>P-tube | 12.00 | 41.00 | 3.5733 | 9.0441 | 0.7657                         |



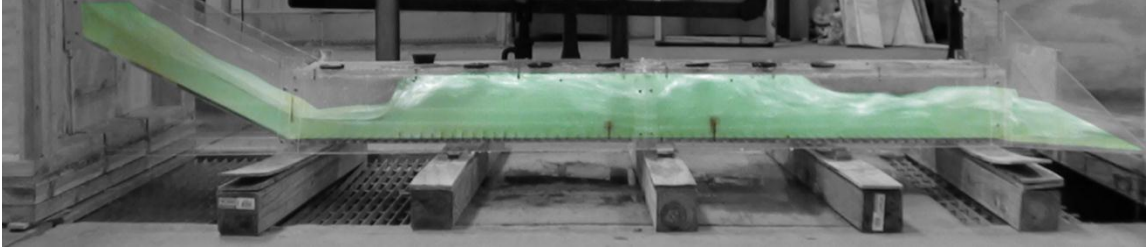


Figure A76: Experiment 26A for 1% Slope

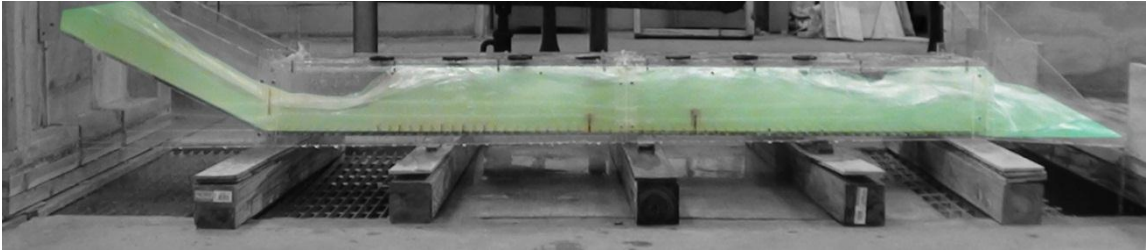


Figure A77: Experiment 26B for 1% Slope

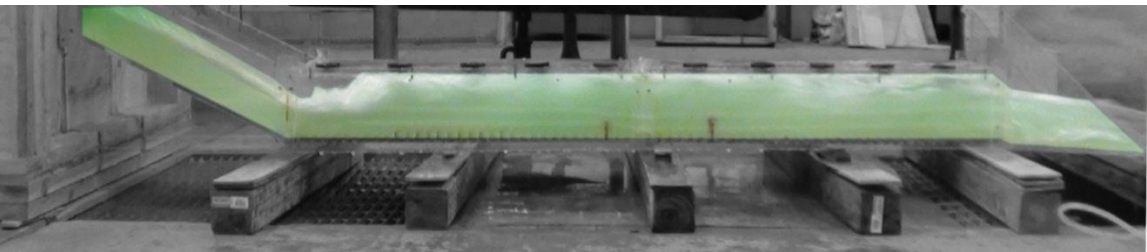


Figure A78: Experiment 26C for 1% Slope

Table A26: Experiment 26 for 1.0% Slope Using Pressure Flow Condition with 30 Flat Faced Friction Blocks and a 1.5" Sill at 37" from the End and a 2" Sill at 27" from the End

| H.J. | Run | H    | W <sub>temp</sub> | Q      | V <sub>u/s</sub> | Y <sub>s</sub> | Y <sub>loc</sub> | Y <sub>1</sub> | Y <sub>2</sub> | Y <sub>d/s</sub> | Fr1 | V <sub>1</sub>   | V <sub>2</sub> | V <sub>d/s</sub> | L     | X     | ΔE     | THL    | E <sub>2</sub> /E <sub>1</sub> |
|------|-----|------|-------------------|--------|------------------|----------------|------------------|----------------|----------------|------------------|-----|------------------|----------------|------------------|-------|-------|--------|--------|--------------------------------|
| Y    | 26A | 0.8d | -                 | 0.9771 | 2.4428           | 2.00           | 1.75             | 1.75           | 8.6127         | 2.75             | 3.8 | 8.2719<br>P-tube | 2.4626         | 4.7758<br>P-tube | 8.00  | 33.00 | 5.3609 | 9.7119 | 0.6303                         |
| Y    | 26B | 1.0d | -                 | 1.2524 | 2.5048           | 2.85           | 2.13             | 2.00           | 8.9499         | 3.25             | 3.5 | 8.1081<br>P-tube | 4.0125         | 5.5065<br>P-tube | 8.00  | 33.00 | 4.6884 | 9.0691 | 0.6710                         |
| Y    | 26C | 1.2d | -                 | 1.6012 | 2.6687           | 3.50           | 3.00             | 3.00           | 10.9599        | 4.25             | 2.9 | 8.2719<br>P-tube | 5.5065         | 6.1858<br>P-tube | 12.00 | 41.00 | 3.8348 | 7.9470 | 0.7565                         |

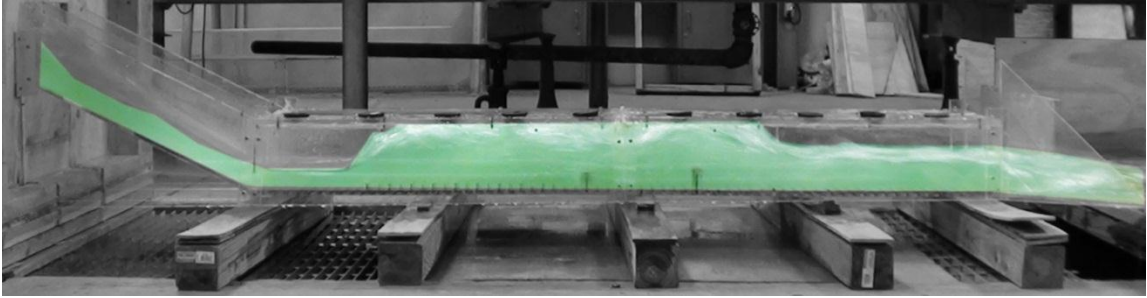


Figure A79: Experiment 27A for 1% Slope

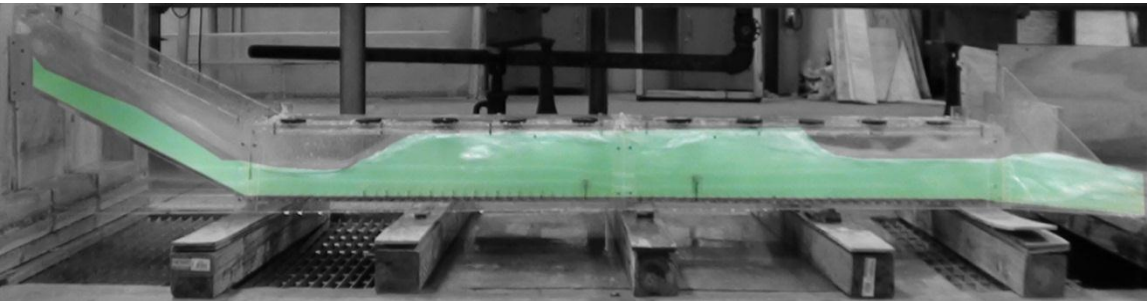


Figure A80: Experiment 27B for 1% Slope

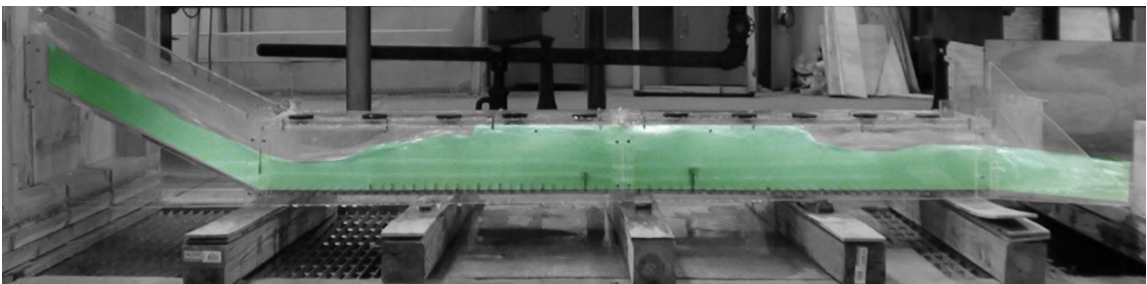


Figure A81: Experiment 27C for 1% Slope

Table A27: Experiment 27 for 1.0% Slope Using Pressure Flow Condition with 45 Flat Faced Friction Blocks and a 1.5” Sill at 37” from the End and a 2” Sill at 27” from the End

| H.J. | Run | H    | W <sub>temp</sub> | Q      | V <sub>u/s</sub> | Y <sub>s</sub> | Y <sub>toe</sub> | Y <sub>1</sub> | Y <sub>2</sub> | Y <sub>d/s</sub> | Fr1  | V <sub>1</sub>   | V <sub>2</sub> | V <sub>d/s</sub> | L     | X     | ΔE     | THL    | E <sub>2</sub> /E <sub>1</sub> |
|------|-----|------|-------------------|--------|------------------|----------------|------------------|----------------|----------------|------------------|------|------------------|----------------|------------------|-------|-------|--------|--------|--------------------------------|
| Y    | 27A | 0.8d | -                 | 0.9648 | 2.4120           | 1.85           | 1.75             | 1.75           | 8.8854         | 2.75             | 3.9  | 8.5118<br>P-tube | 4.0125         | 4.9143<br>P-tube | 7.50  | 34.00 | 5.8409 | 9.4341 | 0.6170                         |
| Y    | 27B | 1.0d | -                 | 1.2524 | 2.5048           | 2.85           | 2.13             | 2.00           | 9.4403         | 3.25             | 3.72 | 8.5118<br>P-tube | 2.3166         | 5.6745<br>P-tube | 9.00  | 33.00 | 5.4538 | 8.7191 | 0.6481                         |
| Y    | 27C | 1.2d | -                 | 1.5762 | 2.6270           | 3.13           | 2.75             | 2.50           | 10.0000        | 3.75             | 3.2  | 8.1904<br>P-tube | 3.2762         | 6.3443<br>P-tube | 10.00 | 34.00 | 4.2188 | 8.0359 | 0.7188                         |

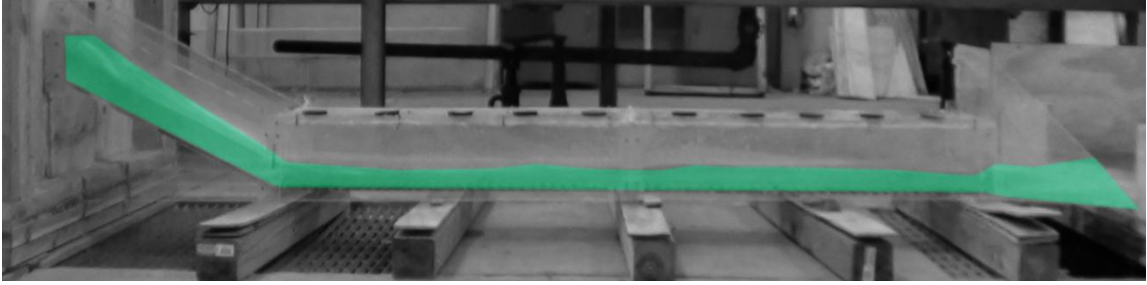


Figure A82: Experiment 28A for 0.6% Slope

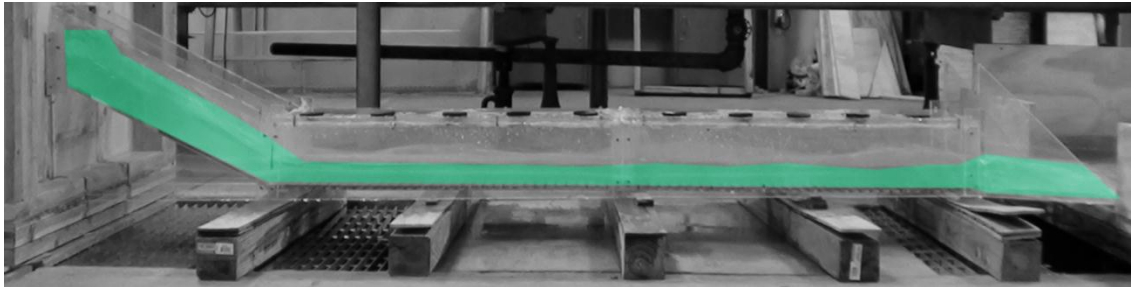


Figure A83: Experiment 28B for 0.6% Slope

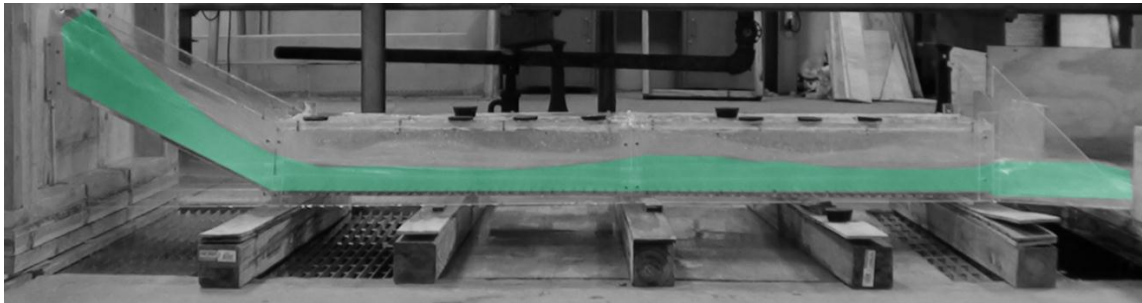


Figure A84: Experiment 28C for 0.6% Slope

Table A28: Experiment 28 for 0.6% Slope Horizontal Channel Using Pressure Flow Condition without any Friction Blocks

| H.J. | Run | H    | $W_{temp}$ | Q      | $V_{u/s}$ | $Y_s$ | $Y_{toe}$ | $Y_1$ | $Y_2$ | $Y_{d/s}$ | Fr1 | $V_1$            | $V_2$  | $V_{d/s}$        | L | X | $\Delta E$ | THL    | $E_2/E_1$ |
|------|-----|------|------------|--------|-----------|-------|-----------|-------|-------|-----------|-----|------------------|--------|------------------|---|---|------------|--------|-----------|
| N    | 28A | 0.8d | -          | 0.9648 | 2.4120    | 2.00  | 1.85      | 1.35  | 1.50  | 1.50      | 4.6 | 8.7081<br>P-tube | 8.1904 | 7.7701<br>P-tube | - | - | -          | 3.9341 | -         |
| N    | 28B | 1.0d | -          | 1.2524 | 2.5048    | 2.75  | 2.25      | 1.85  | 2.00  | 2.00      | 4.0 | 8.8214<br>P-tube | 8.8669 | 8.5118<br>P-tube | - | - | -          | 2.4691 | -         |
| N    | 28C | 1.2d | -          | 1.5862 | 2.6437    | 2.85  | 2.75      | 2.35  | 2.25  | 3.50      | 3.6 | 9.0466<br>P-tube | 8.8971 | 8.6679<br>P-tube | - | - | -          | 1.8023 | -         |

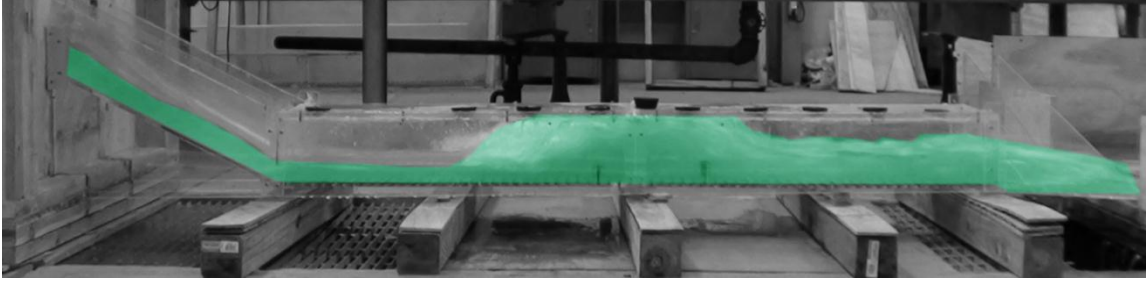


Figure A85: Experiment 29A for 0.6% Slope

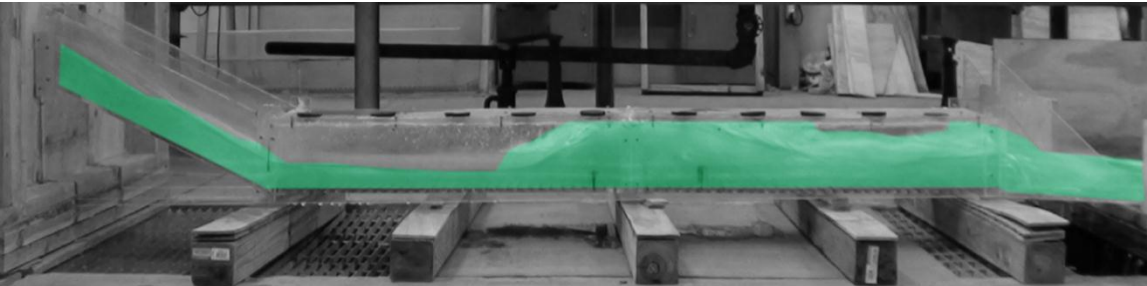


Figure A86: Experiment 29B for 0.6% Slope

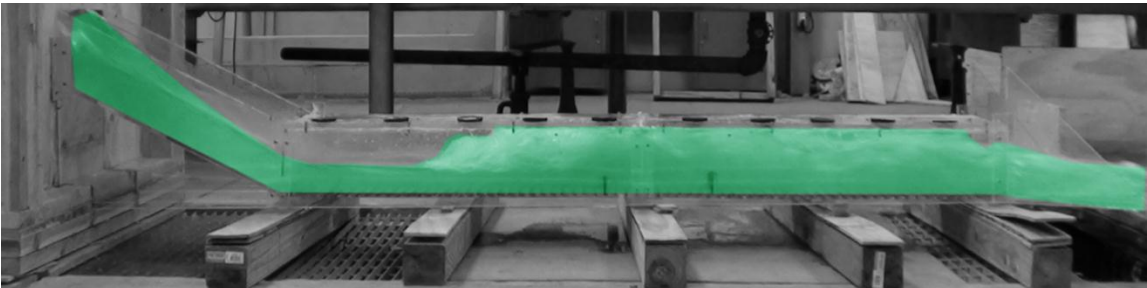


Figure A87: Experiment 29C for 0.6% Slope

Table A29: Experiment 29 for 0.6% Slope Using Pressure Flow Condition and a 1.5" Sill at 37" from the End and a 2" Sill at 27" from the End

| H.J. | Run | H    | $W_{temp}$ | Q      | $V_{u/s}$ | $Y_s$ | $Y_{toe}$ | $Y_1$ | $Y_2$ | $Y_{d/s}$ | Fr1 | $V_1$            | $V_2$  | $V_{d/s}$        | L     | X     | $\Delta E$ | THL    | $E_2/E_1$ |
|------|-----|------|------------|--------|-----------|-------|-----------|-------|-------|-----------|-----|------------------|--------|------------------|-------|-------|------------|--------|-----------|
| Y    | 29A | 0.8d | -          | 0.9648 | 2.4120    | 2.00  | 1.75      | 1.50  | 8.03  | 3.00      | 4.1 | 8.2719<br>P-tube | 3.0646 | 5.1018<br>P-tube | 9.00  | 22.00 | 5.7764     | 8.8341 | 0.5946    |
| Y    | 29B | 1.0d | -          | 1.2524 | 2.5048    | 2.75  | 1.13      | 1.75  | 8.97  | 3.25      | 4.0 | 8.5902<br>P-tube | 4.9143 | 5.6745<br>P-tube | 9.00  | 22.00 | 6.0025     | 8.7191 | 0.6127    |
| Y    | 29C | 1.2d | -          | 1.6086 | 2.6810    | 2.50  | 2.75      | 2.50  | 10.65 | 3.75      | 3.3 | 8.6679<br>P-tube | 4.9143 | 5.6745<br>P-tube | 14.00 | 35.00 | 5.0803     | 9.5893 | 0.6921    |

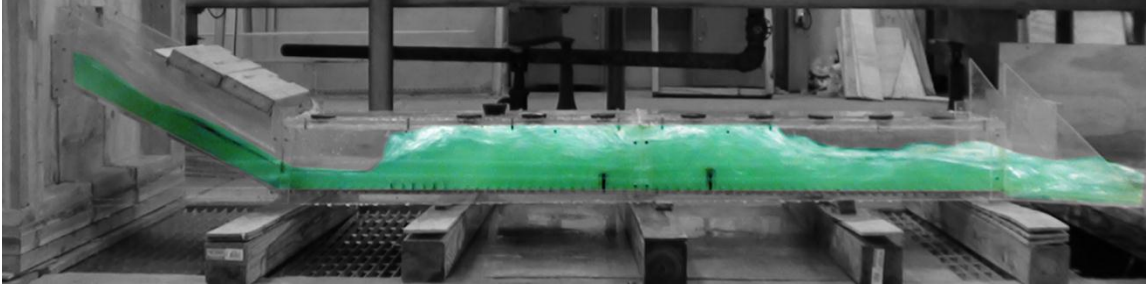


Figure A88: Experiment 30A for 0.6% Slope

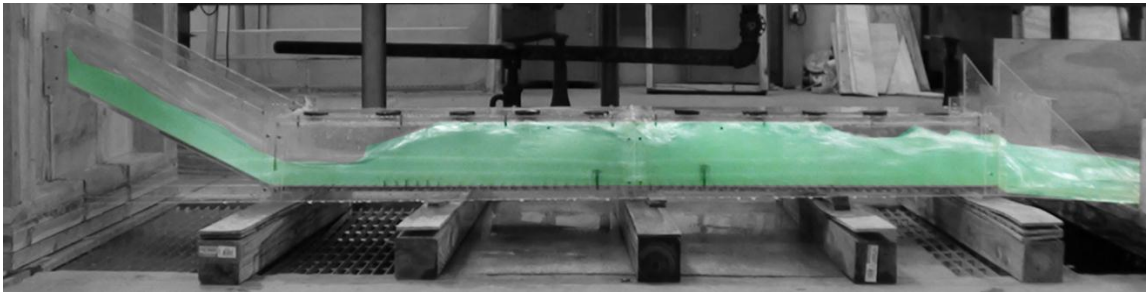


Figure A89: Experiment 30B for 0.6% Slope

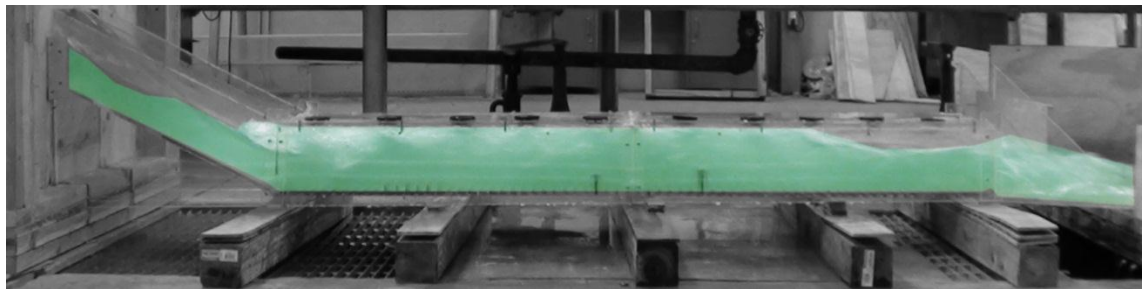


Figure A90: Experiment 30C for 0.6% Slope

Table A30: Experiment 30 for 0.6% Slope Using Pressure Flow Condition with 15 Flat Faced Friction Blocks and a 1.5" Sill at 37" from the End and a 2" Sill at 27" from the End

| H.J. | Run | H    | $W_{temp}$ | Q      | $V_{u/s}$ | $Y_s$ | $Y_{loc}$ | $Y_1$ | $Y_2$   | $Y_{d/s}$ | Fr1  | $V_1$            | $V_2$  | $V_{d/s}$        | L     | X     | $\Delta E$ | THL    | $E_2/E_1$ |
|------|-----|------|------------|--------|-----------|-------|-----------|-------|---------|-----------|------|------------------|--------|------------------|-------|-------|------------|--------|-----------|
| Y    | 30A | 0.8d | -          | 0.9648 | 2.4120    | 1.85  | 1.75      | 1.75  | 8.7518  | 2.75      | 3.9  | 8.3943<br>P-tube | 3.2762 | 4.7079<br>P-tube | 8.00  | 33.00 | 5.6032     | 9.8041 | 0.6234    |
| Y    | 30B | 1.0d | -          | 1.2534 | 2.5068    | 2.85  | 2.25      | 2.13  | 9.9083  | 3.50      | 3.6  | 8.6679<br>P-tube | 4.7079 | 5.5065<br>P-tube | 9.00  | 34.00 | 5.5747     | 8.8209 | 0.6544    |
| Y    | 30C | 1.2d | -          | 1.5812 | 2.6353    | 3.50  | 3.25      | 3.00  | 10.7168 | 4.25      | 2.97 | 8.1081<br>P-tube | 4.7079 | 6.0187<br>P-tube | 11.00 | 41.40 | 3.5733     | 8.2941 | 0.7657    |

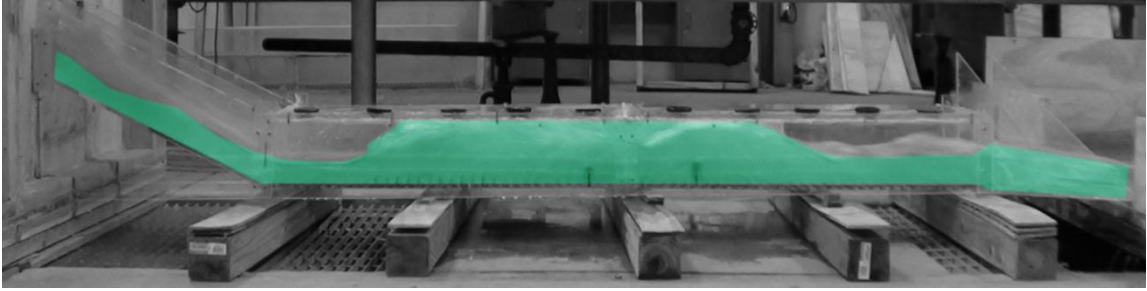


Figure A91: Experiment 31A for 0.6% Slope

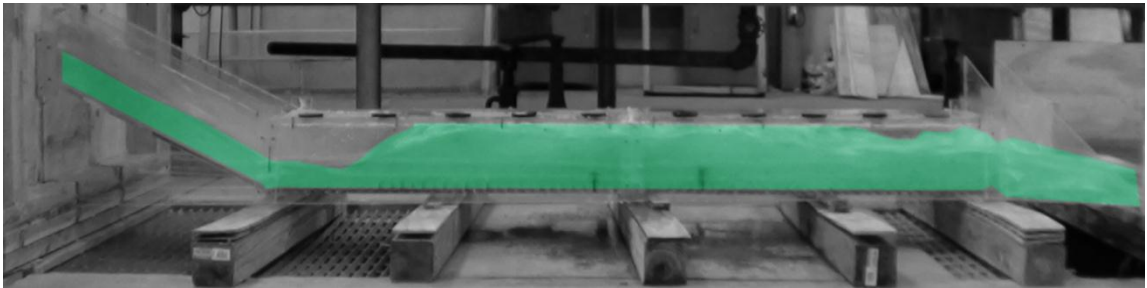


Figure A92: Experiment 31B for 0.6% Slope

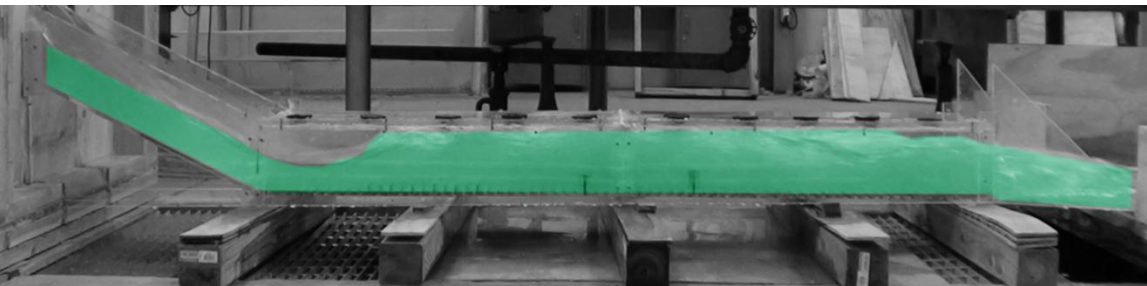


Figure A93: Experiment 31C for 0.6% Slope

Table A31: Experiment 31 for 0.6% Slope Using Pressure Flow Condition with 30 Flat Faced Friction Blocks and a 1.5" Sill at 37" from the End and a 2" Sill at 27" from the End

| H.J. | Run | H    | $W_{temp}$ | Q      | $V_{u/s}$ | $Y_s$ | $Y_{toc}$ | $Y_1$ | $Y_2$   | $Y_{d/s}$ | Fr1 | $V_1$            | $V_2$  | $V_{d/s}$        | L     | X     | $\Delta E$ | THL     | $E_2/E_1$ |
|------|-----|------|------------|--------|-----------|-------|-----------|-------|---------|-----------|-----|------------------|--------|------------------|-------|-------|------------|---------|-----------|
| Y    | 31A | 0.8d | -          | 0.9648 | 2.4120    | 1.85  | 1.75      | 1.75  | 8.8854  | 2.75      | 3.9 | 8.5118<br>P-tube | 4.1763 | 3.4749<br>P-tube | 8.00  | 34.00 | 5.8409     | 11.6841 | 0.6170    |
| Y    | 31B | 1.0d | -          | 1.2524 | 2.4850    | 2.75  | 2.25      | 2.13  | 9.9587  | 3.50      | 3.6 | 8.7081<br>P-tube | 5.2470 | 5.3583<br>P-tube | 9.00  | 34.00 | 5.6549     | 9.1007  | 0.6522    |
| Y    | 31C | 1.2d | -          | 1.5635 | 2.6058    | 3.50  | 2.75      | 2.75  | 10.2577 | 4.25      | 3.0 | 8.0683<br>P-tube | 5.3080 | 6.1292<br>P-tube | 12.00 | 41.40 | 3.7504     | 8.0153  | 0.7480    |

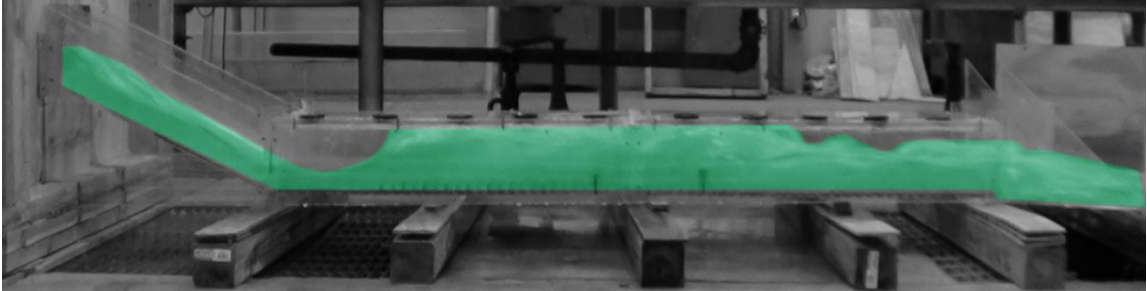


Figure A94: Experiment 32A for 0.6% Slope

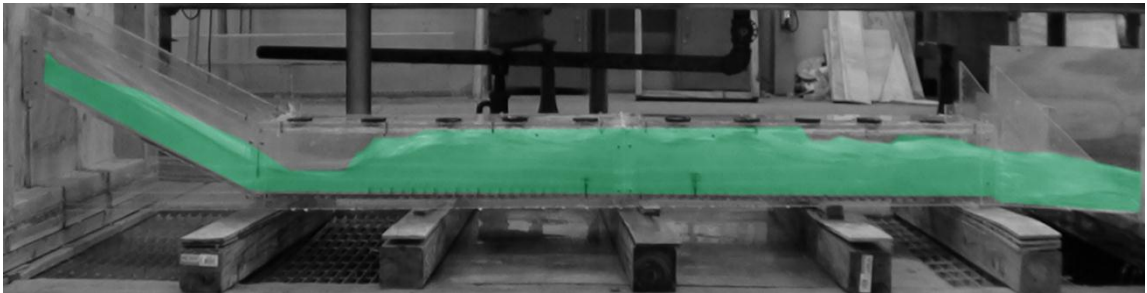


Figure A95. Experiment 32B for 0.6% Slope

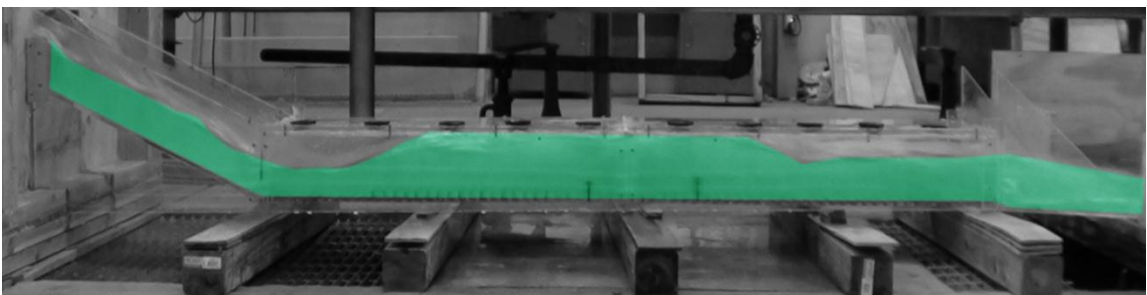


Figure A96: Experiment 32C for 0.6% Slope

Table A32: Experiment 32 for 0.6% Slope Using Pressure Flow Condition with 45 Flat Faced Friction Blocks and a 1.5" Sill at 37" from the End and a 2" Sill at 27" from the End

| H.J. | Run | H    | W <sub>temp</sub> | Q      | V <sub>u/s</sub> | Y <sub>s</sub> | Y <sub>toe</sub> | Y <sub>1</sub> | Y <sub>2</sub> | Y <sub>d/s</sub> | Fr1 | V <sub>1</sub>   | V <sub>2</sub> | V <sub>d/s</sub> | L     | X     | ΔE     | THL    | E <sub>2</sub> /E <sub>1</sub> |
|------|-----|------|-------------------|--------|------------------|----------------|------------------|----------------|----------------|------------------|-----|------------------|----------------|------------------|-------|-------|--------|--------|--------------------------------|
| Y    | 32A | 0.8d | -                 | 0.9648 | 2.4120           | 1.85           | 1.85             | 1.75           | 8.83           | 2.75             | 3.9 | 8.4643<br>P-tube | 3.7712         | 4.7758<br>P-tube | 8.00  | 33.00 | 5.7443 | 9.6841 | 0.6169                         |
| Y    | 32B | 1.0d | -                 | 1.2524 | 2.5048           | 2.75           | 2.13             | 2.00           | 9.44           | 3.25             | 3.7 | 8.5118<br>P-tube | 4.3340         | 5.5550<br>P-tube | 9.00  | 33.00 | 5.4538 | 8.9691 | 0.6481                         |
| Y    | 32C | 1.2d | -                 | 1.5937 | 2.6562           | 3.35           | 2.65             | 2.50           | 10.00          | 4.00             | 3.2 | 8.1904<br>P-tube | 6.4492         | 6.3443<br>P-tube | 11.00 | 34.00 | 4.2188 | 7.8146 | 0.7188                         |

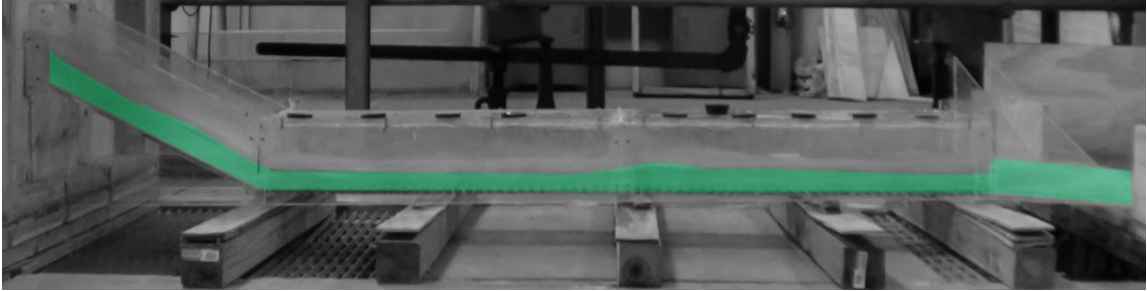


Figure A97: Experiment 33A for 0.3% Slope

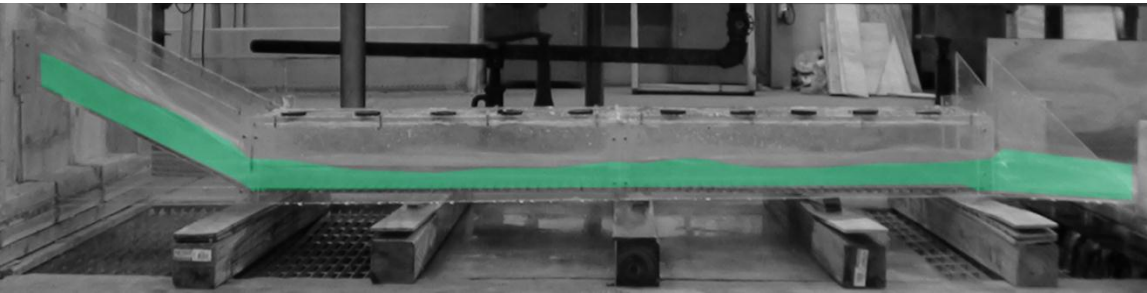


Figure A98: Experiment 33B for 0.3% Slope

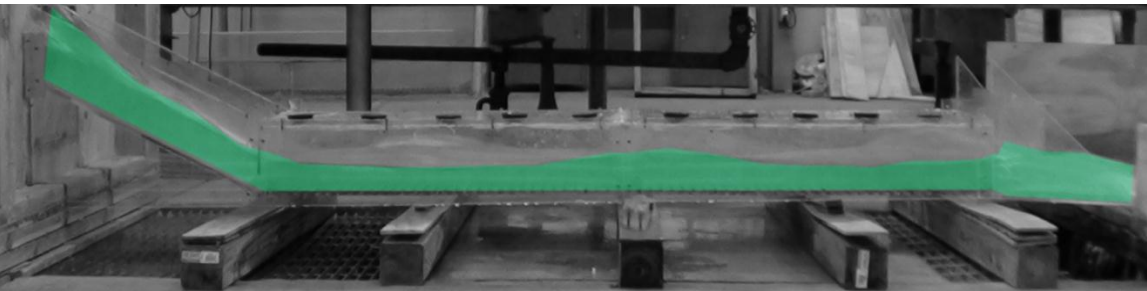


Figure A99: Experiment 33C for 0.3% Slope

Table A33: Experiment 33 for 0.3% Slope Horizontal Channel Using Pressure Flow Condition without any Friction Blocks

| H.J. | Run | H    | $W_{temp}$ | Q      | $V_{u/s}$ | $Y_s$ | $Y_{toe}$ | $Y_1$ | $Y_2$ | $Y_{d/s}$ | Fr1 | $V_1$            | $V_2$  | $V_{d/s}$        | L | X | $\Delta E$ | THL    | $E_2/E_1$ |
|------|-----|------|------------|--------|-----------|-------|-----------|-------|-------|-----------|-----|------------------|--------|------------------|---|---|------------|--------|-----------|
| N    | 33A | 0.8d | -          | 0.9648 | 2.4120    | 1.85  | 1.75      | 1.50  | 1.50  | 1.65      | 4.3 | 8.5902<br>P-tube | 8.4326 | 7.6833<br>P-tube | - | - | -          | 4.0341 | -         |
| N    | 33B | 1.0d | -          | 1.2524 | 2.5048    | 2.85  | 2.13      | 1.85  | 1.85  | 2.13      | 4.0 | 8.8214<br>P-tube | 8.5118 | 8.0250<br>P-tube | - | - | -          | 3.8391 | -         |
| N    | 33C | 1.2d | -          | 1.5962 | 2.6603    | 3.25  | 2.75      | 2.50  | 2.25  | 2.35      | 3.5 | 9.0466<br>P-tube | 8.8971 | 8.4326<br>P-tube | - | - | -          | 3.7188 | -         |



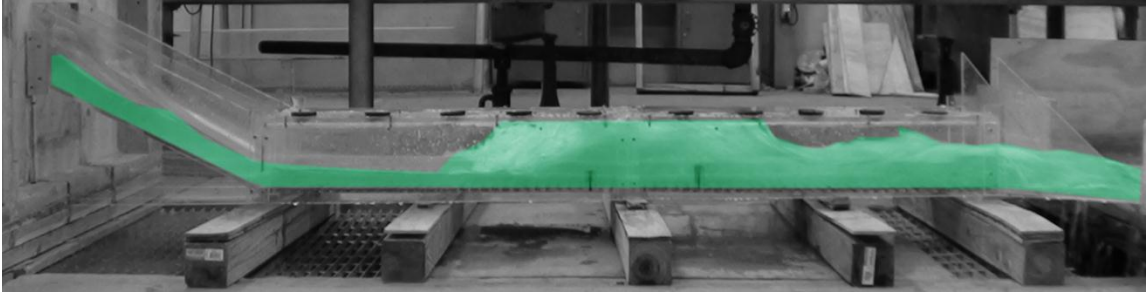


Figure A100. Experiment 34A for 0.3% Slope

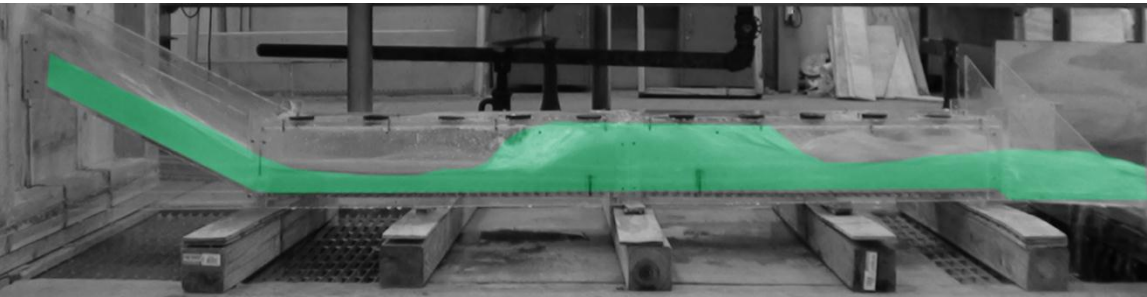


Figure A101: Experiment 34B for 0.3% Slope

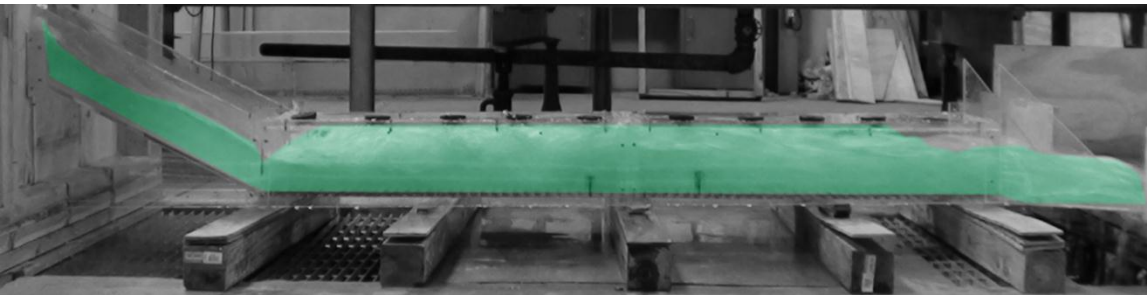


Figure A102: Experiment 34C for 0.3% Slope

Table A34: Experiment 34 for 0.3% Slope Using Pressure Flow Condition and a 1.5" Sill at 37" from the End and a 2" Sill at 27" from the End

| H.J. | Run | H    | W <sub>temp</sub> | Q      | V <sub>u/s</sub> | Y <sub>s</sub> | Y <sub>toe</sub> | Y <sub>1</sub> | Y <sub>2</sub> | Y <sub>d/s</sub> | Fr1 | V <sub>1</sub>   | V <sub>2</sub> | V <sub>d/s</sub> | L     | X     | ΔE     | THL    | E <sub>2</sub> /E <sub>1</sub> |
|------|-----|------|-------------------|--------|------------------|----------------|------------------|----------------|----------------|------------------|-----|------------------|----------------|------------------|-------|-------|--------|--------|--------------------------------|
| Y    | 34A | 0.8d | -                 | 0.9565 | 2.3913           | 1.85           | 1.75             | 1.50           | 8.28           | 2.75             | 4.2 | 8.5118<br>P-tube | 5.7915         | 5.1801<br>P-tube | 8.00  | 24.00 | 6.2759 | 8.9155 | 0.5816                         |
| Y    | 34B | 1.0d | -                 | 1.2460 | 2.4920           | 2.65           | 3.25             | 2.00           | 9.76           | 3.25             | 3.8 | 8.7756<br>P-tube | 6.7540         | 6.1292<br>P-tube | 9.00  | 23.00 | 5.9865 | 7.7072 | 0.6339                         |
| Y    | 34C | 1.2d | -                 | 1.6012 | 2.6687           | 3.25           | 2.85             | 2.50           | 10.44          | 4.25             | 3.3 | 8.5118<br>P-tube | 4.3340         | 6.0187<br>P-tube | 15.00 | 39.00 | 4.7893 | 8.3270 | 0.7007                         |

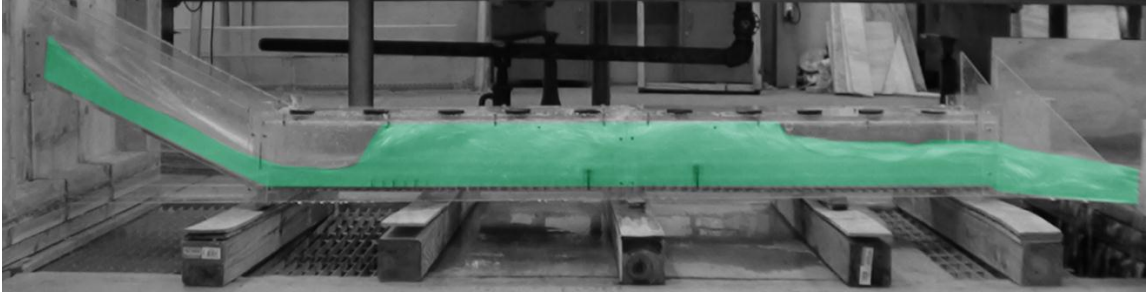


Figure A103. Experiment 35A for 0.3% Slope

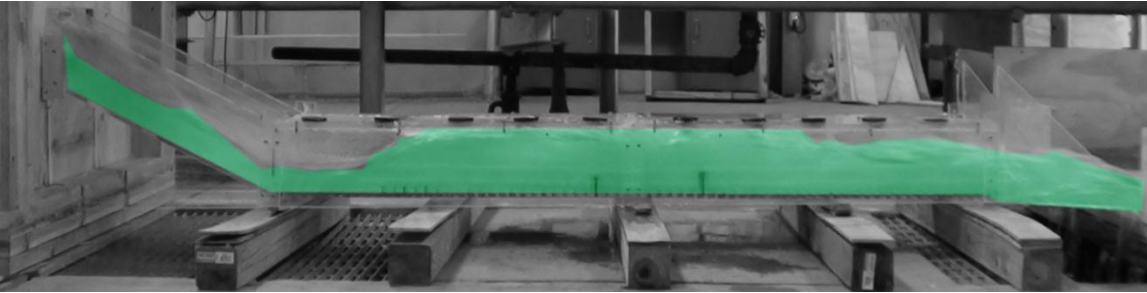


Figure A104: Experiment 35B for 0.3% Slope

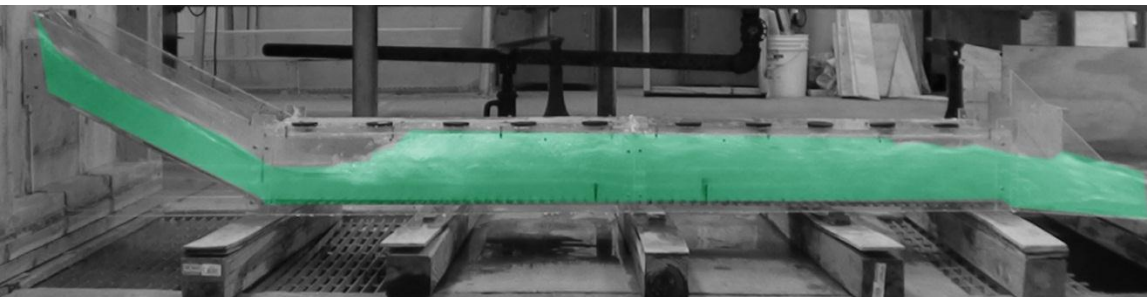


Figure A105: Experiment 35C for 0.3% Slope

Table A35: Experiment 35 for 0.3% Slope Using Pressure Flow Condition with 15 Flat Faced Friction Blocks and a 1.5" Sill at 37" from the End and a 2" Sill at 27" from the End

| H.J. | Run | H    | W <sub>temp</sub> | Q      | V <sub>u/s</sub> | Y <sub>s</sub> | Y <sub>toe</sub> | Y <sub>1</sub> | Y <sub>2</sub> | Y <sub>d/s</sub> | Fr <sub>1</sub> | V <sub>1</sub>   | V <sub>2</sub> | V <sub>d/s</sub> | L     | X     | ΔE     | THL    | E <sub>2</sub> /E <sub>1</sub> |
|------|-----|------|-------------------|--------|------------------|----------------|------------------|----------------|----------------|------------------|-----------------|------------------|----------------|------------------|-------|-------|--------|--------|--------------------------------|
| Y    | 35A | 0.8d | -                 | 0.9565 | 2.3913           | 1.85           | 1.75             | 1.75           | 8.89           | 2.75             | 3.9             | 8.5118<br>P-tube | 3.2762         | 4.7079<br>P-tube | 7.00  | 34.00 | 5.8409 | 9.7855 | 0.6170                         |
| Y    | 35B | 1.0d | -                 | 1.2524 | 2.5048           | 2.75           | 2.25             | 2.13           | 9.96           | 3.75             | 3.6             | 8.7081<br>P-tube | 5.3080         | 5.3080<br>P-tube | 9.00  | 37.00 | 5.6549 | 8.9691 | 0.6522                         |
| Y    | 35C | 1.2d | -                 | 1.5837 | 2.6395           | 3.25           | 3.00             | 3.00           | 10.84          | 4.25             | 2.9             | 8.1904<br>P-tube | 7.0457         | 6.1292<br>P-tube | 12.00 | 41.40 | 3.7035 | 8.0482 | 0.7611                         |

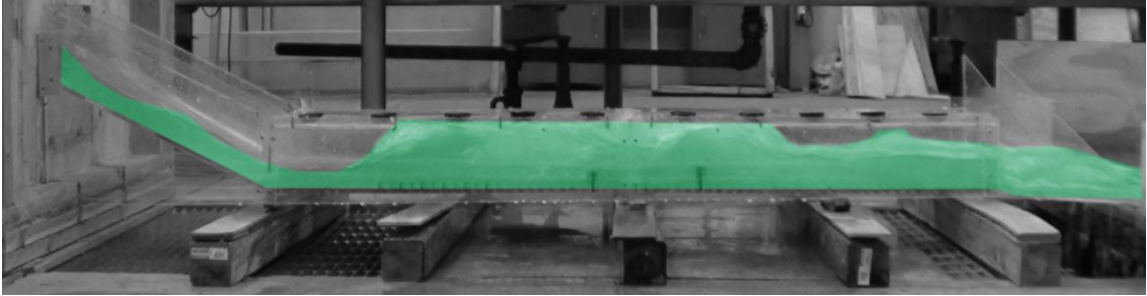


Figure A106: Experiment 36A for 0.3% Slope

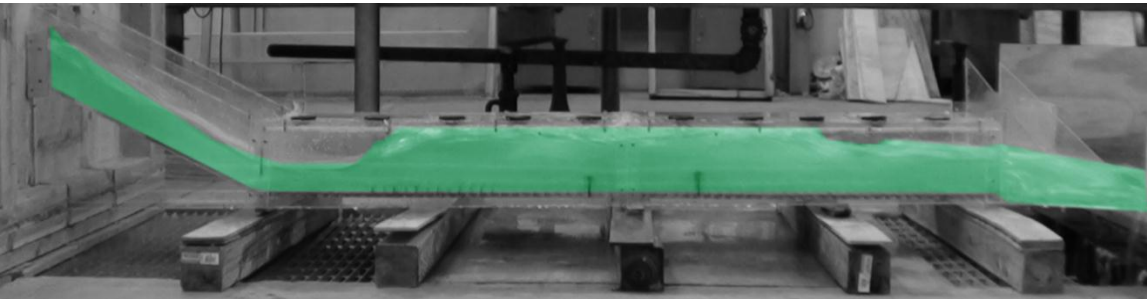


Figure A107: Experiment 36B for 0.3% Slope

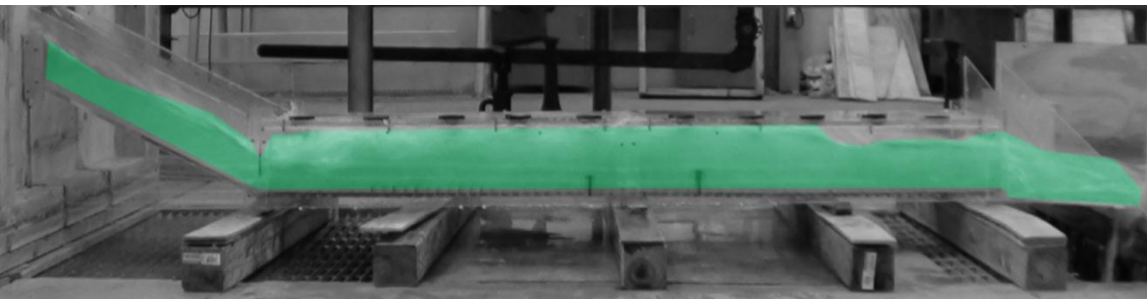


Figure A108: Experiment 36C for 0.3% Slope

Table A36: Experiment 36 for 0.3% Slope Using Pressure Flow Condition with 30 Flat Faced Friction Blocks and a 1.5" Sill at 37" from the End and a 2" Sill at 27" from the End

| H.J. | Run | H    | $W_{temp}$ | Q      | $V_{ws}$ | $Y_s$ | $Y_{toe}$ | $Y_1$ | $Y_2$ | $Y_{ds}$ | Fr1 | $V_1$            | $V_2$  | $V_{ds}$         | L     | X     | $\Delta E$ | THL    | $E_2/E_1$ |
|------|-----|------|------------|--------|----------|-------|-----------|-------|-------|----------|-----|------------------|--------|------------------|-------|-------|------------|--------|-----------|
| Y    | 36A | 0.8d | -          | 0.9648 | 2.4120   | 1.85  | 1.75      | 1.75  | 7.74  | 3.25     | 3.5 | 7.5067<br>P-tube | 3.2762 | 4.7758<br>P-tube | 8.00  | 33.00 | 3.9709     | 9.1841 | 0.6758    |
| Y    | 36B | 1.0d | -          | 1.2460 | 2.4920   | 2.75  | 1.25      | 2.00  | 9.57  | 3.50     | 3.7 | 8.6214<br>P-tube | 4.3340 | 5.4329<br>P-tube | 9.00  | 34.00 | 5.6720     | 8.9572 | 0.6421    |
| Y    | 36C | 1.2d | -          | 1.5987 | 2.6645   | 3.35  | 3.00      | 3.00  | 10.59 | 4.25     | 2.8 | 8.0250<br>P-tube | 5.4329 | 6.2377<br>P-tube | 12.00 | 41.40 | 3.4442     | 7.8229 | 0.7704    |

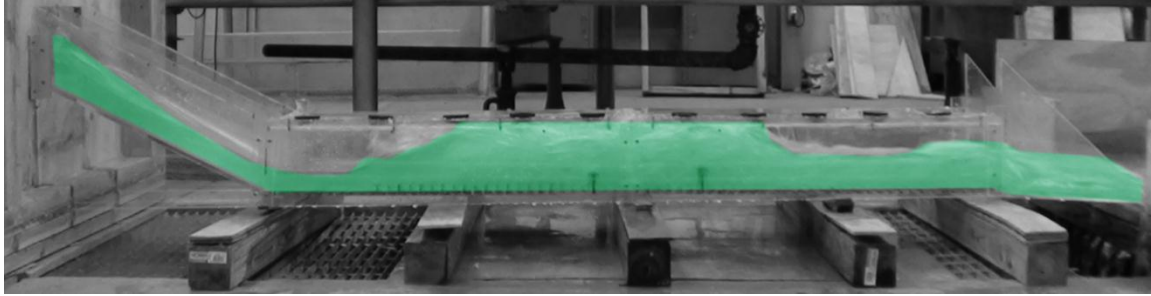


Figure A109: Experiment 37A for 0.3% Slope

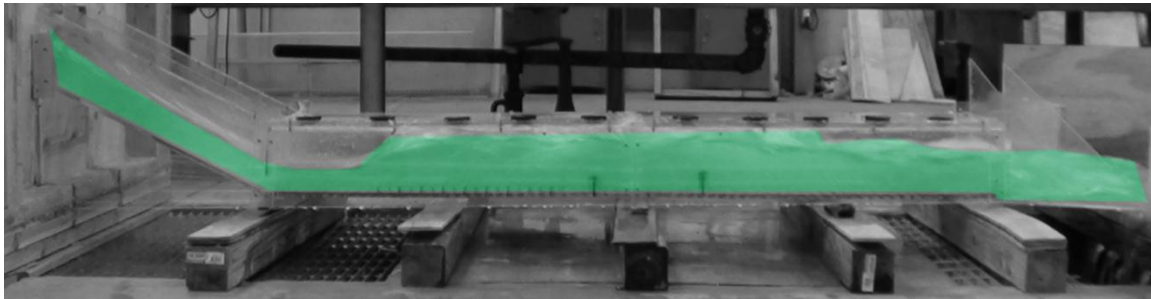


Figure A110: Experiment 37B for 0.3% Slope

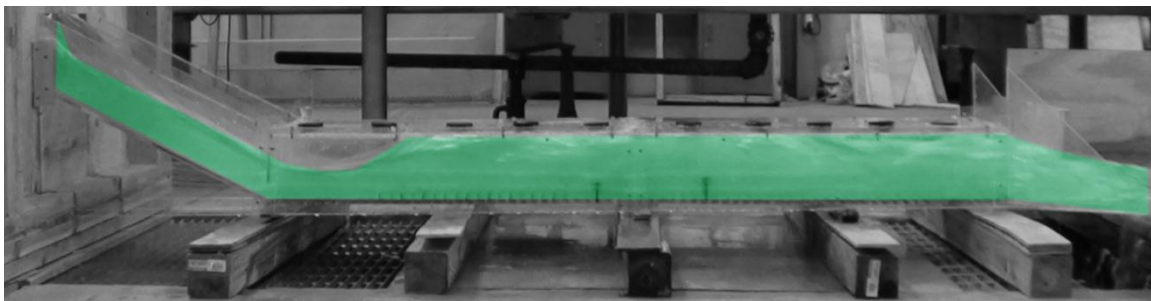


Figure A111: Experiment 37C for 0.3% Slope

Table A37: Experiment 37 for 0.3% Slope Using Pressure Flow Condition with 45 Flat Faced Friction Blocks and a 1.5" Sill at 37" from the End and a 2" Sill at 27" from the End

| H.J. | Run | H    | $W_{temp}$ | Q      | $V_{w/s}$ | $Y_s$ | $Y_{toe}$ | $Y_1$ | $Y_2$ | $Y_{d/s}$ | Fr1 | $V_1$            | $V_2$  | $V_{d/s}$        | L     | X     | $\Delta E$ | THL    | $E_2/E_1$ |
|------|-----|------|------------|--------|-----------|-------|-----------|-------|-------|-----------|-----|------------------|--------|------------------|-------|-------|------------|--------|-----------|
| Y    | 37A | 0.8d | -          | 0.9565 | 2.3913    | 1.85  | 1.65      | 1.50  | 6.94  | 2.75      | 3.6 | 7.2336<br>P-tube | 5.3583 | 4.8317<br>P-tube | 8.00  | 34.00 | 3.8587     | 9.5655 | 0.6570    |
| Y    | 37B | 1.0d | -          | 1.2556 | 2.5112    | 2.75  | 2.25      | 2.13  | 9.25  | 3.25      | 3.4 | 8.1412<br>P-tube | 4.3340 | 5.5550<br>P-tube | 9.00  | 34.00 | 4.5769     | 8.9751 | 0.6839    |
| Y    | 37C | 1.2d | -          | 1.5635 | 2.6058    | 3.50  | 2.65      | 2.50  | 9.78  | 3.75      | 3.1 | 8.0250<br>P-tube | 6.3443 | 6.2377<br>P-tube | 12.00 | 35.00 | 3.9396     | 8.2653 | 0.7283    |



Figure A112: ADV Plugged to Measure the Downstream Velocity  $V_{d/s}$



Figure A113: ADV Instrument

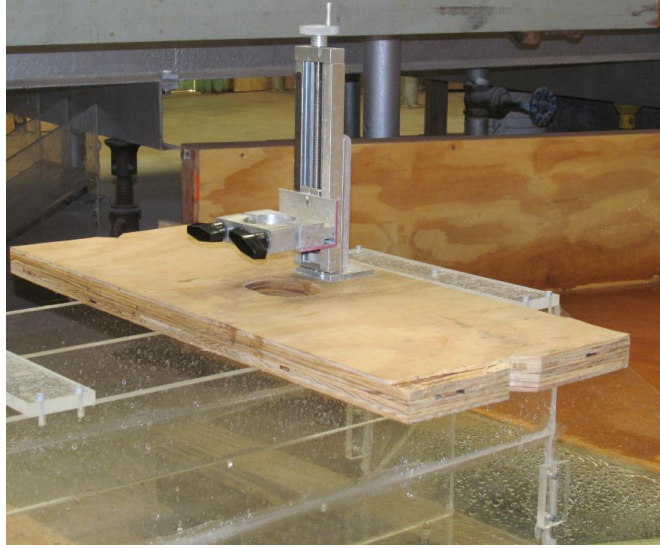


Figure A114: ADV Mount Over Flume

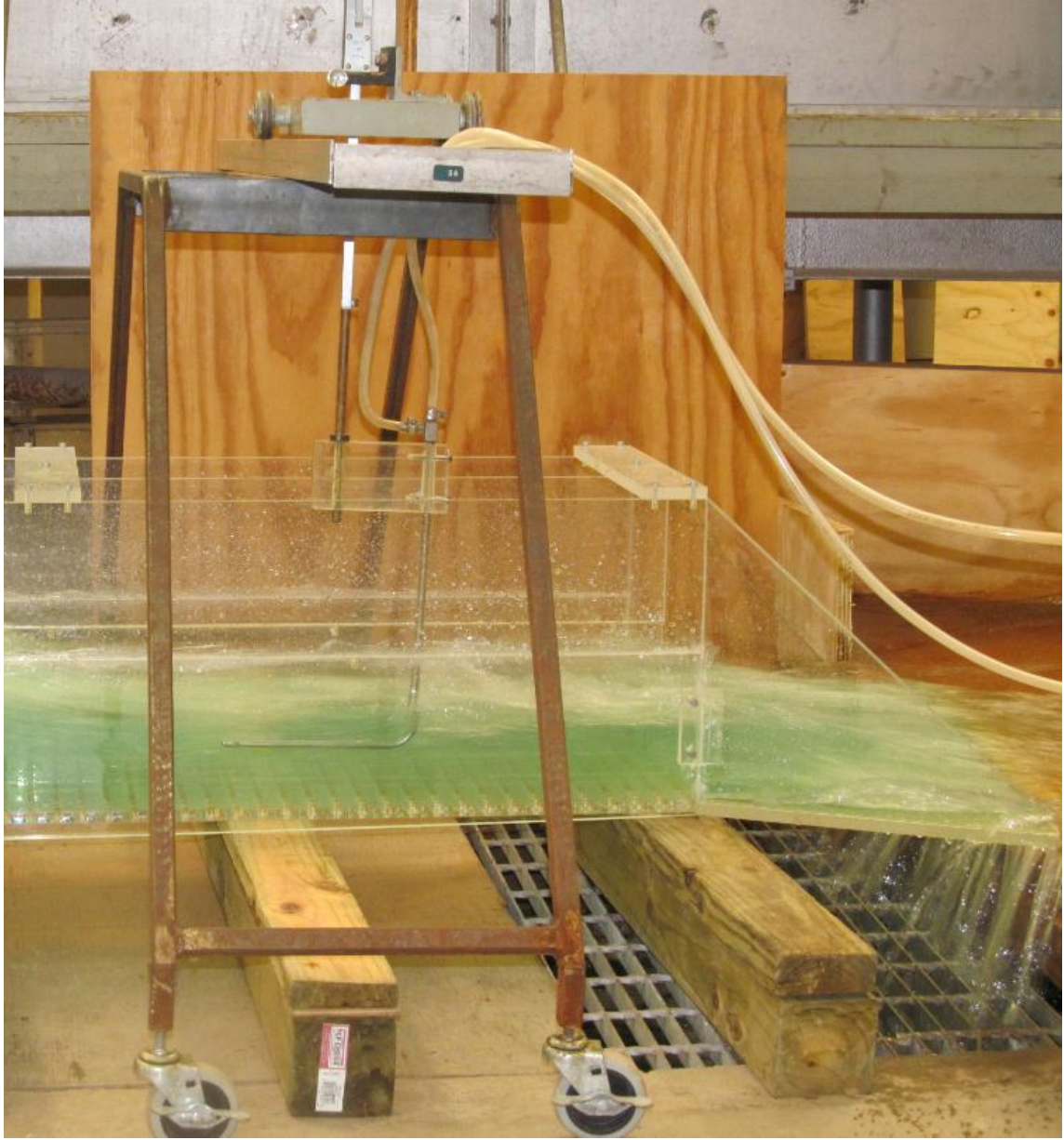


Figure A115: Pitot Tube Plugged in Culverts Downstream to  $V_{d/s}$

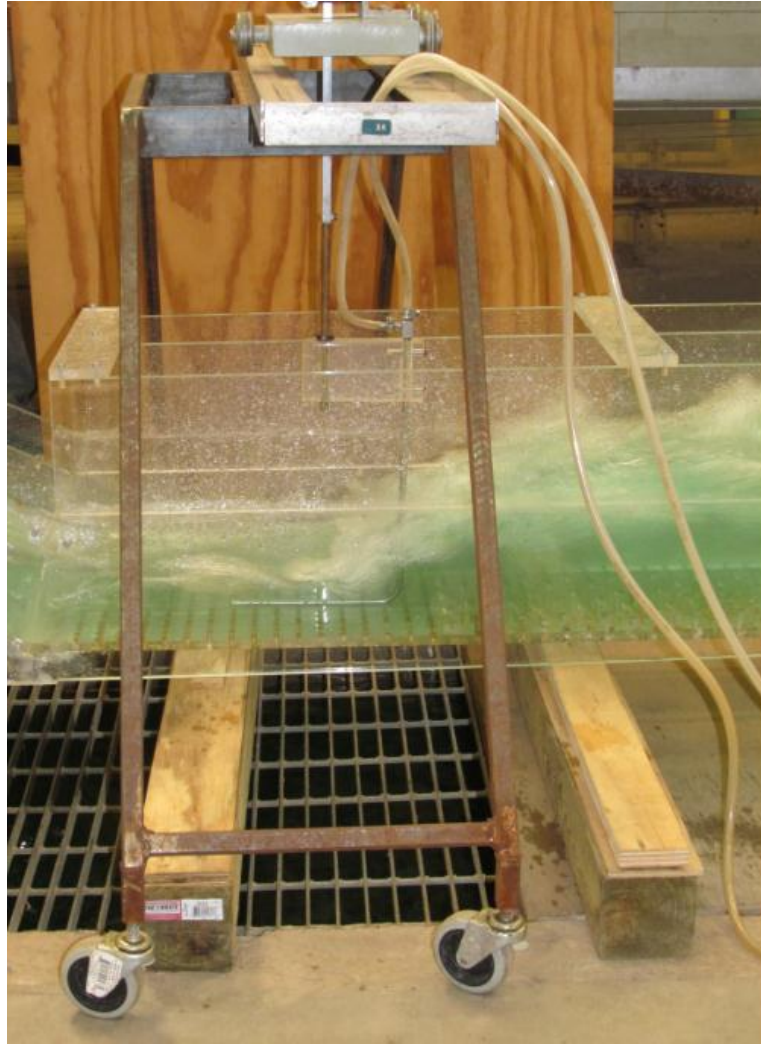


Figure A116: Pitot Tube Plugged in Culverts Upstream to  $V_{wp}$





Figure A117: Pitot Tube.

VITA

Nicholas Michael Johnson

Candidate for the Degree of

Master of Science

Thesis: ANALYSIS OF FLOW THROUGH EIGHTEEN-FOOT BROKEN BACK  
CULVERTS

Major Field: Civil Engineering

Biographical:

Education:

Completed the requirements for the Master of Science in Civil Engineering at  
Oklahoma State University, Stillwater, Oklahoma in May, 2013.

Completed the requirements for the Bachelor of Science in Civil Engineering at  
Oklahoma State University, Stillwater, Oklahoma in 2011.

Experience:

Research Assistant 2011-2013

- Groundwater Hydrology
- Surface Water Hydrology
- GIS-based Modeling
- Open Channel Hydraulics

Teaching Assistant CIVE 3843-Hydrology 2010-2012

Professional Memberships:

American Society of Civil Engineers, ASCE 2013

American Water Works Association, AWWA 2013

Chi Epsilon Civil Engineering Honors Society, XE 2010